INFORMATION TO USERS

This manuscript has been reproduced from the microfilm master. UMI films the text directly from the original or copy submitted. Thus, some thesis and dissertation copies are in typewriter face, while others may be from any type of computer printer.

The quality of this reproduction is dependent upon the quality of the copy submitted. Broken or indistinct print, colored or poor quality illustrations and photographs, print bleedthrough, substandard margins, and improper alignment can adversely affect reproduction.

In the unlikely event that the author did not send UMI a complete manuscript and there are missing pages, these will be noted. Also, if unauthorized copyright material had to be removed, a note will indicate the deletion.

Oversize materials (e.g., maps, drawings, charts) are reproduced by sectioning the original, beginning at the upper left-hand corner and continuing from left to right in equal sections with small overlaps.

Photographs included in the original manuscript have been reproduced xerographically in this copy. Higher quality 6" x 9" black and white photographic prints are available for any photographs or illustrations appearing in this copy for an additional charge. Contact UMI directly to order.

Bell & Howell Information and Learning
300 North Zeeb Road, Ann Arbor, MI 48106-1346 USA
800-521-0600

UMI®

Université d'Ottawa · University of Ottawa

THE ROLE OF NEURONAL APOPTOSIS INHIBITOR PROTEIN IN A MURINE MODEL OF TRAUMATIC BRAIN INJURY

This thesis is submitted in partial fulfillment of the requirements for the degree of

Master of Science (M.Sc.) in the Physiology graduate program

January 18, 2001

Department of Cellular and Molecular Medicine

Faculty of Medicine

University of Ottawa

Rachel Derrane

ACKNOWLEDGEMENTS

I would like to thank Dr. Hutchison, Dr. Fliss, and Dr. MacKenzie for giving me the privilege of studying in their laboratories. I have greatly appreciated their constant encouragement.

I would like to thank the SMA group and Dr. Robertson's laboratory, particularly Dr. Nathalie Gendron and Chris Lee for their technical advice and generous anitbody gifts.

I would like to thank Clare Howlett and Ian Sutcliffe for keeping me sane and making me laugh.

I would like to thank my family for their support, both financial and emotional, and Grey Hound Bus Lines for having eight daily express departures for Toronto.

This thesis is dedicated to Michael Shaye.

Abstract

In models of cell death, the IAPs prevent apoptosis through inhibition of caspases. We postulated that overexpression of NAIP would attenuate apoptosis and improve neurological recovery in a murine model of TBI by inhibiting caspase-3. TBI was performed using a weight drop model. Apoptosis was demonstrated in the cerebral cortex using the ISEL stain on brain sections and PCR amplification of fragmented DNA. The number of apoptotic cells in the cerebral cortex was significantly increased post TBI and the cell types undergoing apoptosis were identified by immunofluoresence as neurons and oligodendrocytes. Immunofluoresence and Western blot techniques were used to reveal that apoptosis was accompanied by a decrease in Naip and an increase in caspase-3 expression. We demonstrate that overexpression of NAIP attenuated DNA fragmentation through the inhibition of caspase-3 using ISEL and Western blot procedures. We were unable to show that NAIP overexpression improved neurological recovery following TBI using the Morris water maze neurological score. Overall, the data presented in this study provide evidence for a role of NAIP in inhibiting apoptosis following TBI.

TABLE OF CONTENTS

LIST OF TABLES

LIST OF FIGURES

LIST OF ABBREVEATIONS

Apaf-1	apoptosis protease activating factor 1
BCL-2	B-cell lymphoma 2
BIR	baculovirus IAP repeat
bp	base pair
BRUCE	bir containing ubiquitin-conjugating enzyme
°C	degrees Celsius
cc	cubic centimeter
CD	cluster definition
cDNA	complementary DNA
ced	cell death
C. elegans	*Caenorhabditis elegans*
cm	centimeter
CMV	cytomegalovirus
CNS	central nervous system
Cp-IAP	*Cydia pomonella* IAP
CSF	cerebral spinal fluid
DNA	deoxyribonucleic acid
DTT	dithiothreitol
EAA	excitatory amino acid
ECL	enhanced chemiluminescence
E. coli	*Escherichia coli*
EDTA	ethylenediamenetetraacetic acid disodium salt

EGTA	ethylene glycol-bis[p-amino ethyl ether]-N,N,N',N'-tetracetic acid
FADD	Fas associated death domain
FITC	fluorescein isothiocyanate
g	gram
x g	gravity
GCS	Glasgow coma scale
HEPES	N-[2 hydroxyethyl] p-perazine-N'-2 ethane sulfonic acid
HIAP	human IAP
IAP	inhibitor of apoptosis protein
I^{CAD}	inhibitor of caspase activated deoxyribonuclease
ICE	interleukin-1β converting enzyme
ICP	intracranial pressure
Ig	immunoglobulin
IGF-1	insulin like growth factor-1
IL-1β	interleukin-1β
ISEL	in situ end label
kb	kilobase
kDa	kilo Dalton
kg	kilogram
L. pneumophila	*Legionella pneumophila*
LM-PCR	ligation mediated - PCR

m	meter
M	molar
MAG	myelin associated glycoprotein
mg	milligram
MHC	major histocompatibility complex
ml	milliliter
mm	millimeter
mM	millimolar
mRNA	messenger ribonucleic acid
NAIP	neuronal apoptosis inhibitor protein
NeuN	neuronal nuclear protein
NF-κB	nuclear factor – kappaB
ng	nanogram
NGF	nerve growth factor
NMDA	N - methyl - D – aspartate
Op-IAP	*Orgyia pseudotsugata* IAP
PARP	poly (ADP) ribose polymerase
PBS	phosphate buffered saline
PCR	polymerase chain reaction
PFA	paraformaldehyde
PMSF	phenyl methyl sufonyl fluoride
PVDF	poly vinyllidene difluoride
RING	really interesting new gene

RNA	ribonucleic acid
rpm	revolutions per minute
RT-PCR	reverse transcription PCR
SDS	sodium dodecyl sulfate
SMA	spinal muscular atrophy
SMN	survival motor neuron
TBI	traumatic brain injury
TNF-α	tumor necrosis factor alpha
TNFR1	TNF receptor 1
TNFR2	TNF receptor 2
TRADD	TNF receptor associated death domain
Tris	tris (hydroxymethyl) aminomethane
U	unit
µg	microgram
µl	microliter
µm	micrometer
µM	micromolar
UTR	untranslated region
XIAP	X-linked IAP

1. Introduction

1.1 Traumatic Brain Injury

1.1.1 Epidemiology of Pediatric Traumatic Brain Injury

TBI is the leading cause of morbidity and mortality in North American children with over 95, 000 children experiencing TBI in the United States every year (2). Several clinical studies have shown that the risk of sustaining TBI is significantly higher in children compared to adults (2, 53, 81). These studies demonstrate that the incidence of TBI steadily increases from newborns to 19 year olds, then gradually decreases until 50 years of age (53). The risk of TBI also differs between genders with 15 to 19 year old males having twice the incidence of head injury and four times the risk of suffering fatal head injuries compared to females in the same age group (53, 81). Data collected in North American emergency wards indicates that most head injuries are caused either by abuse, non-motor vehicle related incidents, or motor vehicle related collisions (107). Regional studies throughout the United States reveal that the most prevalent cause of TBI in children is non-motor vehicle related incidents such as a fall (53). However, the most prevalent cause of severe TBI has been shown to be motor vehicle related collisions involving unrestrained adolescent males (53). Medical science has developed several treatments designed to manage the head injured child and promote recovery.

1.1.2 Classification and Treatment of Mild, Moderate, and Severe Head Injury

Brain damage associated with pediatric TBI is thought to be mediated by acceleration / deceleration forces and elevations in ICP. Due to differences in size and development, the CNS injuries sustained by a child are unique compared to those sustained by an adult following TBI (81). In relation to adults, children are particularly vulnerable to injury caused by acceleration /

deceleration forces as the juvenile head is relatively larger than the body and has less musculoskeletal support (81). Acceleration / deceleration injuries result in diffuse axonal shearing, brain shift, intracranial / intraventricular hematomas, and cell death (81, 93). Compared to adults, children are also particularly vulnerable to increases in ICP (53, 81). Post TBI, ICP rises as increases in cerebral blood flow and volume occur (53). Elevations in ICP occur rapidly and are difficult to reduce in children due to their limited CSF reabsorption range (53). Increased ICP can lead to localized and global ischemia, seizure activity, cytotoxic edema, hydrocephalus, brain inflammation, and cell death (53, 81, 93). It is thought that the cell death that occurs post TBI leads to the neurological deficits observed in patients recovering from trauma. Following TBI, an initial wave of cell death results from mechanical damage to the brain (85). This cell death occurs immediately post TBI and is believed to be non-preventable (81, 85). The second wave of cell death is associated with acceleration / deceleration forces and changes in ICP. This secondary cell death can occur in regions distal to the site of injury and has been associated with deficits in memory retention, olfaction, seizure resistance, and motor function (53). It has been shown in clinical settings that the secondary brain cell death that occurs in children following TBI can be managed using therapeutics directed against elevations in ICP (53, 81).

Children presenting with TBI are assessed using a well described neurological scale and then treated depending on the severity of the injury. During the late 1970's, Drs. Jennett and Teasdale developed a 15 point coma severity scale known as the GCS, that measured motor response, verbal response, and eye opening ability in patients that had sustained TBI (80, 175). Children with a GCS of 15 to 14 are considered to have sustained a mild head injury (81). In mild head injury, the impact force is absorbed by the skull and the intracranial contents are not damaged

(53, 81). Thus, mild head injury is not associated with elevated ICP, acceleration / deceleration forces, or cell death. Patients are monitored for changes in the level of consciousness, pupillary response, and changes in head circumference (81). Children with a GCS of 9 to 12 and a change in the level of consciousness are classified as moderately head injured (81). In moderate head injury, impact forces are transferred from the skull to the brain resulting in acceleration / deceleration and ICP associated injuries (81, 93). Treatment of moderate head injury includes bed rest to stabilize ICP, supportive management, and monitoring for sequelae (i.e.; change in pupillary response to light, change in head circumference) (25). Children that have sustained a severe head injury have a GCS of less than, or equal to, 8 and are often comatose (25). These children are managed with intubation / ventilation, hemodynamic support, and monitoring of ICP (25). To reduce the cerebral edema that can result from dangerously high ICP (30 to 40 Torr) in children with severe head injury, osmotic diuretics such as mannitol or 3% hypertonic saline are often used (25, 81). Mild to moderate hyperventilation and hypothermia may also be used to reduce blood flow to the brain (25, 164). Surgical options to alleviate high ICP in severely head injured patients include decompressive craniotomy and drainage of CSF (121). Due to the aggressive management of elevated ICP, children with moderate and severe TBI have a mortality rate of approximately 30% (81). Nevertheless, even with careful ICP monitoring, the effect of diffuse injury to the brain on cell loss and neurological defects in patients that survive a TBI incident can be profound (81). Animal models of TBI have been used to develop new therapies designed to attenuate cell death at the molecular level and improve neurological outcome following trauma.

1.1.3 Animal Models of TBI

Animal models have been used to investigate cellular changes associated with TBI and to develop therapies designed to promote cell survival following trauma (85). TBI has been studied experimentally using models of acceleration / deceleration injury and brain deformation injury (85). Historically, primates were used in the acceleration / deceleration models because they have comparable head, neck, and spine anatomy with humans (85). Unfortunately cost and housing concerns for the animals have limited the number of acceleration / deceleration injury studies performed. The experimental animals currently used for brain deformation models are rodents, specifically rats and mice (85). Organization of the rodent brain has been extensively studied and has been shown to be homologous to the human brain (82). Additionally, the low cost and easy housing of these animals have made rodents the ideal experimental group to study TBI (85). Over the last 20 years rodent models of TBI have been used to unravel the molecular mechanisms associated with TBI pathophysiology and to develop therapies that promote cell survival (26, 85). However, while animal models of TBI have been invaluable in revealing the biochemical pathways associated with cell death, the results of therapies developed using these models have been disappointing in human clinical trials (26, 85, 115). Reasons for the discrepancy between the animal models and clinical trials include improper dosing of specific therapies in humans, different cell death time courses between humans and rodents, and altered ability of drugs to penetrate the human brain compared to the rodent brain (26). Concerns have also been raised about the type of cell death targeted by the therapeutics (26). Following TBI cells die either by a passive form of death known as necrosis or by an energy requiring, gene mediated form of death known as apoptosis (38, 125, 137, 190). Recent *in vivo* studies have shown that the secondary cell death associated with TBI was caused by apoptosis (137, 139).

However, most therapies developed and used in the clinical trials have been directed against necrosis rather than apoptosis (26).

1.2 Apoptosis

1.2.1 Necrosis versus Apoptosis

During the life span of an organism, cells will either die passively by necrosis or actively through an apoptotic pathway. Cells that receive a sudden extreme injury or are exposed to high levels of a noxious compound that disrupts osmotic balance in the cell often undergo necrotic death. During necrosis, extracellular ions such as calcium enter into the cell and cause damage by inhibiting energy production and activating proteolytic proteases (155). Additional damage occurs when, in an attempt to improve osmotic balance, water enters and causes the cell to swell (155). Cellular contents are eventually spilled through leaky membranes into the extracellular space (138). The inflammatory response initiated by the release of cellular contents often causes extensive damage to neighboring cells (138).

In contrast to necrosis, apoptosis is an energy requiring gene mediated process that is essential for survival of an organism (109). This type of cell death was first observed by Kerr et. al. (1972) who described the morphological changes in non-necrotic dying cells in two stages (86). The first stage involved nuclear and cytoplasmic condensation followed by breakup of the cell into membrane bound vesicles (86). The second stage involved phagocytosis of the vesicles by other cells and recycling of the vesicle contents (86). This form of death prevents the release of pro-inflammatory cellular contents into the extracellular space, thereby avoiding an inflammatory response and damage to surrounding cells (138). Apoptosis, which is a Greek word for 'falling petals or leaves' was the name given to the regulated type of cell death

observed by Kerr (86). Extensive research has shown that apoptosis can occur in all cell types and can be initiated by a variety of stimuli (55, 127). Each apoptotic signal is capable of activating metabolic pathways and specific genes whose action results in the morphological changes associated with apoptosis (55, 127). Apoptosis has been observed in mature tissues and is believed to play an essential role in mediating tissue homeostasis (126). It has also been demonstrated that apoptosis is essential for successful development of organs during embryogenesis (68, 69, 86 129). Apoptotic death has been observed during formation of tubular structures, fashioning of limbs, formation of interdigital clefts and involution of phylogenetic vestiges (86). Apoptosis has also been shown to be essential for the proper formation of the CNS. A remarkable 50% turnover of proliferating CNS neurons occurs during synaptogenesis in order to eliminate excess neurons and those with improper connections (129). Apoptosis during development was thoroughly examined in invertebrate organisms and provided a wealth of information about the biological pathways through which apoptosis is propagated.

1.2.2 Apoptosis During *C. elegans* Development

The genes that are essential for apoptosis during development of the nematode *C. elegans* have been extensively studied. The protein products of three main *ced* genes direct the loss of 131 cells, of which 105 are neuronal, from 1090 somatic cells in the *C. elegans* larvae (67). CED-3 is a proapoptotic protein that exists in the cytosol in an inactive form (68, 69). CED-4 is a proapoptotic protein that is complexed in the cytosol to the antiapoptotic protein CED-9 (68, 69). Following an apoptotic stimulus, CED-9 dissociates from CED-4 which then binds to and promotes activation of CED-3 (6, 69). Activated CED-3 commits the cell to apoptotic death by cleaving specific structural and repair proteins after aspartic acid residues (178). Recent research

has demonstrated that the majority of apoptotic death that occurs in vertebrate organisms involves gene families homologous to the *C. elegans ced* genes (105, 178, 197).

1.2.3 Vertebrate Biochemical Pathways of Apoptosis

Caspases, the mammalian homologues of *ced-3*, are essential to the execution of the two most biologically prevalent pathways of apoptotic death. The caspases were first implicated in cell death when it was revealed that the *ced-3* death gene was related to the mammalian enzyme, ICE which converts the IL-1β precursor to the mature form (196). Eleven human caspases have since been identified and can be divided into three subgroups based on sequence homology (4). The ICE-like subgroup includes caspases-1, -4, and -5, the caspase-2-like subgroup includes caspase -2 and -9, and the CPP32-like subgroup contains caspases-3, -6, -7, -8, -9, and -10 (4). The ICE subfamily appears to be predominantly involved in inflammation while the caspase-2-like and CPP32-like proteases have been shown to promote apoptosis (126). Caspases are expressed in the cytoplasm as inactive 30 - 50 kDa precursor proteins, or zymogens, containing an amino terminal prodomain together with one large (20 kDa) and one small (10 kDa) subunit (178). The zymogens are activated following heterologous and autologous proteolysis to form a heterodimeric structure consisting of two large and two small subunits (178). All of the currently identified caspases, or cysteine aspases, contain a Cys/His diad at the active center and cleave proteins after aspartyl motifs (4). Apoptosis 'initiator' caspases, including caspase -2, -8, -9, and -10, contain long prodomains which allow them to interact with specific cellular adaptor proteins (19). These interactions bring the initiator caspases into close proximity which promotes activation of one zymogen by another and enhancement of the apoptosis signal (19). Apoptosis 'effector' caspases, including caspase-3, -6, and -7, contain a short prodomain and are activated

in a proteolytic cascade by initiator proteases (19). The effector caspases cleave essential structural and regulatory proteins which generates many of the morphological changes that are hallmarks of apoptosis (30, 62, 89, 154, 172, 174, 176, 184).

Caspase-3, the most extensively studied effector caspase, is known to lead to the internucleosomal DNA fragmentation that is characteristic of apoptosis (79). Caspase-3 is activated by cleavage of the inactive 32 kDa proenzyme into 17 and 12 kDa subunits which combine to produce the active heterodimeric form of the enzyme (178). Active caspase-3 contributes to DNA fragmentation by cleaving both the DNAse inhibitor I^{CAD} and the DNA repair enzyme PARP (79, 128 158, 148, 177). As extensive DNA fragmentation irreversibly impairs cellular function, once caspase-3 is activated the cell is considered to be committed to apoptotic death (79).

The caspases are essential to the two most biologically prevalent pathways of apoptotic death: mitochondria induced apoptosis and death receptor induced apoptosis (24). In 1996 it was discovered that an apoptotic program could be induced in the cytosol of non-apoptotic cells by introducing the mitochondrial protein cytochrome c (105). It has since been demonstrated that, following exposure of cells to a variety of apoptotic stimuli, cytochrome c is released from the inner membrane of mitochondria and initiates an apoptotic pathway (150, 191). In the cytosol cytochrome c interacts with the CED-4 homologue Apaf-1 which causes the activation of the initiator protease caspase-9 (101). Caspase-9 then cleaves and activates the effector proteases caspase-3 and –7 (101). The mechanism of the permeability changes in the mitochondrial membrane that result in release of cytochrome c are not yet fully understood but it is believed that the vertebrate CED-9 homologue BCL-2 protein family may play a regulatory role (24, 102). Certain proapoptotic BCL-2 family members are present on the cytoplasmic surface of

mitochondria and are thought to form pores through which cytochrome c can escape once a cell has been exposed to a proapoptotic agent (24, 131).

Cell surface receptors can also stimulate apoptosis through activation of caspases (6). Proapoptotic cell surface receptors, or death receptors, are all members of the TNF / NGF receptor superfamily (24). These receptors contain a cysteine rich repeat in the extracellular domain and a homologous region localized in the cytoplasm known as the death domain (24). The best characterized of the death receptors is the TNF-α receptor, TNFR1 (124). The effects of TNF-α are mediated by two distinct receptors, the high affinity TNFR2 (p75, p80) and the low affinity TNFR1 (p55, p60) (32). TNFR2 is able to bind TNF-α even when extracellular levels of the cytokine are low, does not contain a death domain, and stimulates up regulation of genes involved in cell proliferation and survival through the activation of the transcription factor NF-κB (13, 32, 144, 145). In contrast to TNFR2, the low affinity TNFR1 binds TNF-α only when extracellular levels of the cytokine are abundant and has been shown to mediate TNF-α induced apoptosis (6). Once TNFR1 has bound three ligand molecules the receptor trimerizes and recruits the TRADD protein (124). TRADD associates with the clustered receptor death domains and binds the FADD protein (35, 76). The amino terminus of FADD contains a death effector domain which recruits the inactive initiator protease procaspase-8 (18). Upon recruitment by FADD, procaspase-8 becomes activated by self-cleavage and proteolytically processes procaspase-3 and –7 (123). There is some evidence that the TNF-α apoptotic signal can be amplified through activation of both death pathways (102, 106, 165). Recent *in vivo* and *in vitro* experiments have demonstrated that activated caspase-8 can stimulate the mitochondria death pathway by cleaving the protein Bid (102, 106). Cleavage of this proapoptotic BCL-2 family member by caspase-8 causes translocation of the carboxyl terminal of the protein into the

mitochondria, rapid release of cytochome c into the cytosol, and activation of caspase-9 (102, 106). Thus, extensive research has demonstrated that caspases are essential for the execution of apoptosis death pathways. It is believed that apoptosis in developing and mature organisms is regulated by survival proteins families that interact with cell death mediators and function to prevent apoptosis.

1.2.4 Antiapoptotic Protein Families

Antiapoptotic BCL-2 family members and the IAP family have been shown to inhibit apoptosis *in vitro* and *in vivo* by blocking specific steps in the mitochondria and death receptor pathway (1, 55, 92, 103, 187, 191). The antiapoptotic members of the BCL-2 family, including BCL-2, BCL-Xl, and BCL-w are associated with inhibition of mitochondria initiated cell death upstream from caspase activation (1). These proteins are thought to prevent apoptosis by inhibiting cytochrome c release from the mitochondria or by preventing the interaction of Apaf-1 and procaspase-9 (35, 55, 130, 191). Antiapoptotic BCL-2 proteins are highly expressed in proliferating CNS cells during embryogenesis indicating that these proteins are essential for successful development of the brain and spinal cord (94). However, very low levels of these proteins have been detected in mature CNS structures, suggesting that these proteins do not play an important role in preventing apoptosis in the healthy adult CNS (37, 90, 167, 189).

The IAPs are a recently identified family of antiapoptotic proteins that are differentially expressed throughout the tissues of an organism. Six human IAPs, NAIP, HIAP1, HIAP2, XIAP, survivin, and BRUCE, have been identified (5, 52, 64, 103, 144). The IAPs are characterized by a novel domain of approximately 70 amino acids which can repeat up to three times in the protein (46). This region, known as the BIR domain, is essential for the

antiapoptotic function of the IAPs (46). HIAP1, HIAP2, and XIAP also contain a RING domain which is essential for the function of these proteins (48, 146, 173). Mouse homologues of the human IAPs have also recently been discovered suggesting that the IAP gene family has been conserved in mammals (46). The expression of the IAPs differs throughout tissues in the body. *XIAP* mRNA was found in all adult and fetal tissues tested indicating that it is a ubiquitously expressed member of the family (103). Expression of *HIAP1* and *HIAP2* is highest in the kidney, small intestine, liver, and lung and is quite low in the CNS (195). These proteins are associated with TNFR2 and are thought to promote cell survival by inducing the activation of NF-κB (170). Low levels of *NAIP* expression have been detected in adult liver, placenta, and CNS (147). In contrast to other member of the IAP family, *survivin* expression is rarely detected in healthy adult human and mouse tissues (97). However, recent work has indicated that expression of this IAP is restricted to dividing cells (97). This hypothesis was supported by Ambrosini et. al. (1997) when it was revealed that *survivin* is expressed in a high proportion of the most common forms of cancer (5).

The IAPs appear to function *in vivo* and *in vitro* primarily as antiapoptotic proteins. Overexpression of XIAP, HIAP1, HIAP2, NAIP, or survivin inhibits apoptosis stimulated by a broad variety of agents including TNF-α, menadione, staurosporin, etoposide, Taxol, and growth factor withdrawal (5, 52,100, 103). It has been demonstrated both *in vitro* and *in vivo* that members of the IAP family inhibit both TNF-α and mitochondria induced apoptosis by blocking the activity of specific caspases (47, 48, 146, J. Maier, personal communication). Although the IAPs do not interact with caspase-8, certain members of this protein family have been shown to inhibit the TNF-α apoptosis pathway by interfering with the activity of caspase-3 and -7 (48, 146, J. Maier, personal communication). XIAP, HIAP1, and HIAP2 have also been shown to

block the mitochondria apoptosis pathway by interfering with the activity of caspase-9 (45, 47). Interestingly, recent studies by Deveraux et. al. (1997, 1998) and Roy et. al. (1997) have demonstrated that while binding of the IAPs to caspase-3 and -7 requires activation of these caspases, the IAPs bind to both the activated and unprocessed forms of procaspase-9 (47, 48, 146). As the IAPs are expressed in most adult tissues, including the mature CNS, it has been suggested that these proteins are important post-natal regulators of apoptosis (92).

1.2.5 Apoptosis and Neurodegeneration

Apoptosis is essential for the survival of an organism, however inappropriate apoptosis has recently been implicated in several neurodegenerative disorders (109). Evidence of apoptotic-like cell death has been detected in CNS structures affected by Alzheimer's disease, Huntington's disease, Parkinson's disease, and multiple sclerosis (8, 9, 109). Studies have shown that the cell death occurring in these conditions is associated with internucleosomal DNA fragmentation that can be blocked by caspase inhibitors (39, 62, 183). In neurodegenerative diseases, apoptosis is considered to be a late event resulting from genetic abnormalities within the organism (8). Hence, in regards to these disorders there is on going debate whether damaged CNS cells rescued from apoptotic death are still biologically active and functionally salvageable (8). As a result of the controversy, apoptosis is not a primary target for therapeutics designed to attenuate the pathology arising from neurodegenerative disease. Apoptotic death has also been associated with cellular degeneration resulting from CNS trauma (9). Apoptotic-like death has been observed in *in vitro* and *in vivo* models of stroke, spinal cord injury and TBI (34, 42, 108, 111, 125). This death is associated with activation of various caspases, internucleosomal DNA fragmentation, and cleavage of caspase-3 specific substrates (34, 38, 42, 111, 136, 190). In

contrast to neurodegenerative disease, apoptotic death following trauma is thought to play a significant role in the resulting CNS pathology and is an attractive target for therapeutics (38, 42).

1.2.6 Necrotic and Apoptotic Profiles Following TBI

TBI is characterized by early localized necrotic death and wide spread secondary apoptotic death (38, 111, 125, 137, 190). Several *in vivo* and *in vitro* models of TBI have demonstrated cell death as early as 10 minutes following trauma (3, 38, 137). These cells have the morphological appearance characteristic of necrotic death and are found in the immediate trauma region (38, 111, 137). In experimental models of TBI, the number of necrotic cells has been shown to reach a maximum approximately 3 to 6 hours following injury (3, 38, 136, 137). A second population of dying cells has also been observed in both clinical and experimental TBI models (38, 111, 125, 137, 169). In contrast to the necrotic death, the morphology of these cells appears apoptotic-like (38). Several studies have shown that these cells also contain fragmented DNA, active caspase-3, and cleaved α-spectrin (caspase-3 specific substrate) strongly suggesting that the majority of cells in this second population are undergoing apoptotic death following TBI (38, 136, 190). Apoptosis has been observed as early as 6 hours post TBI in the injury region and as late as 1 year in CNS structures distal to the site of trauma (38, 137). Most recently regionally distinct apoptosis following cortical trauma has been observed in the cortex and subcortical white matter up to 1 week post TBI, striatum up to two weeks post TBI, and thalamus up to 1 month post TBI (38, 137). Due to the prolonged secondary cell death observed in regions distal to the site of injury it is believed that apoptosis rather than necrosis, determines the neuropathologic outcome following TBI (137, 139).

1.2.7 Identification of Apoptotic Cells Following TBI

Gray matter neurons and subcortical white matter oligodendrocytes appear to be particularly vulnerable to apoptotic death following TBI. Immunohistochemical staining techniques have identified cortical apoptotic cells as neurons in several *in vivo* models of TBI (38, 125, 139, 190). Neurons appear to be the primary apoptotic cell type in the cortex as studies have shown that little apoptosis occurs in astrocytes or resident inflammatory cells post trauma (125). Neurons have also been shown to be selectively vulnerable to apoptosis in *in vitro* models of trauma (3, 136). A recent study by Allen et. al. (1999) demonstrated that in mixed cell cultures containing neurons and astrocytes, the neurons undergo apoptosis while the astrocytes proliferate following a mechanical punch trauma (3). Neuronal death during the early post trauma period in *in vivo* and *in vitro* models of TBI has been shown to reach a maximal level at 24 hours following injury, however low levels of neuronal apoptosis has been observed for several months following injury (3, 38, 125, 137). Immunohistochemical staining techniques have identified subcortical white matter apoptotic cells as oligodendrocytes in *in vivo* models of TBI (38). The function of oligodendrocytes is to myelinate neuronal axons in the vertebrate CNS with a single oligodendrocyte interacting with and myelinating several axons (10, 11). There is some evidence that oligodendrocyte and neuronal apoptosis follow the same time course post TBI. Similar to neuronal death, oligodendrocyte death has been observed to reach a maximum level at 24 hours following TBI and to continue at a lower level in tissue distal from the site of injury for several months (38, 42). It is postulated that this oligodendrocyte death may be the result of withdrawal of trophic factors supplied to the cell by the axon (10, 42). Thus, following TBI oligodendrocytes may undergo apoptosis in response to the axonal degeneration and growth

factor withdrawal that occurs as the neurons die (38, 42). However, growth factor withdrawal is probably not the principle apoptotic signal as TBI results in several biological responses that induce both neurons and oligodendrocytes to die.

1.2.8 Death Molecules Associated with TBI

Molecules that induce both necrosis and apoptosis are present in the brain following TBI. EAAs are a major necrosis inducing signal that have been detected in *in vitro* and *in vivo* models of TBI and are thought to cause most of the observed necrotic death (3, 31, 137). CNS cells become transiently depolarized immediately following TBI, an event known as traumatic depolarization (88). The depolarization results in the release of EAA such as glutamate into the extracellular space (88). Much of the necrotic death associated with TBI is thought to arise from the association of glutamate with the NMDA receptor which is present on the plasma membrane of CNS cells (31). In *in vitro* models of TBI, the association of glutamate with the NMDA receptor has been shown to trigger the influx of calcium into neurons which results in an ionic imbalance and activation of calcium dependent proteases (136, 185). It has been demonstrated that neuronal necrosis occurs rapidly following these events. *In vivo* studies have shown that EAA release is a short term, localized response to TBI that is rapidly attenuated following injury (31, 137). Elevated levels of extracellular glutamate and intracellular calcium can be detected in the injured region 5 minutes following experimental TBI but return to basal levels by 3 hours post injury (31, 185). Thus, necrotic death reaches a maximum at approximately 4 hours after *in vivo* and *in vitro* TBI and does not reappear in the injury site or surrounding tissue (136, 137, 185). Due to the transient nature of EAA release, these molecules are not believed to play an important role in mediating the secondary damage that has been observed following TBI (137).

The resident inflammatory response associated with TBI is believed to significantly contribute to the apoptosis that occurs post trauma (7, 17, 88). One of the earliest responses to TBI is activation of the resident inflammatory cells known as microglia (84, 88). Microglia are derived from a bone marrow precursor of monocytic lineage and are deposited in the CNS antenatally (70, 135). In healthy vertebrate organisms, microglia are found through out the CNS in an inactive form (59, 88). Following a neurological insult, microglia become activated in response to elevated levels of extracellular potassium that result from traumatic depolarization (28, 88). Activated microglia are amoeboid shaped motile cells that proliferate and migrate to the site of injury where they phagocytose dying cells and participate in the inflammatory response to TBI (157). Microglia participate in the inflammatory response by expressing T cell adhesion receptors, MHC class II antigen presenting molecules, and by releasing inflammatory mediators known as cytokines (181). *In vivo* models of TBI have shown that microglia are activated throughout the brain as early as 1 hour following trauma and can remain activated up to 3 months post injury resulting in an extensive inflammatory period within the brain (74, 84). Although the activity of microglia can be beneficial to an organism, recent studies have indicated that these cells are involved in mediating cell damage associated with multiple sclerosis, Alzheimer's disease and CNS trauma (21, 84, 139, 171, 186). It is thought that activated microglia damage CNS cells by releasing high levels of the proapoptotic cytokine TNF-α.

TNF-α produced by microglia has been shown to be an important mediator of neuronal and oligodendrocyte apoptosis following TBI (74, 153, 163). TNF-α is a multifunctional cytokine that can mediate a wide range of cellular responses including apoptosis (6, 180). Although brief exposure of cells to TNF-α is often beneficial enabling an organism to mount an immune response to kill an invading pathogen, several studies have shown that exposure of cells to high

levels of TNF-α can be harmful (43, 56, 113, 116, 141, 159, 160, 168). Recently, exposure of the CNS to TNF-α has been implicated in the pathogenesis of bacterial meningitis, multiple sclerosis, cerebral malaria, Alzheimer's disease, Parkinson's disease, and TBI (43, 56, 113, 116, 141). Involvement of TNF-α in the pathology associated with TBI was indicated when elevated levels of TNF-α were found in the cerebrospinal fluid of humans post TBI (143). TNF-α is also increased in clinically relevant models of TBI and has been shown to significantly contribute to the neuronal and oligodendrocyte apoptosis that occurs following trauma. A dramatic increase in TNF-α mRNA has been detected in the injured cortex between 1 hour and 6 hours post TBI in the rat with maximal levels of TNF-α protein observed in injured tissue 6 hours following trauma (56, 87, 161). During the acute post trauma period (48 hours following TBI) TNF-α has been shown to associate with neurons within the damaged region *in vivo* suggesting that this proapoptotic cytokine is involved in the cell death observed following TBI (87). The observation that agents which inhibit TNF-α production or block TNF-α receptors prevent early neuronal apoptosis and improve neurological recovery provide additional evidence that TNF-α plays an important role in mediating the damage associated with TBI (87, 159, 160). TNF-α has also been shown *in vitro* to induce apoptosis of neurons and oligodendrocytes through association with the TNFR1 death receptor (32, 71, 87, 99, 163, 194). Recent studies indicate that the TNF-α stimulated apoptosis of both neurons and oligodendrocytes involves caspase-3 activation, PARP cleavage, and DNA fragmentation (66, 71, 99, 117, 190, 194). The observed elevation of TNF-α following head injury, the association of TNF-α with CNS cells that undergo apoptosis post TBI, and the ability of TNF-α to stimulate apoptosis of neurons and oligodendrocytes through the activation of caspase-3 strongly suggests that TNF-α is an important mediator of the apoptotic death that occurs following trauma.

TNF-α has been shown to be harmful to CNS tissue during the acute period post TBI, however, recent evidence has demonstrated that TNF-α is beneficial to cell recovery in the chronic period following trauma. Holmin et. al. (1999) demonstrated that levels of TNF-α remain elevated above basal levels in the rat brain for up to 3 months. These observations originally lead investigators to speculate that TNF-α may induce the low levels of secondary apoptosis associated with trauma (74). To determine the validity of this hypothesis several studies have examined the effect of extended TNF-α exposure on histological and behavioral recovery in *in vivo* models of stroke and TBI (21, 153). Using a stroke model and mice genetically deficient in TNF-α receptors, Bruce et. al. (1996) demonstrated that wildtype mice had a smaller infarct volume, lower level of damaged neurons, and increased neuronal survival compared to the TNF-α receptor deficient mice (21). These observations indicate that TNF-α had a neuroprotective role during the chronic period following stroke (21). The long term beneficial effect of TNF-α on recovery post TBI has also recently been demonstrated. Using mice deficient in TNF-α production (TNF-/-), Scherbel et. al. (1999) demonstrated that in the acute period post TBI, TNF-/- mice had higher neurological scores and less cortical cell loss than wildtype mice (153). However, the wildtype mice appeared to recover over a 4 week period while the TNF-/- mice continued to show neurological deficits and progressive cortical cell loss (153). These results strongly suggest that although TNF-α is initially cytotoxic, this cytokine is important in facilitating long term CNS recovery following brain injury (153). Researchers have postulated that the dual role of TNF-α with respect to cell recovery may depend on changes in the level of TNF-α and receptor occupancy that occur following TBI. During the acute phase post trauma high levels of TNF-α are present in injured tissue, TNFR1 and TNFR2 are occupied and apoptosis is induced through TNFR1 (32, 163). However, once levels of TNF-α decrease, the

cytokine occupies TNFR2 solely (74, 143). TNFR2 is thought to promote cell recovery by increasing expression of anti-inflammatory cytokines and antiapoptotic proteins (87, 110, 144, 145 153). Thus, there appears to be a critical time window for therapeutics designed to block the interaction of TNFR1 with TNF-α and reduce damage associated with TBI.

1.2.9 Expression of Antiapoptotic Proteins Following TBI

The antiapoptotic BCL-2 protein may play a role in attenuating cell death following TBI. Previous *in vitro* and *in vivo* studies have shown that overexpression of BCL-2 reduces neuropathology and infarct volume in clinically relevant models of stroke (37). Increased expression of endogenous BCL-2 has also been observed in neuronal axons following spinal cord injury (98). These results suggested that BCL-2 might have a role in other models of CNS trauma including TBI (37, 156). Using an experimental model of TBI, Clark et. al. demonstrated that *bcl-2* mRNA and protein were significantly increased in neurons that appeared to be resistant to apoptosis following trauma (37). Further evidence for the neuroprotective role of BCL-2 in CNS trauma was obtained in 1998 when Raghupathi et. al. revealed that BCL-2 overexpressing mice had reduced cortical cell loss following TBI (140). However, the neuroscores obtained from wildtype and BCL-2 overexpressing mice were not significantly different, indicating that the protected neurons in the transgenic animals were not functionally active (140). Additionally, a significant increase in endogenous *bcl-2* mRNA in oligodendrocytes and the attenuation of oligodendrocyte apoptosis following TBI in BCL-2 overexpressing mice has not been reported suggesting that BCL-2 does not influence oligodendrocyte cell death post TBI. (140). *In vitro* studies have demonstrated that BCL-2 is also ineffective in attenuating TNF-α induced apoptosis, which is believed to significantly

contribute to the cell death observed following TBI, due to the inability of BCL-2 to inhibit the caspase-8 pathway (167, 182). The inability of BCL-2 to improve neurological outcome, protect against oligodendrocyte death post TBI, or reliably inhibit TNF-α induced apoptosis, casts doubt on the effectiveness of BCL-2 to attenuate tissue damage following TBI.

Although members of the IAP family have been shown to prevent apoptosis (92), the effect of these proteins on the cell death that occurs following TBI has never been examined. The IAPs block a broader spectrum of apoptotic agents than any other antiapoptotic family and appear to play a significant role in preventing tissue damage associated with various models of neurodegeneration and trauma (73, 92, 187). The protection afforded to CNS tissue may in part be due to the ability of members of the IAP family to effectively prevent TNF-α stimulated apoptosis in most cell types and inhibit the activity of both initiator and effector caspases (47, 48, 92, 103, 146). The antiapoptotic characteristics of the IAPs suggest that members of this protein family could be important mediators of cell survival following TBI. NAIP, the endogenous CNS IAP, was discovered by virtue of its absence in children with the pediatric disorder known as spinal muscular atrophy.

1.3. Spinal Muscular Atrophy

1.3.1. Spinal Muscular Atrophy - General Information.

The spinal muscular atrophies are a group of childhood autosomal neurodegenerative disorders that are classified as either type I (Werdnig-Hoffmann disease), type II, or type III (Kugelberg-Welander disease) depending on age of onset and clinical severity (95, 147). Type I SMA is the most severe form of the disorder with symptoms beginning *in utero* or shortly after birth (20, 65). Afflicted children are not able to sit unaided and rarely survive past age 2 due to weakening

of the respiratory muscles (20).

SMA is primarily the result of inappropriate death of the anterior horn motor neurons (α-motor neurons) of the spinal cord at the lumbar and cervical level (58, 122). It is this death of the α-motor neurons that leads to the symmetrical limb muscle atrophy and weakness observed in SMA patients (51). The molecular defect that causes the inappropriate cell death is not yet fully known. It is suspected that the motor neurons that undergo cell death do so in an apoptotic fashion (57, 149). Motor neurons in SMA spinal cords appear swollen with chromatolysis of cells characteristic of programmed cell death (133). These observations suggest that a defect in the apoptotic pathway causes reactivation or persistence of the cell death that occurs during spinal cord development (129, 149). Thus, it has been hypothesized that the SMAs are diseases resulting from inappropriate apoptosis.

1.3.2 Mapping of the SMA Critical Region

In 1990, it was determined that all three types of SMA were linked to position 5q13 of human chromosome 5 (23, 114). The critical region was found to be contained within a 140 kb region characterized by extreme genetic instability (95, 147, 152). This instability was associated with DNA duplication events resulting in several copies of functional genes as well as a variety of pseudogenes placed in two inverted elements (95, 147, 152). The genetic variability of the region hindered candidate gene identification until 1995 when two potential SMA determining genes *SMN* and *NAIP*, were identified simultaneously (95, 147).

1.3.3 SMN – General Information

The *SMN* gene was identified as a candidate SMA gene by Lefebvre et al. in 1995. *SMN* has

been shown to exist in a telomeric copy (*SMN1* or SMN_{Tel}) and a centromeric copy (*SMN2*, SMN_{Cen} or *cBCD541*) along the 5q13 region of chromosome 5 (95). There is evidence that the two 20 kb genes are oriented in a 'head to head' manner each containing nine exons that code for a 1.7 kb mRNA transcript (95). It has been determined that the centromeric *SMN2* preferentially undergoes alternative splicing of exon 7 which results in a truncated RNA transcript (95). Translation of the truncated RNA generates in a non-functional protein (95). The translation of the full length *SMN1* and *2* mRNA results in a 38 kDa protein which is expressed at a low level in all tissues examined but appears most strongly expressed in CNS tissue (12, 91, 96, 179). The SMN protein has been shown to be involved in RNA metabolism and is essential for embryogenesis (75, 95, 104, 132). Lefebvre *et al.* (1995) demonstrated that genomic rearrangements of *SMN1* occurred in the majority of SMA patients regardless of clinical severity which strongly suggests that *SMN1* is the causative gene in SMA pathogenesis (95).

1.3.4 NAIP– General Information

NAIP was identified as a candidate SMA gene by Roy et al. in 1995 (147). In the 5q13.1 SMA critical region *NAIP* was present as one full length copy in a 'tail to tail' arrangement (5'-3' and 3'-5') next to *SMN1* and as several truncated and internally deleted copies along the 5q13 region (33, 147). *NAIP* occupies 56 kb of genomic DNA and contains 17 exons (33). The 5' UTR spans exons 1 to 3 and part of exon 4 with transcription of exons 4 to 17 resulting in a 6.1 kb mRNA (33). Translation of the mRNA generates a 1403 amino acid full length protein approximately 150 kDa in size (33, 147). NAIP was so named due to its homology with a family of viral inhibitor of apoptosis proteins discovered by Lois Miller in baculovirus and nuclear polyhedrosis virus (15, 41, 147). These viruses were able to suppress insect host cell apoptosis

through the activity of two homologous proteins, Cp-IAP and Op-IAP (92). The antiapoptotic activity of the viral IAPs mapped to two 70 amino acid repeats identified as the BIR domains (92). As NAIP was shown to possess three BIR domains and had a 33% homology to Cp-IAP and Op-IAP, Roy et. al. (1995) postulated that NAIP functioned as a mammalian antiapoptotic protein (147).

NAIP is actively transcribed in select mammalian adult tissues including structures in the CNS. Hybridization of a Northern blot containing a variety of adult non-SMA tissues detected a 6 kb and 7 kb RNA band in liver and placenta, respectively (147). Additionally, RT-PCR using *NAIP* specific primers revealed the presence of *NAIP* transcriptional activity in the spinal cord (147). Using RT-PCR techniques with adult mouse tissue has revealed *Naip* mRNA expression in the spinal cord, liver, lungs, kidney, and spleen (147). The rat homologue of NAIP has also been detected in a variety of adult rat CNS structures (188). Immunohistochemical techniques have revealed the presence of varying levels of NAIP like immunoreactivity in cells of the cortex, hippocampus, thalamus, basal ganglia, cranial nerve nuclei, brainstem relay nuclei, cerebellum, and spinal cord (188). All of these NAIP containing structures show some pathology in type I SMA patients. The identification of NAIP as a potential antiapoptotic protein in addition to its expression in the CNS suggested that a loss of *NAIP* could be involved mediating the apoptotic death of the motor neurons in SMA patients.

1.3.5 Deletions in *NAIP* Associated with SMA

The presence of the IAP *NAIP* in the SMA critical region and the association of neuronal apoptosis with SMA pathology suggested that partial or entire deletion of *NAIP* may affect inhibition of apoptosis in the motor neurons and contribute to SMA pathology (147). It has

recently been demonstrated that *NAIP* exons 4 –5 are homozygously deleted in 60 - 80% of type I patients and in 15 - 42% of type II and III patients (27, 142, 147). As *SMN1* is partially or wholly deleted in the majority of SMA patients an attractive model for SMA is that deletion of *NAIP* and *SMN1* lead to the severe type I phenotype while deletions of *SMN1* alone results in the milder type II and III phenotype (33). In this model *SMN1* is the causative gene for SMA while *NAIP* is the phenotype modifier gene (40, 120).

1.3.6 Function of NAIP

NAIP has been shown to play a significant antiapoptotic role in several *in vitro* and *in vivo* models of cell death. Hela and chinese hamster ovary cell lines transfected with either a NAIP expression plasmids containing exons 4 – 15 or with an adenovirus containing NAIP exons 4 – 15 were dramatically protected against apoptotic death (20 – 90%) compared to non-NAIP expressing cells (103). Using this *in vitro* model, it was revealed that NAIP protected cells against several different apoptotic triggers including serum deprivation, menadione (potent free radical inducer), and TNF-α up to 48 hours following exposure (103). In a similar *in vitro* model, adenovirus was used to express NAIP in rat cerebellar granule neurons which were then treated with low potassium media to trigger apoptosis (162). Cells that expressed NAIP were significantly protected from apoptosis up to 12 hours in low potassium media compared to control cells (162). However, after 40 hours in low potassium media the amount of apoptotic death occurring in the NAIP expressing cells was not significantly different than in the control cells indicating that NAIP delayed but did not attenuate low potassium triggered cell death (162). A delay of apoptosis has also been observed in an *in vivo* model of motor neuron cell death (134). NAIP adenovirus was used to transfect 14% of sciatic motor neurons in 11 day old rats

(134). One week following sciatic axotomy, 40% of motor neurons were protected from cell death (134). However, the protection gradually decreased as expression of the adenovirus decreased indicating that NAIP was necessary to inhibit motor neuron apoptosis (134).

Expression of endogenous NAIP has also been shown to influence apoptosis in *in vivo* models of hippocampal damage. *In vivo* studies in the rat have shown reduced damage in hippocampal neurons that strongly express NAIP or can quickly increase production of NAIP following ischemia (187). Using a mouse line with a targeted deletion of the BIR containing *Naip1* exons 2 and 3, it has been shown that expression of the IAP is not essential for successful embryogenesis but was essential to protect against apoptosis of hippocampal neurons stimulated by kainic acid induced seizures (73). Thus, it has been shown that with varying degrees of success, NAIP can protect against or delay apoptosis initiated by a variety of agents both *in vitro* and *in vivo*. There is evidence that NAIP inhibits apoptosis through the interaction of the BIR domains with the death effector protease caspase-3 (162, J. Maier, personal communication). It is thought that the interaction of the BIR domains with caspase-3 prevents the activity of this protease (J. Maier personal communication). The presence of NAIP in CNS cells, its antiapoptotic function, and the loss of NAIP in type I SMA children suggests that NAIP is an important mediator of CNS cell survival and is consistent with the hypothesis that NAIP is a modifying gene in SMA pathology.

1.3.7 *Naip* is the Murine Homologue of *NAIP*

In 1996 Scharaf et. al. identified the murine region syntenic for the human SMA region on mouse chromosome 13 (151). Murine *Naip* is highly homologous to human *NAIP* with a 68% overall amino acid similarity (193). Additionally, murine *Naip* contains three BIR domains with

76% homology to the three *NAIP* BIR regions and an ATP/GTP binding site that is also present in the human homologue (193). However, in contrast to the human region, *Naip* is present in six distinct copies on murine chromosome 13 (77, 151, 193). Due to the differences in size and sequence of introns between the copies it is thought that the six genes represent a gene family and not copies of the same gene (193). Of the six genes only copies 1 to 3 contain the 5' UTR necessary for translation in the CNS (192, 193). Using RT-PCR and primers specific for either *Naip1, 2,* or *3*, *Naip1* was shown to be expressed in the brain and *Naip2* was shown to be expressed in the spleen (192, 193). This tissue specific expression of the different copies of *Naip* may be the result of differences in the 5' UTR of each gene (193). *Naip1* and *2* show a high degree of similarity in the coding region, however *Naip2* contains multiple 5' UTR exons while *Naip1* contains only one which may lead to alternative regulation of translation of each gene (192, 193).

Recent studies have demonstrated that similar to human NAIP, murine Naip is an antiapoptotic protein. As previously discussed, mice deficient in *Naip1* have increased apoptotic death of hippocampal neurons following kainic acid induced seizures indicating that Naip promotes cell survival following CNS trauma (73). It has also been shown that Naip might play a role in determining susceptibility of macrophages to Legionnaires' disease. Legionnaires' disease is caused by the facultative bacteria *L. pneumophila* which enters macrophages, replicates, and triggers the cell to undergo apoptosis in a caspase-3 dependent manner (61). Macrophages of resistant mouse strains express high levels of Naip following infection (50). In contrast, macrophages from the AJ mouse strain expresses much less Naip than resistant mouse strains and are susceptible to *L. pneumophila* infection (50). The fact that the AJ mice express less Naip suggests the macrophages are not able to protect themselves against the caspase-3 mediated

apoptosis caused by the infection and consequently these animals develop Legionnaires's disease (50, 151). The results are consistent with a role for Naip in inhibiting caspase-3 activity and apoptosis. These recent *in vivo* studies have shown that similar to human NAIP, the murine copies of Naip perhaps function as endogenous antiapoptotic proteins through the inhibition of caspase activity.

1.4 Hypothesis and Principal Objectives

In view of the data above, the hypothesis underlying this study was that elevated NAIP expression in CNS cells in mice would reduce neuronal and oligodendrocyte apoptosis following traumatic brain injury and that the attenuation of apoptosis would improve neurological function. Transgenic mice overexpressing human NAIP were used in these studies and were compared to wildtype controls. Nine principal objectives were investigated in these studies using a murine model of TBI:

1. To determine the quantity and the time course of apoptosis following TBI using staining and gel electrophoresis procedures specific for cleaved DNA.
2. To detect the cleavage of caspase-3 and PARP following TBI using Western blot techniques.
3. To determine the identity and location of cells undergoing apoptosis following TBI using a double stain procedure with antibodies specific for neurons and oligodendrocytes
4. To quantify the expression of the proinflammatory cell marker CD11*b* and the proapoptotic cytokine TNF-α in the cerebral cortex following TBI.
5. To quantify the effect of TBI on the cytosolic levels of Naip using a Western blot procedure, and immunofluorescence staining followed by cell counting with Northern Eclipse software.

6. To detect expression of human NAIP in transgenic C57 mouse brain sections using an immunofluorescent staining procedure with an antibody specific to human NAIP.
7. To determine the effect of NAIP overexpression on post-traumatic DNA fragmentation by comparing the number of apoptotic cells in the cortex and subcortical white matter in mice transgenic for NAIP to wildtype litter mates.
8. To investigate the effect of NAIP overexpression on post traumatic cleavage of procaspase-3 and PARP by comparing activation of caspase-3 and cleavage of PARP in mice transgenic for NAIP to wildtype litter mates using Western blot techniques.
9. To investigate the ability of NAIP overexpression to improve neurological outcome following TBI in NAIP transgenic mice compared to wildtype litter mates using modifications of the Morris water maze.

2. Materials and Methods

All reagents were products of Sigma Chemical (St. Louis, MO) unless otherwise indicated.

2.1 Animal Protocol

2.1.1 Development of a strain of transgenic C57/Bl6 mice expressing the human *NAIP* gene: The pUC18 human *NAIP* vector was constructed in the laboratory of Dr. Alex MacKenzie. A portion of the human *NAIP* gene (coding exons 4-16) was isolated from a phage cDNA library and ligated into a 2.7 kb pUC18 cloning vector (Clontech Laboratories Inc., Palo Alto, CA) for transfection of *E. coli* colonies (147). The pUC18 vector contains a multiple cloning site, a gene conveying resistance to the antibiotic ampicillin, and the α-fragment of the *lac z* gene encoding β-galactosidase. Transcription is under control of a constitutively active CMV promoter (pCMV IV) which is able to drive high levels of gene transcription in almost all mammalian cells (22). The ampicillin resistance element allows for easy selection of *E.coli* transformed with the pUC18 vector. The pUC18 multiple cloning site is located in the *lac Z* α-fragment, resulting in disruption of β-galactosidase activity and the appearance of white *E. coli* colonies on X-gal/IPTG agar plates which allows for selection for recombinant plasmids.

CMV *NAIP* transgenic mice were generated via pronuclear injection of the recombinant plasmids into C57/Bl6 x CBA/J F2 embryos (the embryo contains both male and female nuclei but both nuclear membranes are still intact) in the laboratory of Dr. F. Jurik at the University of British Columbia in 1996 (72). Superovulation was induced in C57/Bl6 female mice using pregnant mare serum and the eggs were harvested and fertilized. The fertilized eggs were placed in an injection chamber and held in place with a glass pipette. The isolated *NAIP* vector was injected into the male pronucleus (usually larger than the female pronucleus and easier to inject)

and eggs were transferred to the oviduct of a pseudopregnant C57/Bl6 mouse. The resulting pups were genotyped for the presence of the human *NAIP* gene. Three heterozygous transgenic mice were transferred to the University of Ottawa Animal care facility and used to establish a breeding colony with C57/Bl6 wildtype mice.

2.1.2 Genotyping of CMV *NAIP* litters: C57/Bl6 mice heterozygous for human *NAIP* were mated to wildtype C57/Bl6 mice (Charles River, QC). The offspring were weaned, their ears tagged, and their tails clipped for DNA isolation. Total genomic DNA was extracted from the tail clipping as follows: in an eppendorf tube containing a tail clipping, 300 µl of STD buffer (1 mM Tris-HCL pH 8.0, 0.5 mM EDTA pH 8.0, and 5 mM NaCl), 200 µl of 2X lysis buffer (Applied Biosystem Inc., Mississauga, ON), 40 µl of 10 mg/ml proteinase K (Boehringer Mannheim, Montreal, QC), and 1.25 µl of 0.5 µg/µl RNAse (Boehringer Mannheim, Montreal, QC) was added. Tubes were incubated overnight at 50^0C in a water bath. Tubes were centrifuged at 14,000 X g for 5 minutes. The supernatant was transferred to new tubes and 400 µl of phenol:chloroform:water (1:1:1) (Applied Biosystem Inc., Mississauge, ON) was added. Tubes were centrifuged at 14,000 x g for 5 minutes and the supernatant was transferred to new eppendorf tubes. The phenol:chloroform:water step was repeated. The supernatant was transferred to new eppendorf tubes, 400 µl of isoamyl alcohol:chloroform (1:50) (Applied Biosysten Inc., Mississauga, ON) was added and the eppendorf tubes were centrifuged at 14,000 x g for 5 minutes. The supernatant was transferred to new eppendorf tubes and the DNA was precipitated with 50 µl of sodium acetate (pH 5.5) and 500 µl of 100% isopropanol (Applied Biosystem Inc., Mississauga, ON). The eppendorf tubes were centrifuged at 14,000 x g for 15 minutes. The supernatant was discarded and the pelleted DNA was washed in 70% ethanol. The

eppendorf tubes were centrifuged at 14,000 x g for 5 minutes, the supernatant was removed and the DNA pellet air-dried. The DNA was resuspended in 50 µl of filter sterilized water.

PCR was performed on isolated DNA to detect human *NAIP*. Two sets of primers (A and B) were used to amplify exons 5-6 and 6-9, respectively. All *Naip* specific primers were obtained from Dr. Z. Yaraghi. Naip primer sequences and exon specificity are listed in table 1 (pg. 42). For primer set A: 6 µl of a 25mM deoxynucleotide solution (Gibco-BRL, Rockville, MD), 5 µl of 10 X PCR buffer (Perkin Elmer, Norwalk, CT), 2 µl of forward and reverse primer set A, 0.4 µl *Thermus aquaticus* (Taq) DNA polymerase enzyme (Gibco-BRL, Rockville, MD), and 33.6 µl of sterile water was added to 1 µl of sample DNA. The same PCR procedure was performed for primer set B with these exceptions: 4 µl of forward and reverse B primers and 29.3 µl of sterile water was added per 1 µl of DNA used. Aliquots containing wildtype mouse genomic DNA and sterile water were used as negative controls for each PCR procedure. An aliquot containing cloned human *NAIP* was used as a positive control for each PCR procedure. Each sample was incubated in a thermal cycler using the following program: 1 cycle of 94°C for 5 minutes, 35 cycles of 94°C for 2 minutes, 60°C for 30 seconds, 72°C for 1 minute, and one cycle of 72°C for 5 minutes. The PCR product was electrophoresed in a 1% agarose gel containing ethidium bromide. The DNA was visualized with an ultra violet light and an animal was considered transgenic when both sets of primers yielded a DNA band of the correct size.

2.1.3 Traumatic brain injury: Wildtype (Charles River, QC) and CMV *NAIP* C57/Bl6 mice (20-25 g) were randomized to control or trauma groups and subjected to blunt head trauma using a modified version of a previously described murine trauma model (63). The head of an anesthetized (1-5% halothane gas) mouse was placed under a teflon impounder and held in place

using a stereotactic apparatus. The tip of the impounder was placed on the head and a 50 g weight was dropped 20 cm so that a blunt injury was administered with a maximum point of impact -1.8 mm from the bregma. Animals developed apnea immediately post TBI, were placed on a 37^0C heating pad, and required administration of 100% oxygen for 2 minutes to stimulate breathing. Approximately 10% of the animals that underwent TBI procedure also demonstrated general seizure activity immediately following the weight drop. However, the mortality rate in both the sham and TBI group was less than 10%. Conscious animals were placed back in caging and allowed free access to food and water. Control animals underwent the same anesthetic and placement in the stereotactic apparatus as trauma animals but the weight was not dropped onto the animal's head. Wildtype mice were sacrificed 6, 24, 48 hours or 7 days following trauma. CMV *NAIP* mice were sacrificed 24 hours following TBI.

Animals whose brains were used for histology were sacrificed under pentobarbital anesthesia (25 mg/kg) and transcardially perfused with a 4% PFA (pH 7.6) solution. The brains were cryopreserved in a 15% sucrose phosphate buffered solution and stored at –80°C in an upright freezer. The cryopreserved brains were sectioned using a CRM cryosectioner into 10 µm sections and mounted on positively charged slides (Surgipath, Winnipeg, MB). Slides were stored at –20°C in an upright freezer.

Animals whose brains were used for biochemical analysis were decapitated under halothane anesthesia (5%). The brains were rapidly removed and placed on a chilled metal plate where the cortex and subcortical white matter under the site of maximum impact was removed. The tissue was cooled to –50°C in a solution of isopentane (Sigma-Aldrich, Missassauga, ON) and stored at –80°C in an upright freezer.

2.2 Apoptosis

2.2.1 In Situ End Labeling: Coronal sections of brain tissue were counter stained for comparative purposes using the general nuclear dye Hoechst 33258 (Bisbenzamide) and the ISEL procedure for visualization of fragmented nuclear DNA. Brain sections were simultaneously fixed and thawed by treating with 1% gluteraldehyde in 0.1M phosphate buffered saline (PBS) and washed thoroughly with PBS. The sections were permeabilized with methanol acetone (1:1), washed with PBS, and treated with proteinase K (20µl/ml) for 15 minutes. Sections were washed with distilled water for 30 minutes and incubated in the dark with Hoechst 33258 (0.05µl/ml) for 30 minutes. The sections were washed briefly and incubated in the dark at 37^0C with a buffered solution containing 2 mM copper cobalt (Boehringer Mannhein, Laval, QC), 10µM 16-d-UTP (Boehringer Mannheim, Laval, QC), and 25 units of terminal transferase enzyme (Boehringer Mannheim, Laval, QC) for one hour. The reaction was arrested by washing the sections briefly with PBS. The slides were incubated in the dark at room temperature with 4X saline sodium citrate buffer containing 2.5 µl/ml avidin-FITC for 30 minutes. The sections were briefly washed with PBS and protected with coverslips (Surgipath, Winnipeg, MB) treated with antifade solution (1 mg/ml p-phenylenediamine, 90% glycerol in PBS). A positive control for brain sections was prepared by incubating the brain tissue with 5 U/ml of DNAse I prior to terminal transferase treatment.

2.2.2 PCR Amplification of DNA Fragmentation and Agarose Gel Electrophoresis: This work was performed in the laboratory of Dr. J. M^{c}Manus by I. Rasquinha and was observed by Rachel Derrane. Nuclear DNA was extracted from non-perfused control and 24 hours post trauma cortex and subcortical white matter tissue. The tissue was homogenized in an equal

volume of 4^0C buffer containing 10 mM Tris-HCL, 25 mM EDTA, 100 mM NaCl (pH 8.0) with a polytron homogenizer at 10,000 rpm for 30 seconds. To each 100 µl of crude homogenate 1.25 ml of lysis buffer containing 10 mM Tris-HCL, 25 mM EDTA, 100 mM NaCl, 1% SDS (pH 8.0) was added. The solution was incubated at room temperature for 15 minutes and centrifuged for 15 minutes at 13,000 x g in a microcentrifuge at room temperature. The supernatant containing genomic DNA was transferred to fresh tubes and incubated at 60^0C for 1 hour with 100 µg/ml proteinase K. The DNA was precipitated at -20^0C overnight in a solution of 50% ethanol and 0.5 M NaCl. The DNA was pelleted following centrifugation at 13,000 x g at 4^0C. The ethanol was gently removed and the DNA was allowed to air dry for 30 minutes. The DNA was resuspended in 500 µl of TE buffer (10 mM Tris-HCL, 1 mM EDTA, pH 8.0) and purified with one phenol:chloroform (1:1) wash and one chloroform wash. Following centrifugation at 13,000 x g, the aqueous phase was removed and transferred to a clean tube. The ethanol precipitation was repeated and pelleted DNA was resuspended in 50 µl of sterile water.

Traditionally, freshly isolated fragmented DNA has been visualized directly on an agarose gel. In systems where apoptosis occurs asynchronously, the DNA fragments may not be visible. Ligation mediated detection of fragmented DNA uses PCR to selectively amplify the DNA ladder and allows visualization of the ladder on an agarose gel. A 0.5 µg aliquot of genomic DNA was mixed with 35µl of ligation mix (Clontech, Palo Alto, CA). The reaction mixture was heated to 55^0C and cooled over 1 hour to 10^0 C to allow the adaptor 24' mer oligonucleotide (5' - AGCACTCTCGAGCCTCTCACCGCA - 3') (Clontech, Palo Alto, CA) to anneal to the fragmented DNA. The reaction was incubated at 10^0C for 10 minutes and 0.5 µl of T4 DNA ligase was added (Clontech, Palo Alto, CA). The reaction was incubated at 16^0C overnight. For each sample a PCR reaction mixture was prepared as follows: 10µl 10X LM-PCR mix

(Clontech, Palo Alto, CA), 50-159 ng of adaptor-ligated DNA, 2 µl of 50 X advantage cDNA polymerase mix (Clontech, Palo Alto, CA), and sterile water to make up to 100µl (Clontech, Palo Alto, CA). Each sample was incubated in a thermal cycler using the following program: 1 cycle of 72^0 C for 8 minutes, 30 cycles of 94^0C for 1 minute followed by 72^0C for 3 minutes, and one cycle of 72^0C for 15 minutes. The PCR product was electrophoresed on a 1.2% agarose gel containing ethidium bromide. DNA ladder was visualized with a UV lamp.

2.2.3 Western Blot of Procaspase-3, PARP, and Naip: Changes in procaspase-3, PARP and in the cortex and subcortical white matter Naip following TBI were determined using standard Western blotting techniques and antibodies specific for these proteins. Brain tissue (approximately 250 µg) was homogenized on ice with a 1 cc syringe and 18 gauge needle in 500 µl of sucrose buffer containing 0.3 M sucrose, 1 mM EGTA, 25 mM NaCl, 15 mM Tris-HCL (pH 6.8), 0.5 mM DTT, 0.5 mM spermidine, 0.15 mM spermine, and 5 µg/ml aprotinin, leupeptin, and pepstatin. The homogenate was centrifuged at 4^0C for 20 seconds at 8,000 x g in a Hettich micro/rapid K centrifuge. The supernatant was discarded and the cell pellet was resuspended in 250 µl of the sucrose buffer. Cells were homogenized using a motor driven teflon pestle set at 3,000 rpm and a 2 ml tissue grinder. The homogenate was centrifuged at 4^0C for 20 seconds at 8,000 x g in a Hettich micro/rapid K centrifuge. The supernatant was removed from the pellet and centrifuged at 4^0C for 10 minutes at 13,000 x g in a Hettich micro/rapid K centrifuge. The supernatant containing the cytosolic proteins was removed and aliquoted on ice. To lyse the nuclear membrane, the pellet was resuspended in a high salt buffer containing 0.75 M NaCl, 0.05 M HEPES, 12.5% glycerol, 0.75 mM $MgCl_2$, 0.5 mM EGTA, 5 mM DTT, 1 mM PMSF, 2 µg/ml leupeptin, and 5µg/ml aprotinin. The suspension was vortexed 5 times for 10 seconds each. Between each vortex the sample was kept on ice for 5 minutes. The sample was

then centrifuged at 4^0C in a Hettich micro/rapid K centrifuge for 10 minutes at 13,000 x g. The supernatant containing the nuclear proteins was removed and aliquoted on ice. The cytosolic and nuclear protein concentration was determined using the Bradford protein assay. Bovine serum albumin was used as the protein standard (New England Biolabs, Mississauaga, ON). Protein samples of a known concentration were electrophoresed on a 12% polyacrylamide gel (procaspase-3) or on a 15-4% polyacrylamide gradient gel (PARP, Naip) (Bio Rad Laboratories, Hercules, CA) and transferred to a PVDF membrane (Millipore Corporation, Bedford, MA). The membranes were blocked overnight in a phosphate buffered saline containing 0.1% tween (PBS-T) and 5% skim milk. The membranes were incubated for 2 hours at room temperature in a solution of PBS-T and 5% milk containing the primary antibody. For the procaspase-3 Western a 1/1000 dilution of a polyclonal 0.2 mg/ml rabbit anti-mammalian procaspase-3 IgG stock solution was used (Santa Cruz Biotechnology, Santa Cruz, CA). A 1/1000 dilution of a monoclonal 1 mg/ml mouse anti-mammalian PARP IgG stock solution was used for the PARP Western (Chemicon International, Temecula, CA). For the Naip Western a 1/2500 dilution of a polyclonal 1 mg/ml rabbit anti-mouse Naip IgG stock solution was used (developed in house). The membrane was then thoroughly washed with PBS-T for an hour. The membrane was incubated for 1 hour at room temperature in PBS-T and 1% skim milk containing the appropriate secondary antibody conjugated to horseradish peroxidase. For procaspase-3 and Naip a 1/1500 dilution of a polyclonal 1 mg/ml donkey anti-rabbit IgG stock solution was used (Amersham Pharmacia Biotech, Piscataway, NJ). For the PARP Western a 1/1500 dilution of a polyclonal 1 mg/ml donkey anti-mouse IgG stock solution was used (Amersham Pharmacia Biotech, Piscataway, NJ). The membrane was washed thoroughly in PBS-T for 1 hour and the protein bands were visualized with ECL chemiluminescence onto X-ray film according to

manufacturer's instructions (Amersham Pharmacia Biotech, Piscataway, NJ). The protein band intensity was quantified by densitometry analysis using Molecular Analyst Software (Bio Rad Laboratories, Hercules, CA).

To ensure that the protein concentration in each sample was equal, positive control Westerns were preformed. The initial primary and secondary antibodies were removed by incubating the membrane at 50^0 C for 30 minutes with strip buffer containing 0.1M Tris-HCL (pH 6.7), 2% SDS, and 0.70% beta-mercaptoethanol. The membrane was then treated for 2 hours at room temperature with a 1/4000 dilution of a polyclonal 0.2 mg/ml rabbit anti-mouse α-catenin IgG stock solution (Amersham Pharmacia Biotech, Piscataway, NJ). The membrane was washed and incubated at room temperature for 1 hour with a 1/1500 dilution of donkey anti-rabbit IgG conjugated to horseradish peroxidase (Amershan Pharmacia Biotech, Piscataway, NJ). The protein band was visualized as described above.

2.3 Immunofluorescence

2.3.1 Identification of Apoptotic Neurons and Oligodendrocytes: Apoptotic cells in the cortex and subcortical white matter were identified using an ISEL / immunofluorescence double stain procedure with primary antibodies specific for proteins expressed by neurons and oligodendrocytes. Slides were subjected to 3 washes of PBS, 10 minutes per wash. To reduce background staining slides were treated with 10% normal blocking serum in PBS (serum is from the animal that the secondary antibody was raised in). For neurons and oligodendrocytes, slides were incubated with 10% donkey blocking serum for 20 minutes. The three PBS washes were repeated and the slides were incubated overnight at 4^0C with a solution of PBS and 0.3% triton-X 100 containing the primary antibody. To label neurons, a 1/50 dilution of a monoclonal 1

mg/ml mouse anti-human NeuN primary antibody stock solution was used (generous gift from Dr. Michael McBurney). To label oligodendrocytes, a 1/200 dilution of a monoclonal 1 mg/ml mouse anti-human MAG primary antibody stock solution was prepared (generous gift from Dr. John Bell). The slides were washed 3 times for 10 minutes each in PBS, and then incubated for three hours at room temperature with a solution of PBS and 0.3% triton-X 100 containing the secondary antibody. For both neurons and oligodendrocytes, a 1/200 dilution of a stock polyclonal 1.3 mg/ml donkey anti-mouse secondary antibody conjugated to the fluorchrome CY3 was used (Jackson ImmunoResearch Laboratories, Inc. West Grove, PA). The sections were washed 3 times for 10 minutes each in PBS. A modified version of the ISEL procedure was used in order to detect apoptotic cells and maintain the NeuN and MAG immunofluorescence stain. Slides were treated with a solution of methanol:acetone (1:1) for 4 minutes and then washed twice with PBS for 5 minutes. Sections were incubated with the mild detergent Neuropore (Trevigen, Gaithersburg, MD) for 30 minutes at room temperature and washed twice with deionized water for 15 minutes. Slides were incubated with the ISEL reaction mix at 37^0C for 1 hour and washed 3 times in PBS for 1 minute. Sections were incubated at room temperature for 30 minutes in the 2.5 μg/ml avidin-FITC solution, washed 3 times in PBS for 1 minute, and coverslipped with antifade mounting media. The double labeled sections were viewed using a fluorescent microscope (Zeiss Axiophot, Germany).

2.3.2 Detection of Tumor Necrosis Factor Alpha, activated microglia, murine and human NAIP: Immunofluorescence techniques were used to detect the presence of activated microglial cells, tumor necrosis factor-alpha (TNF-α), murine Naip, and human NAIP in the cerebral cortex. The sections were washed 3 times in PBS for 10 minutes each. The sections were

treated for 20 minutes with 10% normal blocking serum in PBS. For TNF-α, murine Naip, and human NAIP 10% goat blocking serum was used. For Cd11*b* (adhesion receptor expressed by activated microglia), 10% donkey blocking serum was used. Sections were washed 3 times in PBS for 10 minutes each. For human NAIP, slides were incubated with neuropore (Trevigen, Gaithersburg, MD) for 30 minutes at room temperature and washed twice in PBS for 15 minutes. Sections were then treated with undiluted polyclonal 1 mg/ml rabbit anti-human J2 antibody (developed in house) overnight at 4^0C. For all other immune staining, sections were incubated overnight at 4^0C with primary antibody diluted in a solution of PBS and 0.3% triton-X 100. For activated microglia, a 1/2 dilution of the 50 ug/ml stock monoclonal rat anti-mouse CD11*b* primary antibody was used (Developmental Studies Hybridoma Bank, Iowa City, IA). To detect TNF-α, a 1/100 dilution of the 1 mg/ml stock polyclonal rabbit anti-mouse TNF-α primary antibody was prepared (Genzyme Diagnostics, Cambridge, MA). Cerebral cortex cells expressing murine Naip were detected with a 1/25 dilution of the polyclonal 1 mg/ml stock rabbit anti-mouse α1.7 primary antibody (developed in house). Sections were washed 3 times for 10 minutes each with PBS. Slides were incubated for 3 hours at room temperature with secondary antibody diluted in a solution of PBS and 0.3% triton-X 100. For CD11*b*, a 1/200 dilution of a stock polyclonal 1 mg/ml biotinylated donkey anti-rat secondary antibody was prepared (Jackson ImmunoResearch Laboratories, Inc., West Grove, PA). For TNF-α, murine Naip, and human NAIP, a 1/100 dilution of a stock polyclonal 1 mg/ml goat anti-rabbit secondary antibody conjugated to FITC was used (Cedarlane Laboratories Ltd., Hornby, Ont.). Sections were washed 3 times for 10 minutes each. CD11*b* slides were incubated for 30 minutes in the dark at room temperature with a 2.5 *u*g/ml avidin-FITC solution and washed for 3 times 10 minutes in PBS. All sections were coverslipped with antifade, and stored in the dark. Sections

were viewed with a fluorescent microscope (Zeiss Axiophot, Germany) and fluorescent cells were counted using Northern Eclipse Software (Empix, Mississauga, ON).

2.3.3 Visualization of Tumor Necrosis Alpha Association with Neuronal Cells: A dual immunofluorescent staining procedure was used to visualize the association of TNF-α with cortical neurons following trauma. Sections were washed 3 times for 10 minutes each in PBS and incubated at room temperature with neuropore (Trevigen, Gaithersburg, MD) for 30 minutes. Slides were washed 3 times for 10 minutes each in PBS and blocked in 10% donkey blocking serum or 20 minutes. Sections were washed and incubated with the first primary antibody diluted in PBS + 0.3% triton X-100 overnight at 4^0C. For NeuN, a 1/50 dilution of a monoclonal 1 mg/ml mouse anti-human NeuN stock primary antibody was used (gift from Dr. Michael McBurney). Sections were washed 4 times for 5 minutes each with PBS and incubated for 3 hours at room temperature with the secondary antibody diluted in PBS + 0.3% triton X-100. For NeuN, a 1/200 dilution of a stock polyclonal 1.3 mg/ml donkey anti- mouse secondary antibody conjugated to the fluorchrome CY3 was used (Jackson ImmunoResearch Laboratories, Inc. West Grove, PA). Sections were washed 3 times for 10 minutes each and incubated at room temperature with 10% goat blocking serum for 20 minutes. Slides were washed and incubated overnight in the second primary antibody diluted in PBS + triton X-100. For TNF-α, a 1/100 dilution of a polyclonal 1 mg/ml stock rabbit anti-mouse TNF-α primary antibody was used (Genzyme Diagnostics, Cambridge, MA). Sections were washed 4 times for 5 minutes each in PBS and incubated for 3 hours at room temperature with the secondary antibody diluted in PBS + 0.3% triton X-100. For TNF-α, a 1/100 dilution of the 1 mg/ml stock polyclonal goat anti-rabbit secondary antibody conjugated to FITC was used (Cedarlane Laboratories Ltd., Hornby,

Ont.). Sections were washed, coverslipped with antifade and stored in the dark at -20^{0}C. Sections were viewed with a Zeiss fluorescent microscope (Axiophot, Germany).

2.4 Neurological Outcome Following TBI

2.4.1 Morris Water Maze Neurological Score: The effect of TBI on the spatial memory of wildtype and CMV *NAIP* transgenic C57/Bl6 mice was assessed using the Morris water maze test (119). The Morris water maze apparatus consisted of a large, white, circular pool 1.5 m in diameter and 0.60 m deep and a clear Plexiglass platform 15 cm in diameter. On each day the testing pool was refilled with water and maintained at a temperature of 23 +/- 1^{0}C. The platform was submerged approximately 2.5 cm below the surface of the water. The platform was stationed in the south position approximately 15 cm from the side of the pool. Transgenic and wildtype mice were randomized to sham or TBI procedure and allowed to recover for 48 hours. Mice were given five trials per day in the water maze over a five day period. For each trial, the mouse was placed in the water facing the wall at one of four randomly chosen locations separated by 90^O (designated north, south, east, and west). Mice were allowed to search for the submerged platform for 60 seconds per trial and the time to find the platform (latency time) was recorded. Mice that failed to find the platform within the 60 seconds were gently placed on the platform for 15 seconds. Mice were given 60 seconds to rest between trials. Once all five trials were completed, mice were towel-dried and placed in a cage under a heating lamp. The animals were then returned to their cages and given free access to food and water. The average latency time per day for each group was calculated.

2.5 Statistical Analysis

All data represent the mean +/- standard deviation of measurements from 3-6 mice from each experimental group. The differences between the groups were analyzed using one-way analysis of variance (ANOVA) and post hoc Tukey tests. Values of $p < 0.05$ were considered to be statistically significant.

Primer Name	*Naip* exon	Strand	Sequence
A	5	Forward	5' TCTGGGATTCAGTGCTTCTGCTG 3'
A	6	Reverse	5' CATTTGGCATGTTCCTTCCAAGG 3'
B	6	Forward	5' AAAGCCTCTGACGAGAGGATC 3'
B	9	Reverse	5' AAAAGAGTCCAGCCGTAGTTC 3'

Table 1: Exon location, strand location, and sequence of *NAIP* specific primers used in the PCR of total genomic DNA from offspring generated through mating of CMV NAIP overexpressing mice and wildtype mice.

3.0 Results

3.1 Apoptosis in the Cerebral Cortex of Wildtype C57/Bl6 Mice Following TBI

The ISEL stain and ligation mediated PCR amplification of DNA was used to probe damaged tissue for the presence of apoptotically cleaved DNA and to determine the time course of apoptosis following TBI. In pilot experiments, animal that had undergone control or trauma were sacrificed and the brains removed at 6, 24, 48 hours, or 7 days following the procedure. The brain was coronally sectioned anterior to posterior into 10 μm brain sections which were placed on slides. ISEL positive cells were observed in the brain section located directly below the impounder in our model of TBI (figure 1). The ISEL positive cells were predominantly observed in the cortex and subcortical white matter (cerebral cortex) following TBI (figure 1). Minimal ISEL positive cells were observed in the hippocampus or other subcortical structures. In subsequent experiments, ISEL positive cells were counted in three coronal sections of the cerebral cortex through the site of maximum impact in control, 6 hour, 24 hour, 48 hour, and 7 days post TBI brains and the results are represented graphically in figure 2. ISEL positive cells were not observed in other regions of the brain. Compared to control brains, the number of ISEL positive cells in the three sections was significantly increased in the cortex and subcortical white matter at 6, 24, and 48 hours following TBI (figure 2). At 7 days following TBI the number of ISEL positive cells in the region of the cortex that receives maximum impact (section 4, bregma −1.8 mm) was still significantly increased compared to control (figure 2). We observed that, compared to all other groups, the number of ISEL positive cells in the cortex and subcortical white matter peaked at 24 hours following TBI in the region directly under the site of maximum impact (figure 2). As the cell death that we observed occurred over the course of a week in a

localized area of the brain, we used a sensitive method to amplify the DNA fragmentation signal known as LM PCR. Figure 3 shows the presence of the characteristic fragmentation pattern in DNA extracted from the cortex and subcortical white matter at 24 hours following TBI. In contrast, DNA fragmentation was not detected in DNA extracted from cortex and subcortical white matter of control animals.

The expression of procaspase-3 and cleavage of PARP following TBI was detected using Western blot techniques with cytosolic protein from TBI and control cerebral cortex tissue and primary antibodies to either procaspase-3 or PARP. The densitometry of procaspase-3 protein bands from each group are represented graphically in Figure 4C. At 6 hours following TBI the level of 32 kDa procaspase-3 was significantly decreased in the cortex and significantly increased in the subcortical white matter compared to control (figure 4A and C). At 24 hours following TBI, the amount of procaspase-3 was still significantly decreased in the cortex compared to control and the amount of procaspase-3 was significantly decreased in the subcortical white matter compared to 6 hour post TBI (figure 4B and C). It had previously been reported that active caspase-3 specifically cleaves the 116 kDa DNA repair enzyme PARP into 89 kDa and 24 kDa fragments (128, 158). Thus, to determine if the decrease in procaspase-3 observed following TBI was associated with an increase in the active form of the enzyme, cleavage of PARP was assessed. The densitometry of the 116 kDa full length PARP protein and 89 kDa PARP fragment from each group is represented graphically in Figure 5 B1 and B2. Western blot analysis of nuclear protein extracts revealed that the amount of 116 kDa PARP was significantly decreased while the amount of the 89 kDa fragment is significantly increased in the cortex and subcortical white matter at 24 hours following TBI compared to control (figures 5 A, B1, and B2). The 105 kDa α-catenin was used as a loading control to ensure that equal amounts

of protein from each group were probed in the Western blots (figures 4 A and B and 5 A).

Given that the region of the cerebral cortex where ISEL positive cells were observed was known to contain a large population of neurons and oligodendrocytes, we postulated that these were the probable cell types undergoing cell death in our model of TBI. A double labeling immunofluorescent technique with the ISEL stain and primary antibodies to specific cell markers for neurons and oligodendrocytes was used to identify the dying cells. Using the double labeling procedure with an antibody directed against MAG, which is a specific cell marker for oligodendrocytes, revealed that oligodendrocytes were predominantly located in the subcortical white matter (figure 6 A). The ISEL positive cells in the subcortical white matter also appeared to be stained with the anti MAG antibody (figure 6 B and C). A few of the ISEL positive cells in the cortex also stained positive with the MAG antibody. However, using the double labeling procedure with an antibody directed against NeuN protein, which is a specific cell marker for neurons, the majority of the ISEL positive cells in the cortex appeared to be stained with the anti NeuN antibody (figures 6 D, E and F).

3.2 Inflammation in the Cerebral Cortex of Wildtype C57/Bl6 Mice following TBI

To determine if inflammation in the cerebral cortex occurred in our model of TBI, we attempted to detect activated microglia and TNF-α in the brain and determine the time course for each following trauma. Activated microglia were identified using an immunofluorescent staining procedure with a primary antibody to CD11*b*, an adhesion receptor specifically expressed on the activated resident inflammatory cells (181). The amoeboid shaped activated microglia were predominantly observed in the injured region of cerebral cortex following TBI (figure 7 A and B). In contrast, no activated microglia were observed in brain sections from control animals

(figure 7 C). The number of activated microglia present in a region of damaged cerebral cortex at each time point following TBI is expressed graphically in figure 7 F. The number of activated microglia was significantly increased compared to control at 6, 24, and 48 hours following TBI with maximum microglial activation occurring at 24 hours following TBI (figure 7 F). A double labeling immunofluorescent technique with primary antibodies specific to TNF-α, and NeuN was used to detect the presence of TNF-α and the association of TNF-α with neurons. As figure 7 D demonstrates, TNF-α (green stain) was observed in the injured cortex and subcortical white matter and was often associated with the cell membrane of neurons (red stain) following TBI. TNF-α staining was observed in the extracellular space and did not appear within the cytosol of cells in the cerebral cortex. No TNF-α staining was observed in the cerebral cortex from control animals (figure 7 E). The amount of TNF-α present in a region of damaged cerebral cortex at each time point following TBI is represented graphically in figure 7 E. Compared to the control group, the amount of TNF-α was significantly increased at 6 hours, 24 hours, 48 hours, and 7 days following TBI (figure 7 F). Maximal levels of TNF-α in the cerebral cortex was observed at 6 and 24 hours following TBI (no significant difference in the level of TNF-α at 6 and 24 hours post TBI) (figure 7 F).

3.3 Expression of Naip following TBI

We attempted to determine the effect of TBI on the expression of endogenous mouse Naip in our model. Changes in the expression of Naip following TBI were detected using Western blot and immunofluorescent techniques with a primary antibody specific for murine Naip. The densitometry of the Naip protein bands from each group are represented graphically in figure 8

C. The number of cells expressing Naip in a section of cerebral cortex is expressed graphically in figure 9 D. Western blot analysis of cytosolic protein extracts reveal that at 6 hours following TBI, the level of Naip and associated fragments in the injured cortex and subcortical white matter was significantly increased compared to control (figure 8 A and C). However, at 24 hours following TBI, the level of Naip and associated fragments in the cortex and subcortical white matter appeared to be significantly decreased compared to control (figure 8 B and C). The 105 kDa α-catenin was used as a loading control to ensure that equal amounts of protein from each group were probed in the Western blots (figures 8 A and B). Immunofluorescent staining techniques revealed that at 6 hours following TBI the number of cells expressing Naip in the injured cerebral cortex was significantly increased compared to control, with the majority of cells displaying a diffuse staining pattern throughout the cytosol and nucleus (figure 9 A and B and D). The number of cells expressing Naip in the cortex at 24 hours following TBI was significantly decreased compared to 6 hours post trauma but was still significantly increased compared to control (figure 9 A, B, C, and D). At 24 hours post TBI, the number of cells expressing Naip in the subcortical white matter was not significantly different than in control subcortical white matter (figure 9 D). Naip expression appeared in the cytosol and nucleus of cells 24 hours post TBI, but the staining pattern was not as diffuse as that observed at 6 hours following trauma.

3.4 Detection of the CMV NAIP Construct and Protein in Transgenic C57/Bl6 Mice

Mice that express human *NAIP* were used to determine if an overexpression of the IAP could attenuate cell death in the cerebral cortex following TBI. Transgenic mice were identified from wildtype litter mates using a PCR technique with primers specific for *NAIP* exons 5-6 and 5-9.

Thirty cycles of PCR were used to visualize the 380 bp exon 5-6 specific product and the 840 bp exon 5-9 specific product from the genomic DNA of transgenic animals (figure 10 A). Neither PCR product was present in the genomic DNA from wildtype litter mates. As a positive control, the cloned human *NAIP* gene was used in both PCR procedures (lane P, figure 10 A). To ensure that the primers were specific for human *NAIP*, wildtype mouse genomic DNA was used in both PCR procedures as a negative control (lane N_1, figure 10 A). A "blank" PCR reaction containing no DNA was used to ensure that components of each PCR mixture were not contaminated (lane N_2, figure 10 A).

Immunofluorescent techniques with a primary antibody specific for human NAIP was used to detect the presence of this protein in the cerebral cortex of transgenic mice. As shown in figure 10 B, NAIP appeared to be expressed in neuron-like cells throughout the cortex of transgenic mouse brain (figure 10 B). NAIP expression was also detected in both oligodendrocyte-like cells (small round cells) and astrocyte-like cells (larger, star shaped cells) throughout the subcortical white matter of transgenic brain (figure 10 D). In contrast, NAIP positive cells were absent in the cortex and subcortical white matter of wildtype animals (figure 10 C and E).

3.5 Apoptosis in the Cerebral Cortex of Transgenic C57/Bl6 Mice Following TBI

We determined the effect of overexpression of NAIP on cell survival, DNA fragmentation, procaspase-3 expression, and PARP cleavage in the brain following TBI. The ISEL stain was used to identify cells with fragmented DNA in sections of brain from control and 24 hour post TBI wildtype and NAIP transgenic mice. The number of ISEL positive cells in the cortex and subcortical white matter from each group are represented graphically in figure 11. In the transgenic cortex and subcortical white matter, the number of ISEL positive cells at 24 hours

post TBI was significantly decreased compared to the number observed at the same time point in the wildtype cortex (figure 11). Most notably, the number of ISEL positive cells in the subcortical white matter at 24 hours post TBI was not significantly different than the number observed in control subcortical white matter (figure 11).

Western blot techniques were used with primary antibodies to procaspase-3 and PARP to determine the effect of NAIP overexpression on procaspase-3 expression and PARP cleavage in samples of cortex and subcortical white matter following TBI. Densitometry of the procaspase-3 protein band from each group is represented graphically in figure 12 C. In both wildtype and transgenic animals at 24 hours post TBI, expression of procaspase-3 in the cortex was significantly decreased compared to control (figure 12, A, B, and C). However, at 24 hours following trauma the expression of procaspase-3 in the subcortical white matter from transgenic brain was not significantly different than the expression of procaspase-3 in control subcortical white matter (figure 12 B and C). Densitometry of the 116 kDa full length PARP and 89 kDa PARP fragment from each group are represented graphically in figure 13 C1 and C2. The amount of PARP cleavage observed in transgenic cortex and subcortical white matter at 24 hours post TBI was significantly decreased compared to that observed in wildtype cortex from the same time point (figure 13 A, B, C1, and C2). The 105 kDa α-catenin protein was used as a loading control to ensure that equal amounts of protein from each group were probed in the procaspase-3 and PARP Western blot (figures 12 and 13).

3.6 Inflammation in the Cerebral Cortex of CMV NAIP Transgenic C57/Bl6 Mice Following TBI

Expression of CD11*b* and TNF-α in the cerebral cortex of CMV *NAIP* mice following TBI was

investigated to determine if a similar response to TBI occurred in transgenic and wildtype brains. Immunofluorescent staining with a primary antibodies to CD11*b* and TNF-α were used to detect the presence of activated microglial cells and expression of TNF-α in the cerebral cortex. The number of activated microglia and the expression of TNF-α in the cerebral cortex and subcortical white matter is expressed graphically in figure 14. The increase in the expression of CD11*b* and TNF-α induced by trauma at 24 hours post TBI was not significantly different between wildtype and transgenic mice (figure 14).

3.7 *Neurological Outcome in Wildtype and CMV NAIP Transgenic C57/Bl6 Mice Following TBI*

We examined the effect of NAIP overexpression on neurological outcome in our model of TBI. To test neurological outcome in transgenic and wildtype C57/Bl6 mice that had undergone the control or TBI procedure, a modification of the Morris water maze was used (119). Transgenic and wildtype mice that had undergone control or TBI procedure were allowed to recover for 48 hours. Animals were then given five trials per day in the water maze over a five day period. Latency times for each trial were recorded and the average for each day is represented graphically in figure 15. The average latency time for each group appeared to decrease over the first four days of the water maze testing period (figure 15). However, due to the large standard deviations in latency time in each group, none of the average latency times between transgenic and wildtype groups were significantly different.

Figure 1: ISEL positive cells in the cerebral cortex of wildtype C57/Bl6 mice. The ISEL procedure was used to detect fragmented DNA in injured brain tissue. ISEL positive cells were observed in the subcortical white matter (A, arrows) and the cortex (B, arrows) (100 X magnification). The staining in the TBI brains was compared to the staining observed in control (no trauma) white matter (C) and cortex (D) (100 X magnification). (n = 5 mice / group)

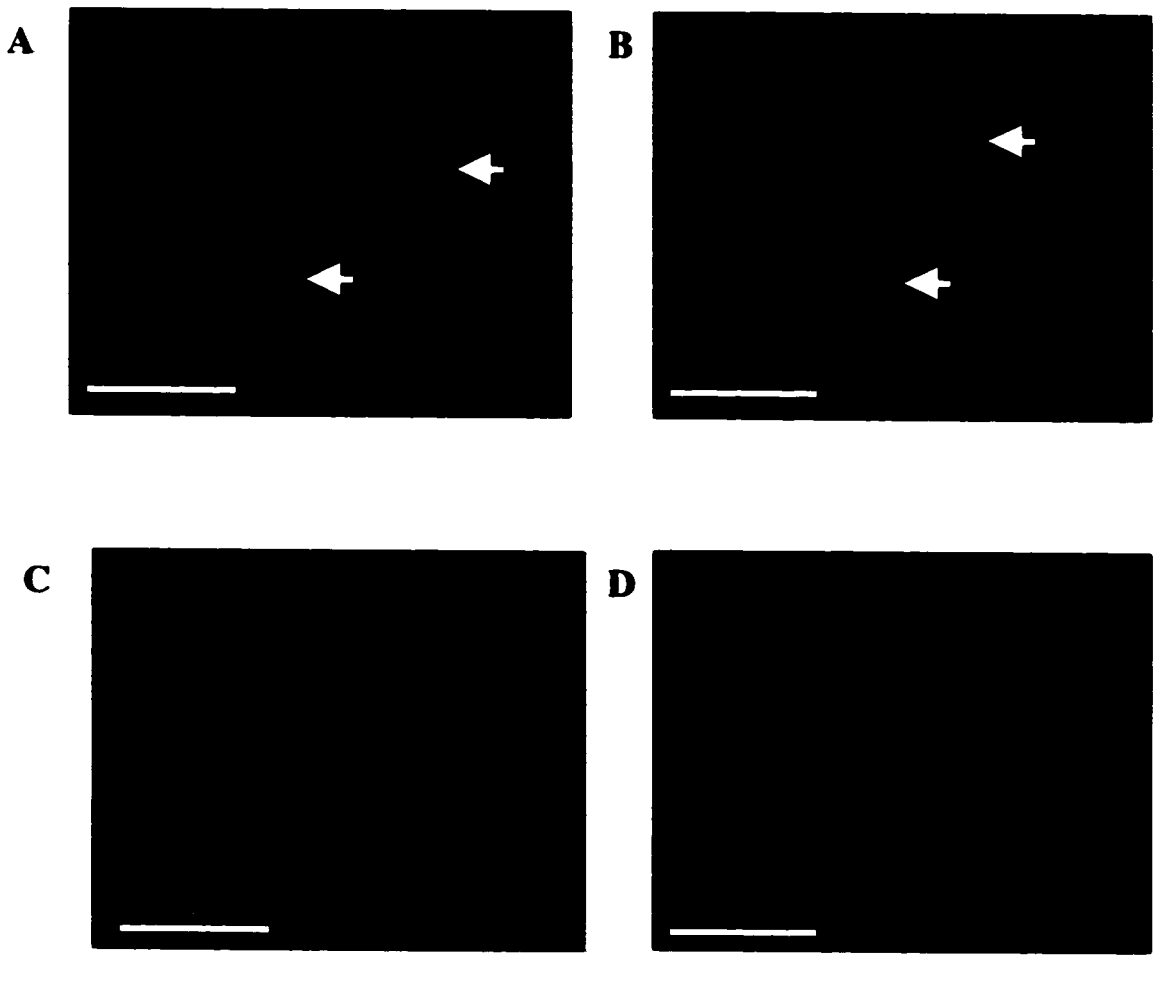
A
B
C
D

Figure 2: Counts of ISEL positive cells in the subcortical white matter (A) and cortex (B) from wildtype mice following TBI. ISEL positive cells were counted in three coronal sections through the impact region from sham, 6 hour, 24 hour, 48 hour, and 7 days post TBI mice. *$p < 0.05$ compared to control, #$p < 0.05$ compared to all other groups. ($n = 5$ mice / group)

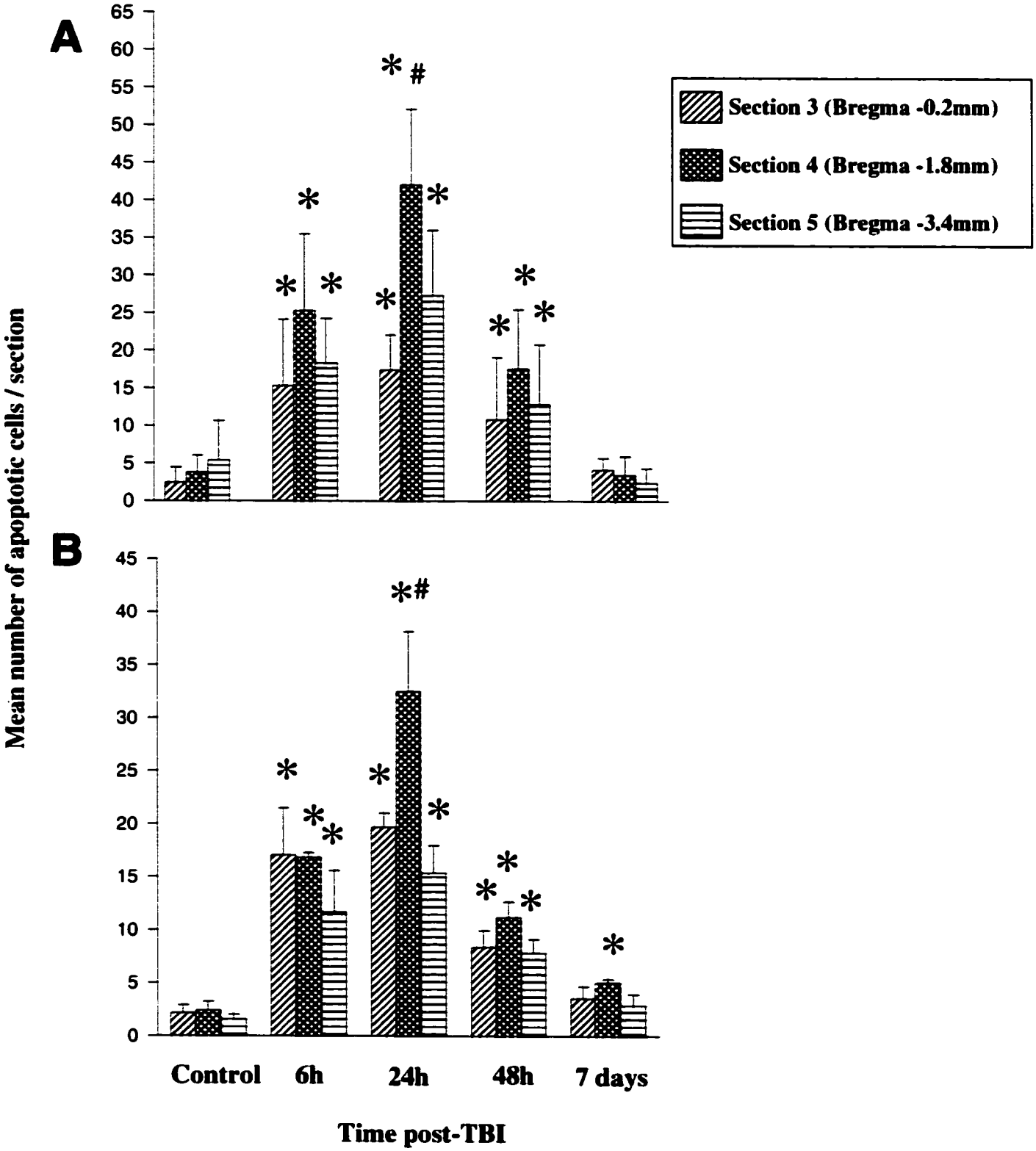
A
B
Section 3 (Bregma -0.2mm)
Section 4 (Bregma -1.8mm)
Section 5 (Bregma -3.4mm)
Mean number of apoptotic cells / section
Control
6h
24h
48h
7 days
Time post-TBI

Figure 3: Ligation mediated PCR amplification of fragmented DNA in samples of brain from wildtype C57/Bl6 mice. Using specific adaptor oligonucleotides, DNA cleaved between nucleosomes in brain samples was amplified after a total of 30 cycles of PCR (2 samples / group are shown). Lane L designates the SalI digested lambda DNA ladder used for the molecular weight marker. The laddering pattern characteristic of internucleosomal DNA cleavage was visible in samples of cortex (C) and subcortical white matter (W) at 24 hours following trauma. The DNA ladder was not visualized in samples of cortex or subcortical white matter removed from control brains (no trauma). Brain samples pooled from 5 mice.

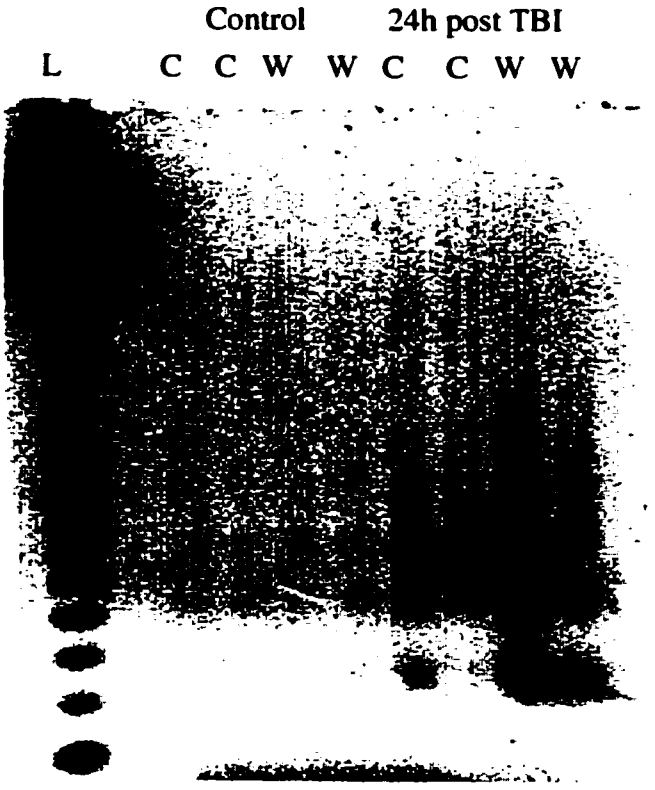
Control
24h post TBI
L
C C W W C C W W

Figure 4: Expression of procaspase-3 protein, detected using Western blot techniques, in wildtype C57/Bl6 brain. Western immunoblots of procaspase-3 protein were measured in samples of brain taken from control animals (no trauma) and animals at 6 hours (A) and 24 hours (B) following trauma [control cortex (CC) and subcortical white matter (CW), trauma cortex (TC) and subcortical white matter (TW)]. The density of the protein band in the TBI groups is represented as a percentage of the optical density of the protein band measured in the respective control group (C). *$p < 0.05$ compared to control, #$p < 0.05$ compared to 6h post TBI. ($n = 5$ mice / group)

A

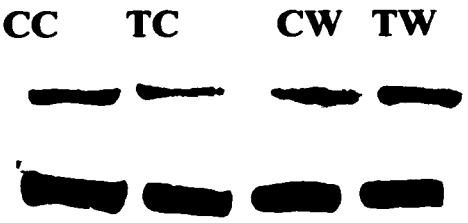

32 kDa

105 kDa α-catenin

B

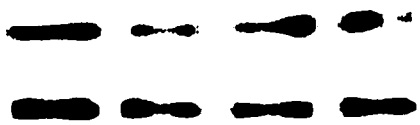

32 kDa

105 kDa α-catenin

C

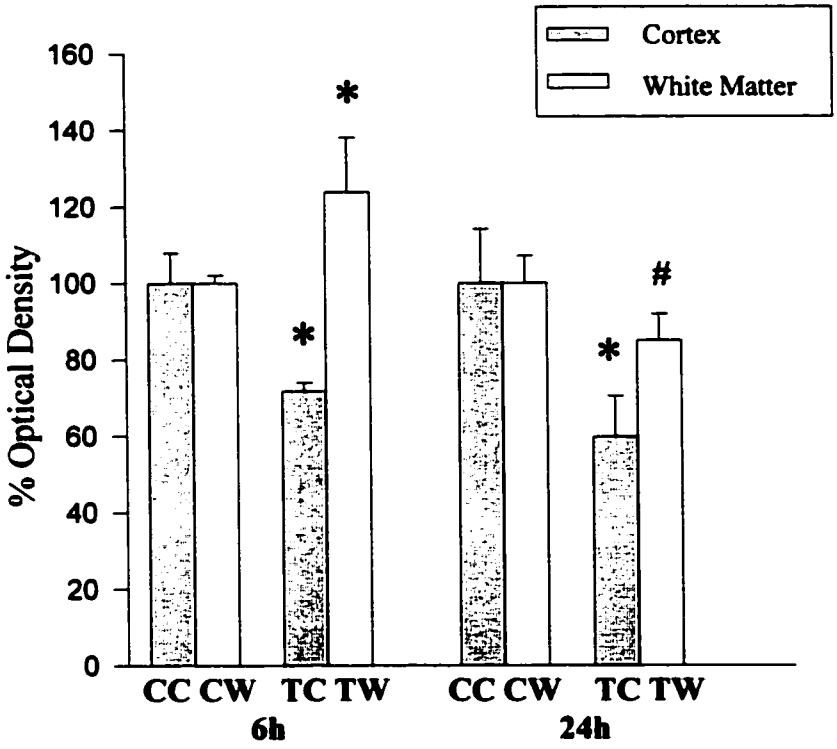

Time post TBI

Figure 5: Cleavage of PARP, detected using Western blot techniques, in wildtype C57/Bl6 brain. The full length PARP protein and the PARP fragment were measured in control (no trauma) cortex (CC) and subcortical white matter (CW), at 24 hours post trauma in the cortex (TC), and at 24 hours post trauma in the subcortical white matter (TW) (A). Density of the full length PARP protein (B1) and PARP fragment (B2) band in the TBI groups is represented as a percentage of the optical density of the protein band measured in the respective control group. *$p < 0.05$ compared to control. ($n = 5$ mice / group)

A

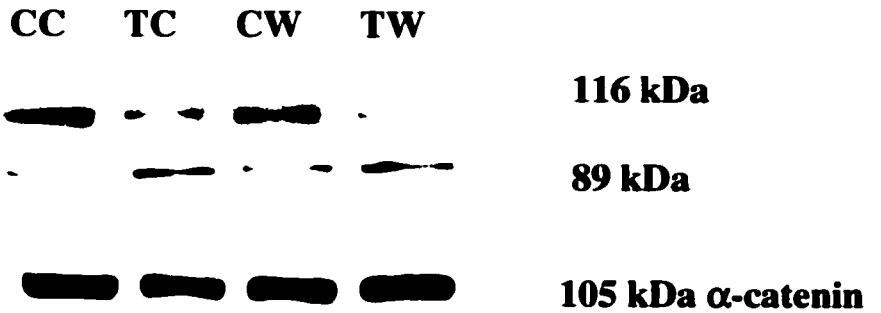
CC
TC
CW
TW
116 kDa
89 kDa
105 kDa α-catenin

B1

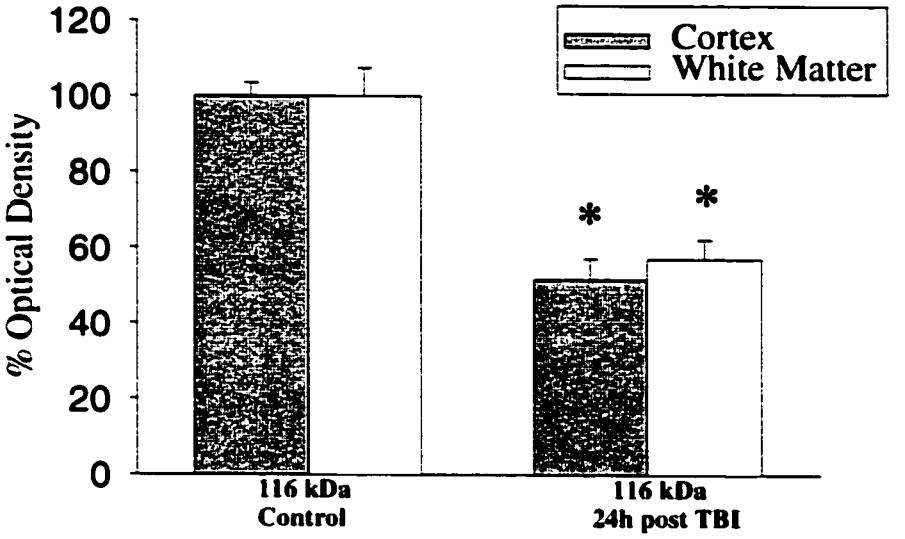
120
100
80
60
40
20
0
% Optical Density
Cortex
White Matter
*
*
116 kDa
Control
116 kDa
24h post TBI

B2

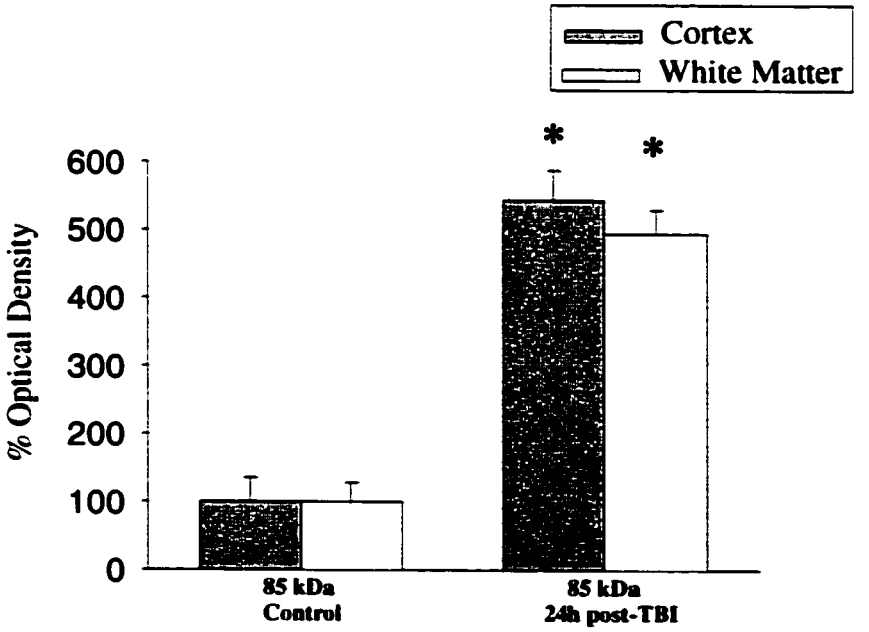
Cortex
White Matter
600
500
400
300
200
100
0
% Optical Density
*
*
85 kDa
Control
85 kDa
24h post-TBI

Figure 6: Identification of ISEL positive subcortical white matter oligodendrocytes and cortical neurons following TBI. Immunoflourescent staining of myelin associated glycoprotein (MAG) labels oligodendrocytes in the subcortical white matter and cortex (A, 10 X magnification). Cells that are ISEL positive within the subcortical white matter (B, arrow) also stain with MAG (C, arrow) (100 X magnification). Immunofluorescent staining for neuronal nuclear protein (NeuN) labels neurons in the cortex (D, 10 X magnification). Cells that are ISEL positive within the cortex (E, arrows) also stain with NeuN (F, arrows) (100 X magnification). (n = 5 mice / group)

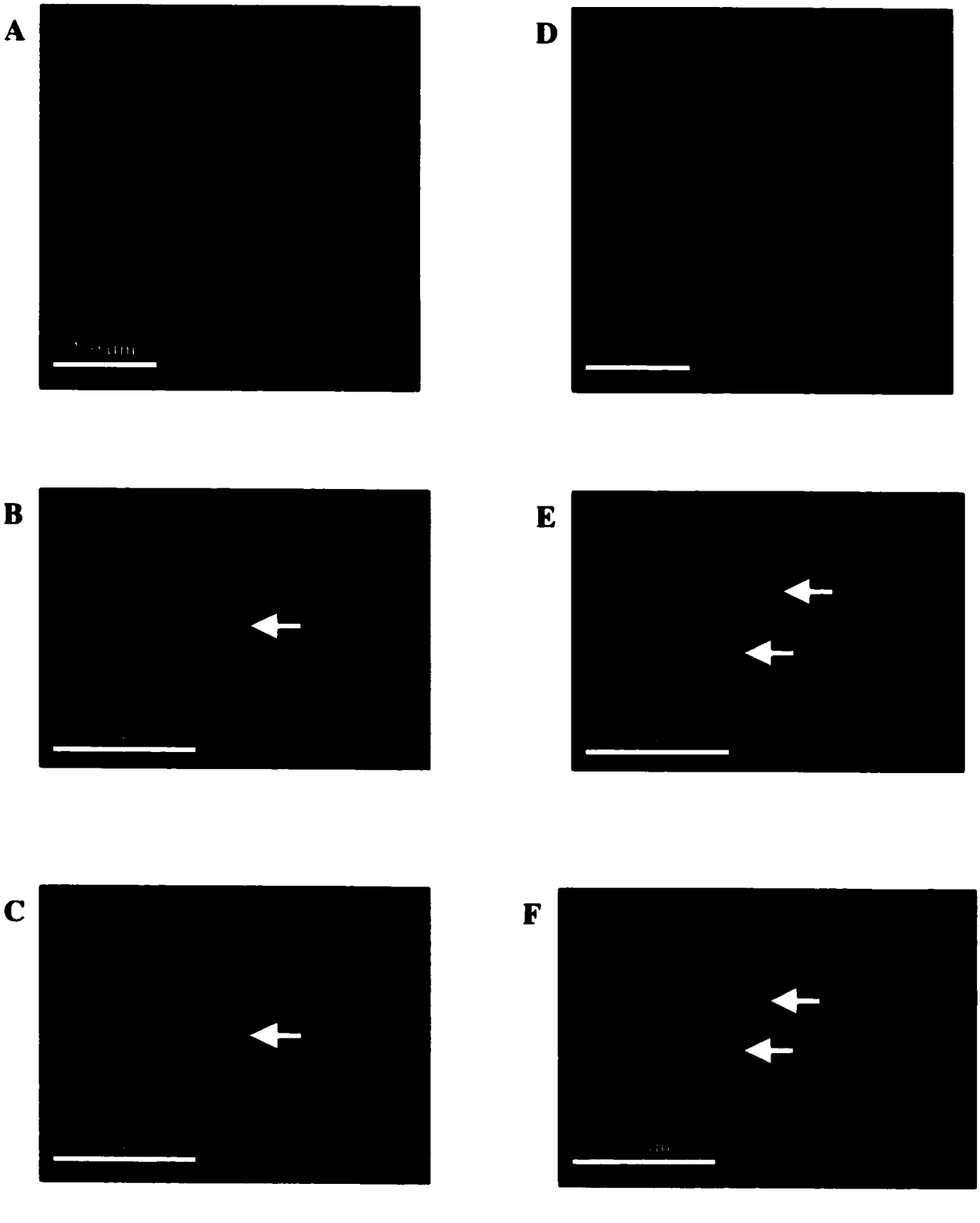
A
D
B
E
C
F

Figure 7: Expression of CD11*b* and TNF-α in wildtype C57/Bl6 cerebral cortex. Brain sections from the injured region of wildtype and transgenic animals were stained for the presence of the activated microglial marker CD11*b*. Activated microglia were observed in the injured region of the cortex (A, 10 X magnification) and subcortical white matter (B, 100 X magnification) following trauma. The staining in the trauma brains was compared to the staining observed in the cerebral cortex from the control animals (no trauma) (C, 10X magnification) to estimate the levels of background. Brain sections from wildtype animals were stained for the presence of TNF-α. TNFα was observed in the injured region of the cortex and subcortical white matter following TBI. TNF-α was often associated with neurons in the cortex (D, arrows, 100 X magnification) following TBI. The staining in the trauma brains was compared to the staining observed in the cerebral cortex from control animals (no trauma, stained for the presence of CD11*b*) (E, 10 X magnification). The number of activated micrglia and the level of TNF-α in a 10μm section of injured cerebral cortex from wildtype animals is represented graphically (F). *$p < 0.05$ compared to control. (n = 5 mice / group)

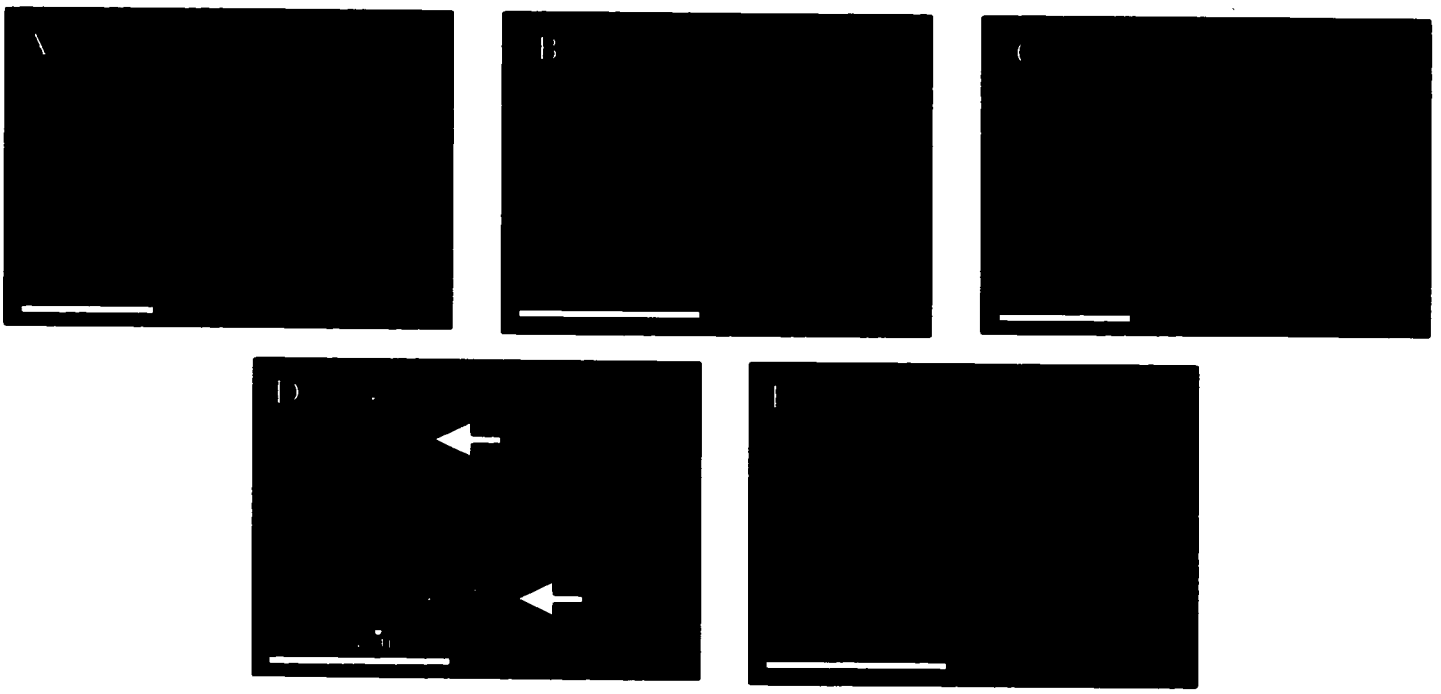

F

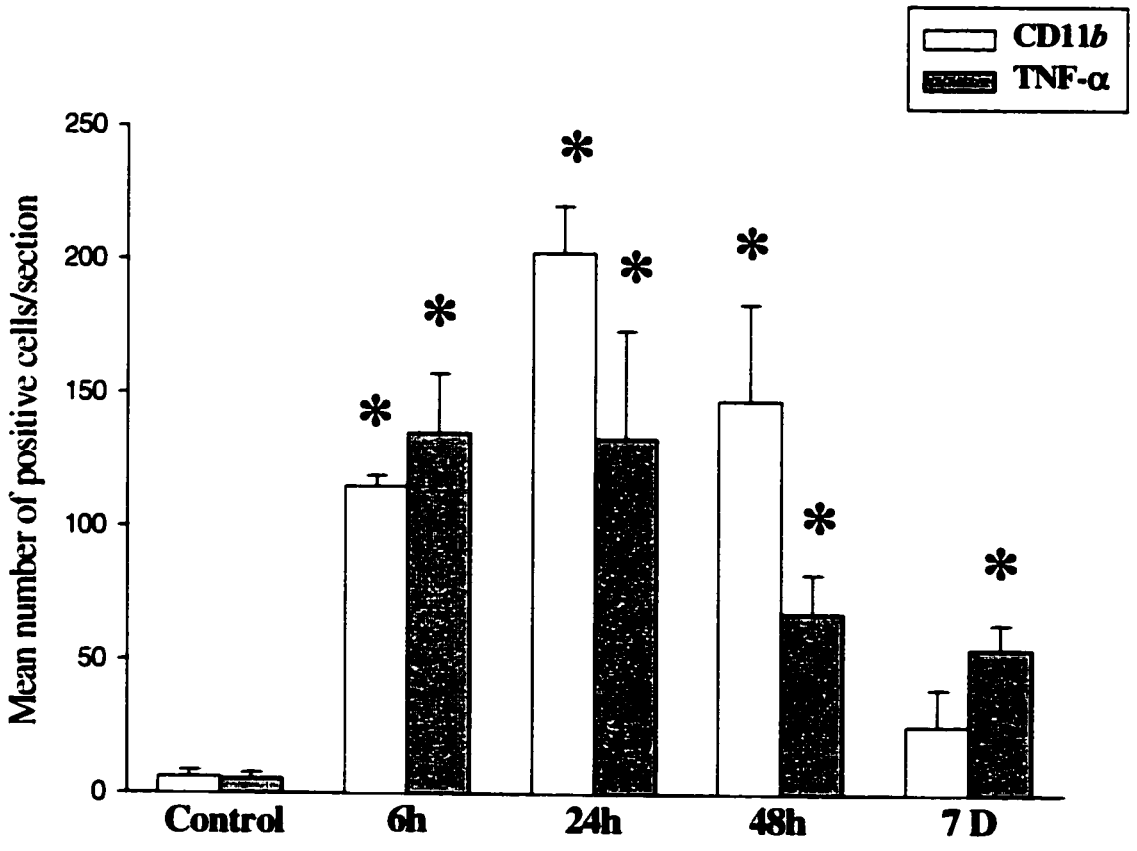
CD11b
TNF-α
Mean number of positive cells/section
250
200
150
100
50
0
Control
6h
24h
48h
7 D
Time post-TBI

Figure 8: Expression of Naip, detected using Western blot techniques, in wildtype C57/Bl6 brain. Expression of Naip and associated fragments were measured in brains from control (no trauma) animals, and at 6 hours (A) and 24 hours (B) following trauma [control cortex (CC) and subcortical white matter (CW), trauma cortex (TC) and subcortical white matter (TW)]. Density of the full length Naip bands are represented graphically as a percentage of the optical density of the protein band measured in the control group (C). *$p < 0.05$ compared to control, #$p < 0.05$ compared to 6 hour post TBI group. ($n = 5$ mice / group)

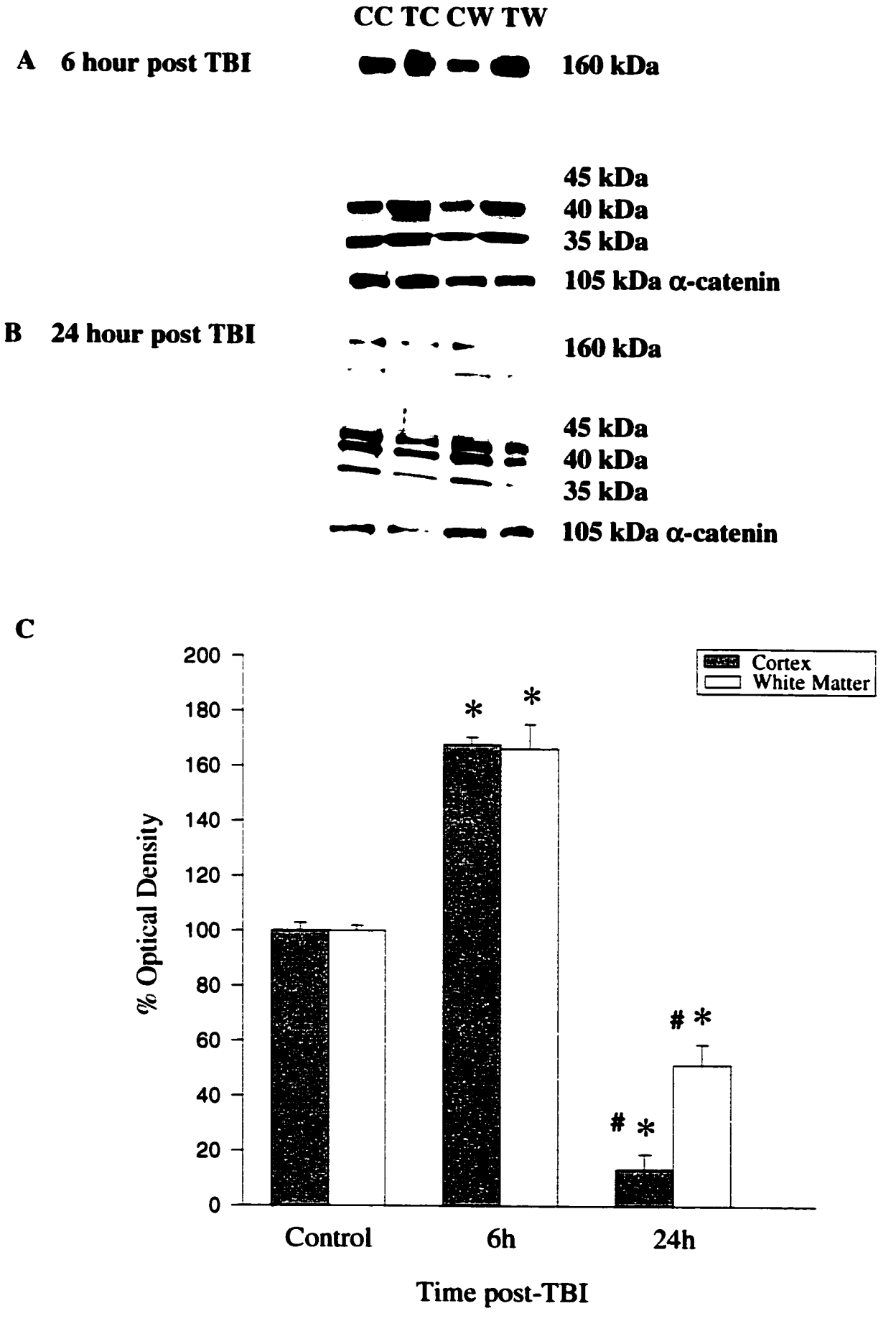
CC TC CW TW
A 6 hour post TBI
160 kDa
45 kDa
40 kDa
35 kDa
105 kDa α-catenin
B 24 hour post TBI
160 kDa
45 kDa
40 kDa
35 kDa
105 kDa α-catenin
C
Cortex
White Matter
% Optical Density
200
180
160
140
120
100
80
60
40
20
0
*
*
*
*
Control
6h
24h
Time post-TBI

Figure 9: Expression of Naip, detected using immunofluorescence techniques, in C57/Bl6 wildtype brain. Naip positive cells in sections of cerebral cortex from control (A, no trauma), 6 hours post TBI (B), and 24 hours post TBI (C) (100 X magnification). The number of positive cells observed in 10μm sections of the injured cerebral cortex from control, 6 hours post TBI, and 24 hours post TBI brains are represented graphically (D). *$p < 0.05$ compared to control, #$p < 0.05$ compared to 6 hour post TBI group. ($n = 5$ mice / group)

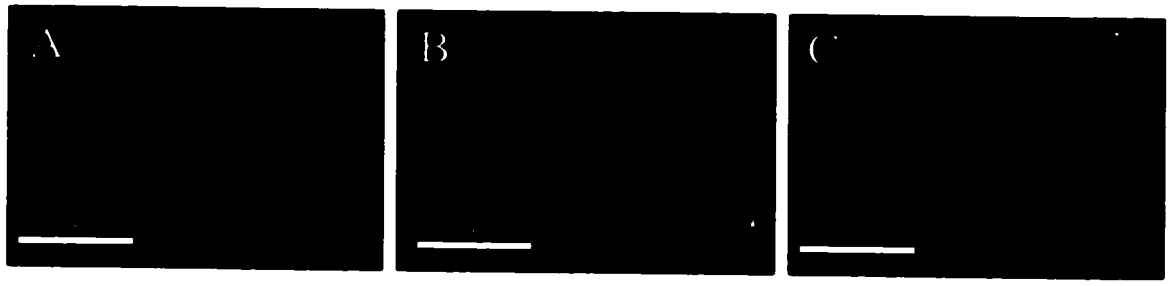
A
B
C

D

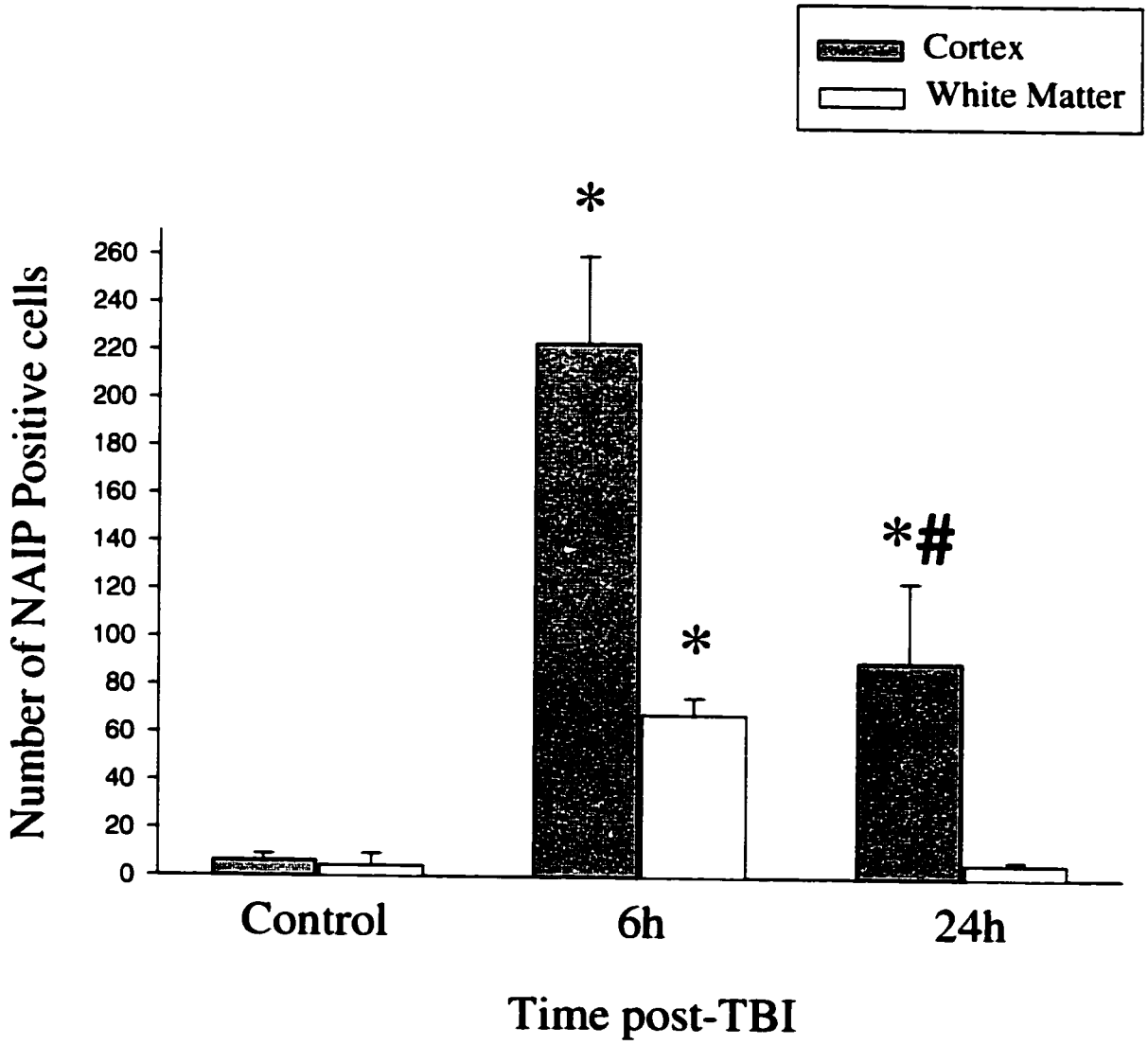
Cortex
White Matter
Number of NAIP Positive cells
260
240
220
200
180
160
140
120
100
80
60
40
20
0
*
*
*#
Control
6h
24h
Time post-TBI

Figure 10: Detection and expression of *NAIP* and in CMV *NAIP* C57/ Bl6 mice. Using two sets of specific primers, *NAIP* was amplified in the genomic DNA from tail samples of CMV *NAIP* transgenic pups and wildtype litter mates following 30 cycles of PCR. Lane N1and N2 designate the wildtype mouse genomic DNA and "blank" negative controls, respectively. Lane P designates the cloned *NAIP* positive control. Lane M designates the 1 kb ladder used for the molecular weight marker. The remaining lanes represent DNA from separate litter mates (wildtypes and heterozygotes for *NAIP* transgene). Aliquots were electrophoresed on a 1% agarose gel to resolve the expected 380 bp (amplification of *NAIP* exons 5 - 6) and 840 bp (amplification of *NAIP* exons 5 - 9) fragments. Expression of the NAIP protein in the cerebral cortex from transgenic animals was detected using immunofluorescent techniques. NAIP positive cells were observed throughout sections of cortex (B, 20 X magnification) and subcortical white matter (D, 100 X magnification) from transgenic animals. No cellular staining for NAIP was observed in the cortex (C, 20 X magnification) or subcortical white matter (E, 100 X magnification) in sections of brain from wildtype litter mates.

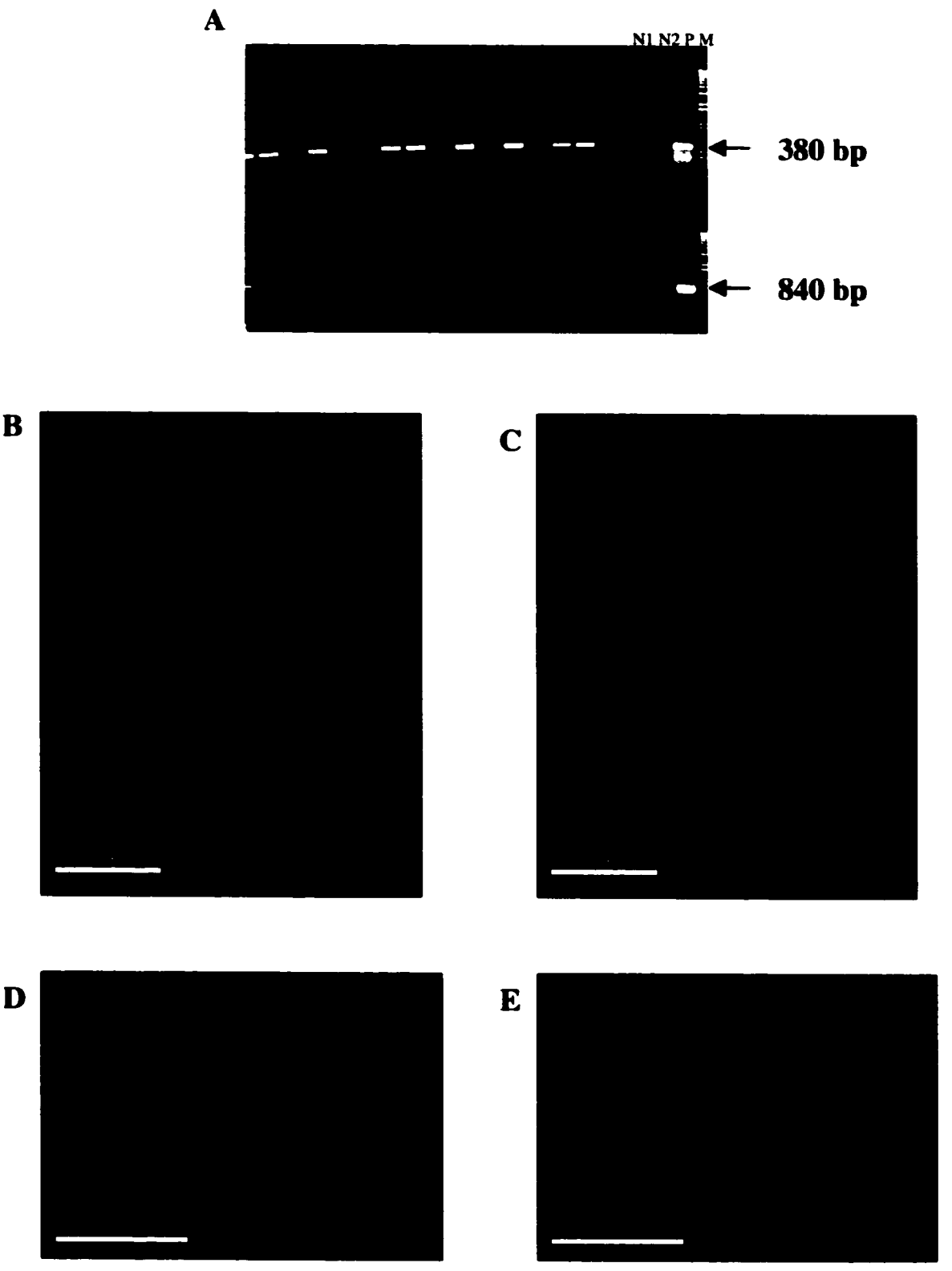
A
N1 N2 P M
380 bp
840 bp
B
C
D
E

Figure 11: Counts of ISEL positive cells in the subcortical white matter (A) and cortex (B) of CMV *NAIP* and wildtype C57/Bl6 mice. The number of ISEL positive cells in three coronal sections through the impact region from control (no trauma) and 24 hour post TBI wildtype and transgenic groups. *$p < 0.05$ compared to control, #$p < 0.05$ compared to all other groups. ($n =$ 5 mice / group).

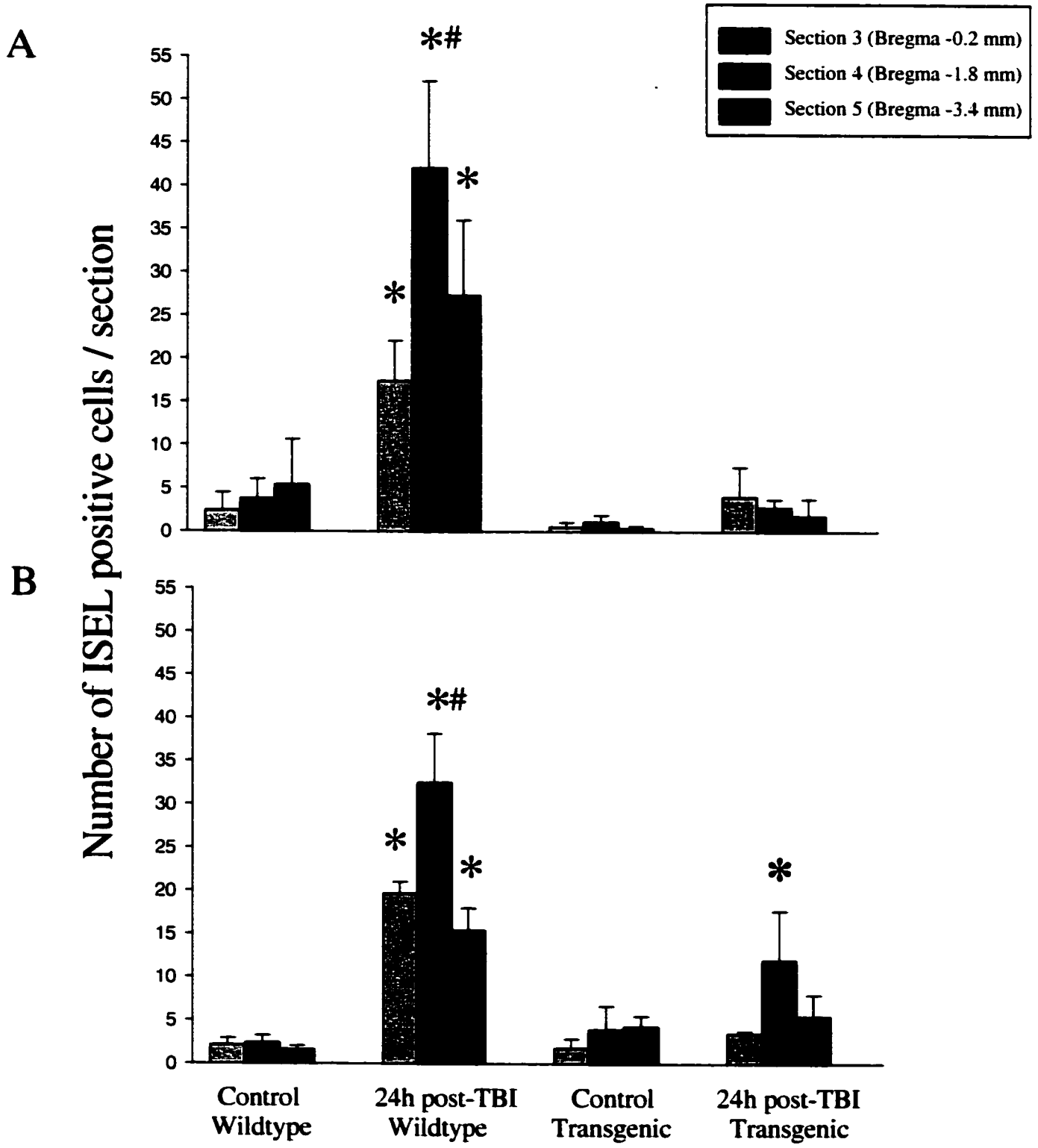
A
B
Section 3 (Bregma -0.2 mm)
Section 4 (Bregma -1.8 mm)
Section 5 (Bregma -3.4 mm)
Number of ISEL positive cells / section
55
50
45
40
35
30
25
20
15
10
5
0
*#
*
*
*
*#
*
*
*
Control Wildtype
24h post-TBI Wildtype
Control Transgenic
24h post-TBI Transgenic

Figure 12: Expression of procaspase-3 protein, detected using Western blot techniques, in wildtype and CMV *NAIP* C57/Bl6 brains. Procaspase-3 protein was measured in control (no trauma) cortex (CC) and subcortical white matter (CW) and 24 hour post trauma cortex (TC) and subcortical white matter (TW) in both wildtype (A) and CMV *NAIP* transgenic (B) animals. The density of the protein band in the TBI groups is represented as a percentage of the optical density of the protein band measured in the respective control group (C). *$p < 0.05$ compared to control. (n = 5 mice / group)

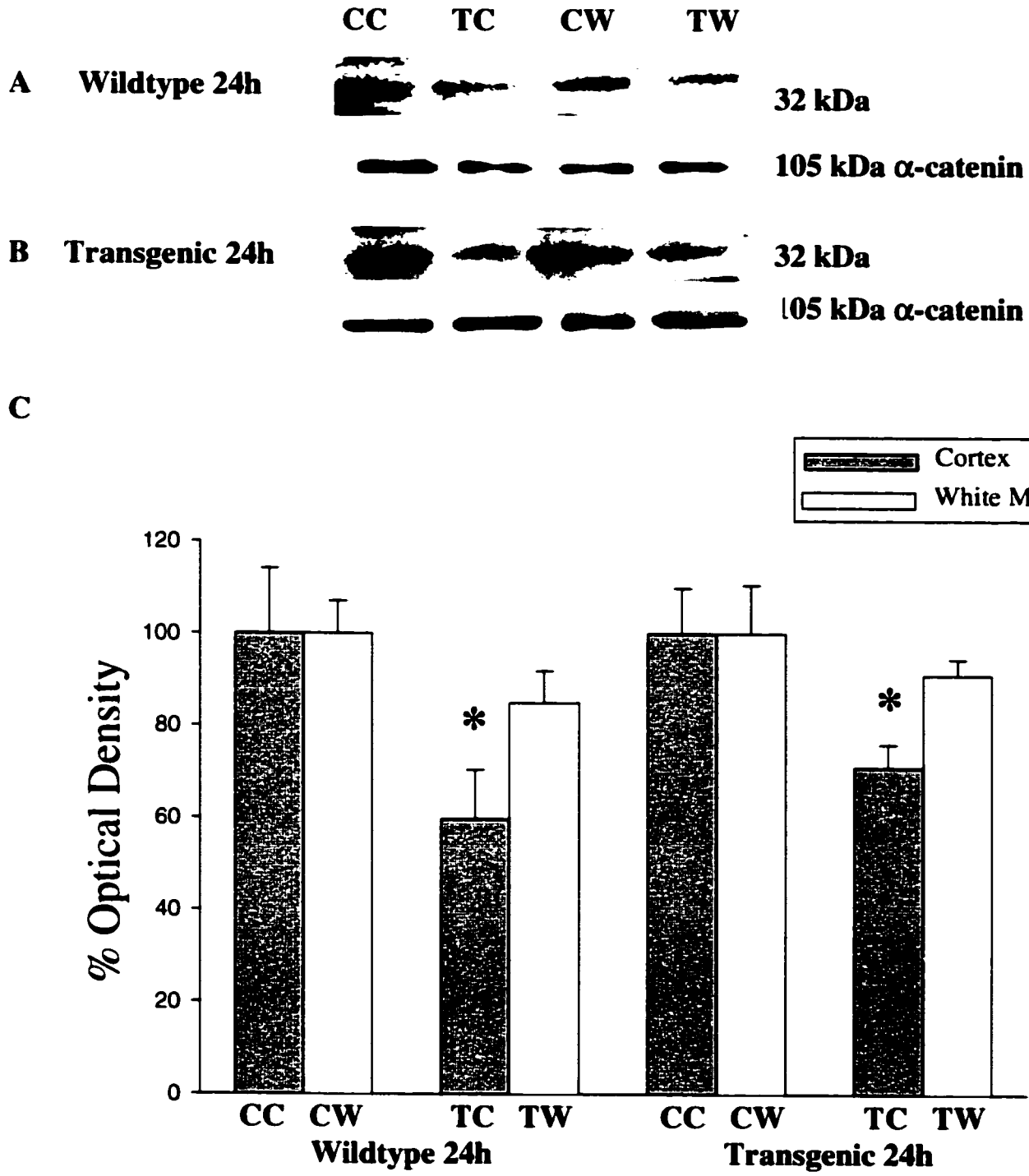
CC
TC
CW
TW
A
Wildtype 24h
32 kDa
105 kDa α-catenin
B
Transgenic 24h
32 kDa
105 kDa α-catenin
C
Cortex
White Matter
% Optical Density
120
100
80
60
40
20
0
*
*
CC
CW
TC
TW
CC
CW
TC
TW
Wildtype 24h
Transgenic 24h
Time post TBI

Figure 13: Cleavage of PARP, detected using Western blot techniques, in wildtype and CMV *NAIP* C57/Bl6 brains. The full length PARP protein and the PARP fragment were measured in control (no trauma) cortex (CC) and subcortical white matter (CW) and 24 hour post trauma cortex (TC) and subcortical white matter (TW) in both wildtype (A) and CMV *NAIP* transgenic mice (B). Density of the full length PARP protein (C1) and PARP fragment (C2) band in the TBI groups is represented graphically as a percentage of the optical density of the protein band measured in the respective control group. !$p < 0.05$ compared to wildtype group, *$p < 0.05$ compared to control. ($n = 5$ mice / group)

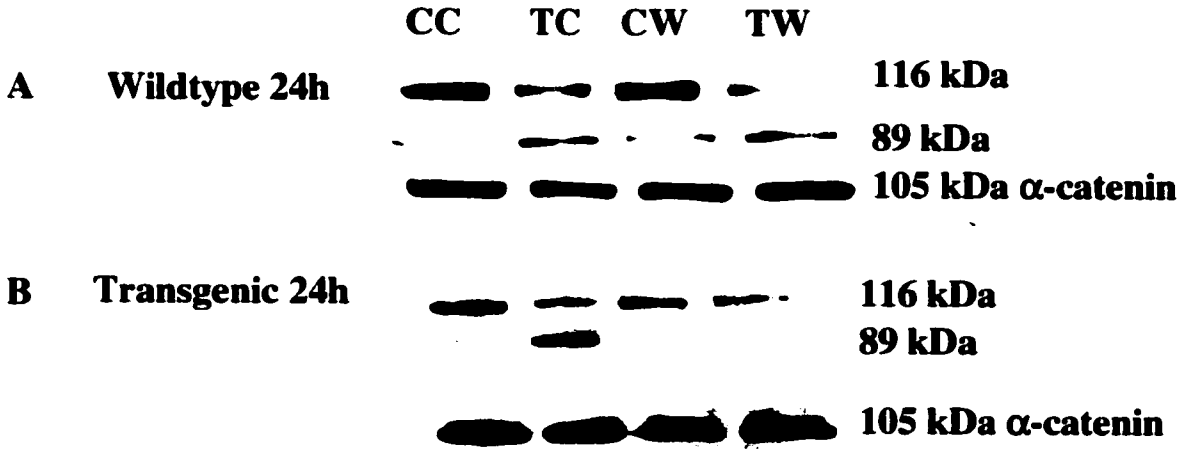
CC
TC
CW
TW
A
Wildtype 24h
116 kDa
89 kDa
105 kDa α-catenin
B
Transgenic 24h
116 kDa
89 kDa
105 kDa α-catenin

C1

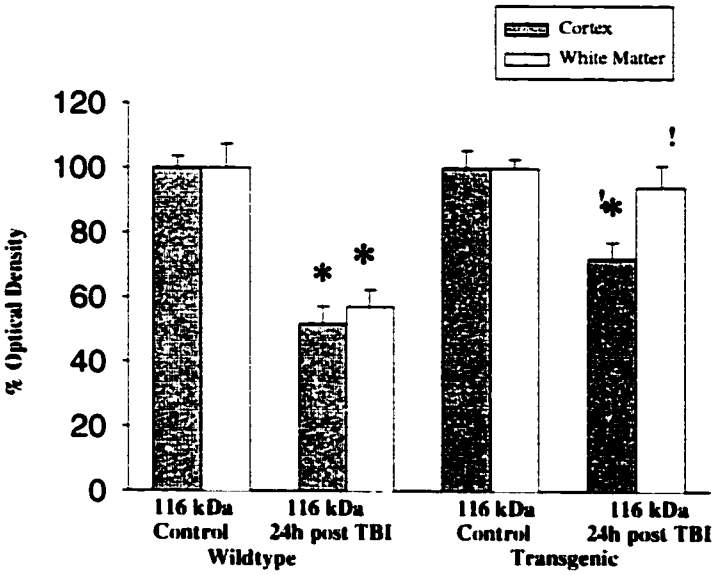
Cortex
White Matter
% Optical Density
120
100
80
60
40
20
0
116 kDa Control
116 kDa 24h post TBI
116 kDa Control
116 kDa 24h post TBI
Wildtype
Transgenic

C2

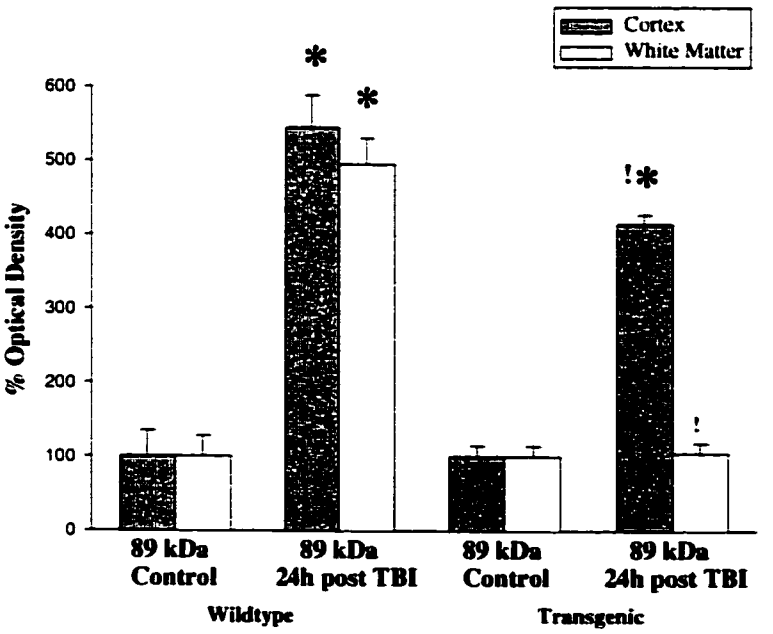
Cortex
White Matter
% Optical Density
600
500
400
300
200
100
0
89 kDa Control
89 kDa 24h post TBI
89 kDa Control
89 kDa 24h post TBI
Wildtype
Transgenic

Figure 14: Expression of CD11*b* and TNF-alpha in wildtype and CMV *NAIP* C57/Bl6 brain. Expression of CD11*b* and TNF-α was quantified in the injured region of the cortex and subcortical white matter at 24 hours following TBI in wildtype (Wt) and transgenic (Tg) mouse brains. *$p < 0.05$ compared to control (5 wildtype mice / group, 3 CMV *NAIP* transgenic mice / group)

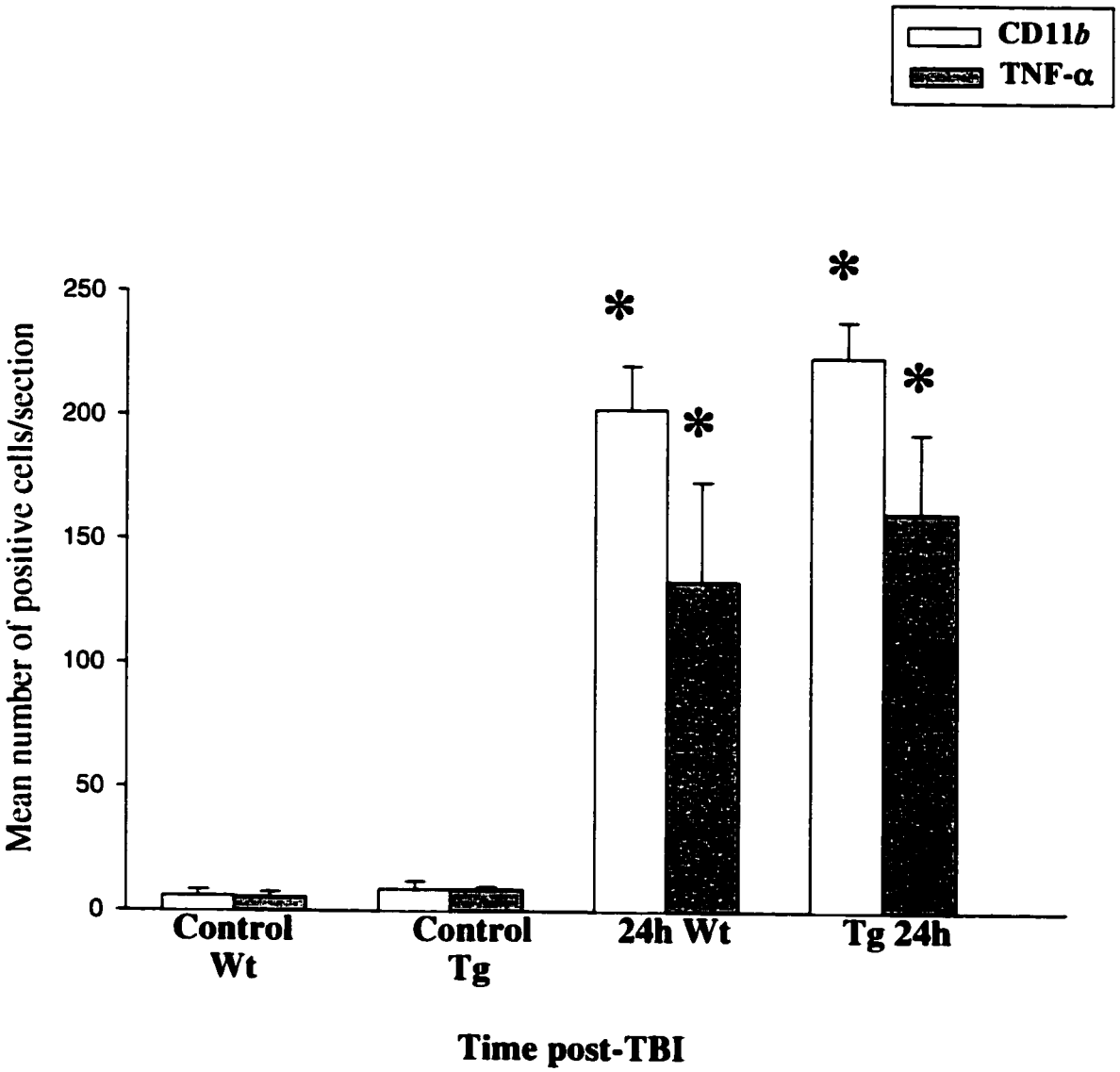
CD11b
TNF-α
Mean number of positive cells/section
250
200
150
100
50
0
*
*
*
*
Control Wt
Control Tg
24h Wt
Tg 24h
Time post-TBI

Figure 15: Morris water maze latency times for wildtype and CMV *NAIP* transgenic mice. Beginning 48 hours post TBI or sham procedure, mice were given five trials a day for five days and the latency time was recorded for each trial. The mean +/- standard deviation water maze latency time for each group on each day is represented graphically. (n = 6 mice / group)

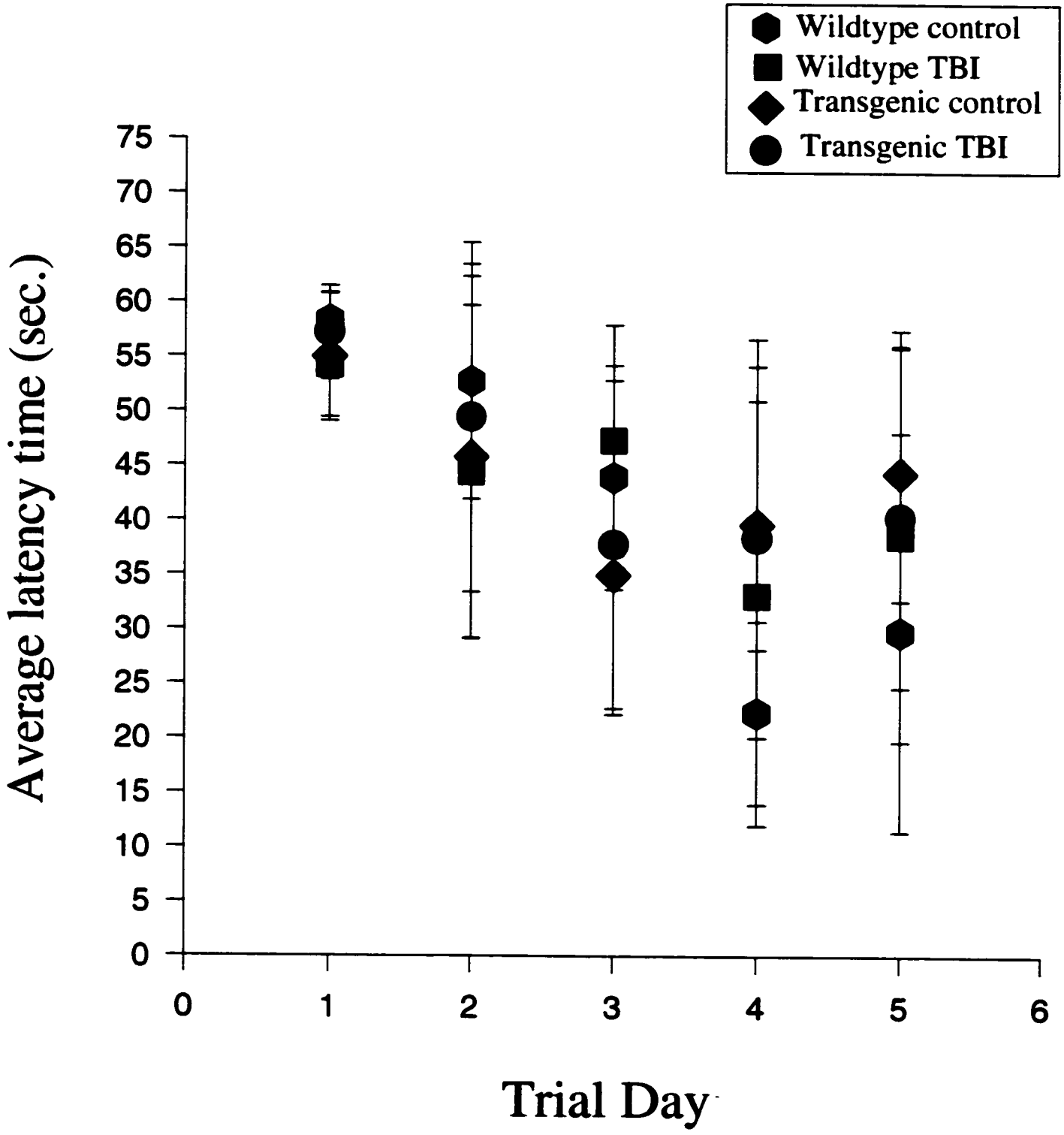
Wildtype control
Wildtype TBI
Transgenic control
Transgenic TBI
Average latency time (sec.)
75
70
65
60
55
50
45
40
35
30
25
20
15
10
5
0
0
1
2
3
4
5
6
Trial Day

4.0 Discussion

4.1 Apoptosis in C57/Bl6 Wildtype Brain Following TBI

Apoptosis of cortical neurons and subcortical white matter oligodendrocytes had been observed in several *in vivo* models of TBI (38, 137). This apoptotic cell death had been shown to cause neurological deficits and to involve internucleosomal DNA fragmentation and caspase-3 activation (38, 60 137, 140, 190). In contrast to other well described TBI models, the experimental animals used in this study were mice, the scalp of the mouse was closed during the procedure, and severe brain deformation was not generated (37, 38, 56, 60, 111, 112). Given the central role of apoptosis in mediating TBI pathology, we were interested in identifying the time course of apoptotic death, biochemical mediators of apoptosis, and the cell type undergoing apoptosis in our model of TBI.

Apoptosis in the cerebral cortex of wildtype brains post TBI was distinguished through the detection of DNA fragmentation and caspase-3 activation, the two best accepted hallmarks of apoptosis. The increased number of ISEL positive cells observed in the regions of the cortex and subcortical white matter that received an impact force in our model, indicated that DNA fragmentation occurred in cells of the injured cerebral cortex up to 7 days following TBI. Similar to results reported from other *in vivo* TBI models, the maximum number of ISEL positive cells present in the cortex and subcortical white matter was observed at 24 hours post TBI in the region that received maximum impact (38). Evidence that the ISEL positive cells represented apoptotic cell death was obtained from the observation of 'ladders' indicating internucleosomal DNA cleavage in agarose gels of DNA from the cortex and subcortical white matter at 24 hours post TBI. Although recent studies had suggested that this type of DNA fragmentation could occasionally occur in necrotic cells as well, internucleosomal DNA

fragmentation is still considered to be the primary hallmark of apoptosis (29, 49, 79). A second hallmark of apoptosis observed in most cell types is the proteolytic cleavage of procaspase-3 to form active caspase-3 (49). Compared to control and 6 hour post TBI groups, a decrease in the level of procaspase-3 in the cortex and subcortical white matter was observed at 24 hours following TBI suggesting that at the time point when the maximum number of ISEL positive cells were observed in the cerebral cortex, the proenzyme was cleaved and active caspase-3 was generated. Cleavage of specific substrates, such as the DNA stabilizing protein PARP, by active caspase-3 generates many of the degenerative changes associated with apoptosis (128, 158, 178). PARP cleavage was detected in the cortex and subcortical white matter at 24 hours post TBI which, taken together with the decrease in the proenzyme observed at this time point, indicated that caspase-3 was activated in injured tissue 24 hours following trauma. Thus, the detection of ISEL positive cells, internucleosomal DNA fragmentation, and activated caspase-3 in the region of the cerebral cortex that received injury provided strong evidence for the occurrence of apoptosis in our model of TBI. Data from this study also indicated that following TBI cortical neurons and subcortical white matter oligodendrocytes were the primary cell types sensitive to apoptosis. These observations are in agreement with several *in vivo* studies that had demonstrated selective apoptosis of cortical neurons and subcortical white matter oligodendrocytes following TBI (38, 125, 139,190).

4.2 Inflammation in C57/Bl6 Wildtype Brains Following TBI

Inflammation is increasingly being recognized as a contributing factor to the apoptosis that occurs following CNS trauma (21, 84, 87, 139, 160, 161, 171, 186). This study revealed that inflammation occurred in the injured cerebral cortex following trauma, and the data indicated

that a proapoptotic cytokine might mediate apoptosis following TBI. Previous studies had demonstrated that both activated microglia and infiltration of blood borne inflammatory cells could contribute to CNS inflammation post TBI (168). However, inflammatory cells that entered the brain through the injured blood brain barrier did not significantly accumulate until 18 – 24 hours post TBI while microglial activation was often observed immediately following trauma which suggested that the early inflammatory response to TBI was mediated by activation of the resident inflammatory cells (56, 84, 88, 168). The data from this study revealed that microglial activation was an early event with a maximum number of activated microglia observed in the cerebral cortex at 24 hours following TBI. The blood brain barrier did not appear to be extensively disrupted and infiltrating blood borne inflammatory cells were not observed at any time point following TBI. These results provide additional evidence that activated microglia generate the early inflammatory response to TBI.

Microglia release several factors, such as the proapoptotic cytokine TNF-α, that play a role in the immune response and in mediating the damage associated with CNS trauma (56, 74, 153, 163). Although TNF-α is produced largely by glial cells following CNS trauma, neurons have also been observed to produce this cytokine (87). TNF-α derived from microglia is considered to be a proinflammatory and proapoptotic agent while neuronally derived cytokines appear to be involved in information transfer between cells (14). In this study, the presence of high levels of TNF-α in the cerebral cortex during maximum microglial activation and the observation that TNF-α was not present within the cytosol of cerebral cortex cells indicated that this cytokine originated from the microglia. Several studies had demonstrated that TNF-α associated with neurons following TBI and was a potent apoptotic stimulus for both cultured neurons and oligodendrocytes (32, 87, 99, 163, 194). In this study, we demonstrated that TNF-α associated

with neurons during the acute period post TBI, which suggested that TNF-α might have stimulated the cell death observed in our model of TBI. The data also provided further support for the role of TNF-α in mediating neuronal and oligodendrocyte apoptosis following TBI.

Recent reports by Bruce et al. (1996) and Scherbel et al. (1999), had suggested that TNF-α might play a dual role in head trauma, accelerating cell death during the acute phase and facilitating cellular and neurological recovery during the chronic phase post TBI (21, 153). Although the chronic effect of TNF-α was not examined in this study, the sustained presence of TNF-α in the injured cerebral cortex after most apoptotic death had occurred provided additional evidence for the theory that this cytokine might have a nonapoptotic role during the chronic period following TBI.

4.3 The Role of Naip in Mediating Cell Survival Following TBI

This was the first study to report alterations in the expression of endogenous Naip following TBI and the data suggested that the role of Naip could be to promote cell survival in the cerebral cortex post trauma. Using Western blot and immunofluorescent techniques, a dramatic increase in Naip expression was observed at 6 hours post TBI in the cortex and subcortical white matter. The increased expression of Naip occurred when TNF-α levels were at a maximum and early changes in procaspase-3 were observed which suggested that levels of Naip were elevated in response to these proapoptotic signals. Several *in vitro* and *in vivo* studies had demonstrated that exposure of neurons and oligodendrocytes to high levels of TNF-α stimulated apoptosis through the TNFR1 receptor and involved activation of caspases-8, –9, and –3 (32, 87, 99, 102, 106, 109, 163, 194). It had been shown that the antiapoptotic protein BCL-2 was only partially able

to block TNF-α induced apoptosis due to the inability of this protein to influence the activity of caspase-8 or –3 (117, 182). As NAIP was believed to prevent apoptosis by interacting with caspase-3 and had been shown *in vitro* to effectively inhibit TNF-α stimulated apoptosis, it was postulated that this IAP would have a more significant role than BCL-2 in preventing death receptor induced death (103, J. Maier, personal communication). Thus, it is tempting to speculate that in cortical and subcortical white matter cells Naip expression was rapidly increased following TBI in an attempt to block caspase-3 activity and TNF-α induced apoptosis. The theory that increased Naip expression might promote cell survival following TBI is supported by observations from Xu et. al. (1997) where hippocampal neurons resistant to apoptosis induced by ischemia were shown to increase the expression of this IAP (187). Although the transcriptional pathway responsible for increased expression of *Naip* following CNS trauma has not been described, the transcription factor NF-κB might be involved. *In vitro* cell culture studies had demonstrated that expression of two members of the IAP family, HIAP1 and HIAP2 were increased following TNFR2 induced NF-κB activation (170). It is believed that these two IAPs are sequestered at TNFR2 and, although able to inhibit caspases *in vitro*, do not interact with the TNFR1 apoptotic pathway *in vivo* (144, 147). These reports indicated that NF-κB played a role in IAP transcription and therefore suggests that this transcription factor could increase expression of *Naip* in response to TNFR1 induced apoptosis.

Western blot analysis revealed that cytosolic levels of Naip were significantly decreased in the cortex and subcortical white matter compared to sham during the time when maximum apoptosis was observed providing further evidence for the protective role of endogenous Naip following TBI. As Naip levels decreased between 6 and 24 hours following TBI, the number of apoptotic cells present in the cortex and subcortical white matter directly under the site of maximum

impact almost doubled. Taken together, the 6 hour and 24 hour post TBI Naip data demonstrated that the ability of the cells to prevent apoptosis decreased as levels of Naip decreased, which suggested that an increase in Naip expression promoted cell survival and a decrease in Naip expression allowed apoptosis to proceed following TBI. Recent reports by Xu et al. (1997), Holchik et al. (2000), and Perrelet et al. (2000) had demonstrated that a similar decrease in Naip expression was associated with increased neuronal apoptosis in *in vivo* models of stroke, epilepsy, and motor neuron damage (73, 134, 187). These studies, together with the data presented in this report indicated that Naip had a role in mediating cell survival following CNS trauma. The apparent discrepancy between the level of Naip and the number of cells expressing Naip in cortex tissue at 24 hours post TBI compared to control might be due to different sensitivities between the two methods used to detect the protein. Alternatively, Naip might move from the cytosol to the nucleus following TBI which would generate inconsistencies in the measurements of Naip protein level and the number of cells expressing Naip. It had been observed *in vitro* that following exposure of cells to an apoptotic stimulus, Naip translocates from the cytosol to the nucleus (David Barnes, personal communication). Thus, exposure of the cerebral cortex cells to TNF-α (or other unidentified proapoptotic stimuli) in our model of TBI might trigger translocation of Naip into the nucleus at 24 hours following TBI (as noted the staining pattern of Naip was more nuclear and not as diffuse at 24 hours following TBI compared to 6 hours following TBI). As the cytosolic protein extracts were used in the Naip Western blots, the level of cytosolic Naip could appear to decrease while the number of cells expressing Naip could still be elevated compared to sham. Western blots of the nuclear protein extracts and confocal microscope analysis of Naip location at 24 hours post TBI would aid in determining if translocation of the protein occurred following TBI.

This study provided additional evidence for the role of NAIP in promoting cell survival in SMA patients. One of the primary unanswered questions in the molecular pathogenesis of SMA pathology is whether loss of endogenous NAIP expression exacerbates α-motor neuron death and SMA phenotype (27, 142). The apoptotic morphology of the motor neurons observed in the spinal cords of affected children had lead to the speculation that SMA was the result of inappropriate apoptosis (149). In 1995, *NAIP* and *SMN1* were identified as the two candidate causative genes for SMA (95, 147). Recent work by Lefebvre (1995) and others had demonstrated that deletions of *SMN1* exon 7 were associated with virtually all cases of SMA and the remaining cases presented different mutations and deletions in *SMN1* (95, 179). These studies strongly indicated that *SMN1* was the causative gene in mediating SMA pathology (95, 179). In comparison, NAIP had also been detected in tissues that demonstrate SMA pathology and found to be deleted in 60 - 80% of type I patients and in 15 - 42% of type II and III patients which suggested that expression of NAIP aids in determining phenotype severity (40, 120, 147). Additionally, several studies had revealed that NAIP was a potent antiapoptotic agent able to inhibit apoptosis stimulated by a wide variety of triggers (92). Thus, *NAIP* was proposed to be a modifying gene in SMA pathogenesis (27, 142). In this model, deletion of *NAIP* and *SMN1* result in extensive motor neuron apoptosis and the severe type I phenotype while deletions of *SMN1* alone results in limited apoptosis and the milder type II and III phenotype (33). The data presented in this study, together with recent reports which revealed that a decrease in endogenous Naip expression lead to enhanced apoptosis in models of CNS injury provided further evidence for the role of *NAIP* as a modifying gene in SMA pathology (73, 187).

4.4 Apoptosis in CMV NAIP C57/Bl6 Transgenic Brain Following TBI

Historically, transgenic animals had been widely used in medical science to gain a better understanding about the molecular mechanisms involved in gene transcription, embryogenesis, and disease pathology (72). In this study, *NAIP* transgenic mice were used to further evaluate the role of NAIP with regards to caspase-3 activation and DNA fragmentation following TBI and the data indicated that this IAP promoted cell survival through the inhibition of caspase-3 activity. To generate the transgenic mice used to establish a heterozygous breeding colony, a *NAIP* construct under transcriptional control of the CMV promoter was injected into the pronucleus of a newly fertilized mouse egg. Pronuclear injection is the most common technique employed to develop transgenic animal strains (78). In this procedure foreign DNA integrates into random sites within the genome usually at the one cell stage of embryo development (72). Thus, every cell of the mature animal contains the foreign DNA. In this study, PCR techniques were successfully utilized to identify transgenic mice from wildtype litter mates. The CMV element is one of the most common promoters employed to generate transgenic animals (22). This promoter is unregulated and constitutively active resulting in continuous expression of the foreign DNA (22). For this reason, it was believed that *NAIP* would be expressed in all cells that contained the construct, including the cells in the region of the cerebral cortex where apoptosis was observed in wildtype mice. Immunofluorescent techniques were used to demonstrate the expression of NAIP in neuron - like and oligodendrocyte - like cells throughout the cerebral cortex of mice containing the CMV *NAIP* construct.

This was the first study to demonstrate that an overexpression of NAIP enhanced cell survival in the cortex and subcortical white matter at 24 hours following TBI. DNA fragmentation, detected using the ISEL stain, was significantly reduced in the cortex and subcortical white

matter of transgenic animals at 24 hours post TBI compared to wildtype brain from the same time point. In particular, the number of ISEL positive cells in the subcortical white matter from transgenic animals at 24 hours post TBI was not significantly different than the number observed in the transgenic sham brains. These results suggested that NAIP overexpression was protective against DNA fragmentation and enhanced cell survival of both cortical and subcortical white matter cells at 24 hours following TBI. A similar attenuation of cortical cell death following TBI in mice overexpressing BCL-2 was recently observed by Ragupathi et. al. (1998). However, although BCL-2 was expressed in cells throughout the brain, an attenuation of subcortical white matter cell death was not reported (140). As both cortical neurons and subcortical white matter oligodendrocytes had been shown to be the primary apoptotic cell types following TBI, the data presented in this study indicated that NAIP could have a greater potential to prevent the cell death associated with TBI compared to BCL-2. It had been speculated that the enhanced ability of NAIP to prevent TNF-α induced apoptosis and cell death following TBI might be due to the interaction of NAIP with caspases downstream from the site of BCL-2 activity (73, 117, 182, J. Maier, personal communication).

In this study, NAIP overexpression appeared to enhance cortical cell survival at 24 hours following TBI and the data indicated that this protection might result from decreased caspase-3 activity at this time point. The interaction of the BIR domains of NAIP with active caspase-3 had been observed *in vitro* and it is through this interaction that NAIP is believed to exert its antiapoptotic effect (92, J. Maier, personal communication). In this study, Western blot analysis revealed that procaspase-3 levels were significantly decreased in the transgenic cortex at 24 hours post TBI compared to control. These results did not differ significantly from the results obtained from the wildtype animals. The data suggested that NAIP overexpression did not have

an effect on activation of caspase-3 or on activation of caspases upstream from caspase-3 at this time point. Western blot analysis of PARP cleavage was used to indirectly detect the presence of active caspase-3 in the cortex and to examine the effect of NAIP overexpression on caspase-3 activity following TBI. Although PARP cleavage was significantly increased following TBI in the transgenic cortex compared to control, the amount of PARP cleavage was significantly reduced in the transgenic cortex post TBI compared to the cleavage observed in wildtype cortex at the same time point following TBI. Taken together with the ISEL data, these results suggested that the reduced cortical cell death observed in the transgenic cortex 24 hours after TBI was due to a heightened inhibition of caspase-3 activity compared to wildtype and provided further evidence that the antiapoptotic effects of NAIP are mediated through the interaction with active caspase-3. However, as the ISEL and Western blot data show, NAIP overexpression was insufficient to completely attenuate DNA fragmentation and PARP cleavage in the transgenic cortex 24 hours post TBI. Thus, it appeared that NAIP overexpression was not able to totally prevent caspase-3 activity in the cortex at this time point. These results are complementary to a study by Simons et. al. (1999) where NAIP was shown to delay, but not attenuate, cell death in cerebellar granule neurons exposed to low potassium media (162). It had been suggested that the inability of NAIP to permanently halt apoptosis in some cells was reflective of saturation of the protein with active caspase-3 (J. Maier, personal communication). As there is no evidence that NAIP interacts with caspases upstream from caspase-3 or that NAIP can interact with more than one active caspase-3 enzyme it was thought that progressive cleavage of procaspase-3 would result in increased occupation of NAIP with active caspase-3 (146, J. Maier, personal communication). Eventually the entire cytosolic NAIP pool would be occupied and further caspase-3 activation would result in DNA fragmentation and cell death. The complete effect of

NAIP overexpression on caspase-3 activity and cortical cell death cannot be determined in this study due to the fact that the apoptosis time course in the cortex of transgenic animals following TBI was not investigated. It is possible that caspase-3 activation, DNA fragmentation, and PARP cleavage continue in the cortex and that NAIP overexpression does not permanently inhibit cortical cell death but rather delays apoptosis following TBI. However, overexpression of NAIP might prolong the therapeutic window for other antiapoptotic therapies following TBI.

In the transgenic brain, subcortical white matter cells appeared to be profoundly protected from apoptosis at 24 hours post TBI and the data indicated that the protection observed at this time point was due to inhibition of active caspase-3. In the subcortical white matter, procaspase-3 levels following trauma did not differ between wildtype and transgenic animals but there was a marked attenuation of PARP cleavage in NAIP transgenic animals compared to wildtype mice following trauma. Taken together with the ISEL data, these results strongly suggested that at the 24 hour time point following trauma in the NAIP transgenic animals, activation of caspase-3 in the subcortical white matter was dramatically reduced compared to wildtype. These results provided additional evidence that NAIP promoted cell survival through the inhibition of active caspase-3. However, attenuation of apoptosis in the subcortical white matter of transgenic animals might be mediated by factors other than NAIP. Several studies had demonstrated that oligodendrocyte survival depended on the presence of growth factors that originated from neuronal axons (10, 11, 194). These growth factors had been shown *in vivo* and *in vitro* to promote survival by inhibiting oligodendrocyte apoptosis (10, 194). The importance of CNS growth factors in attenuating TNF-α induced apoptosis was recently shown by Ye and D'Ercole (1999) who demonstrated that, following exposure to TNF-α, IGF-1 promoted oligodendrocyte survival either through the inhibition of the apoptotic pathway upstream from caspase-3 or by

blocking TNF-α stimulation of apoptosis (194). Therefore, the attenuation of caspase-3 activation and cell death observed in the subcortical white matter of the NAIP transgenic brains at 24 hours following TBI might be due to the enhanced survival of the cortical neurons which release axonal growth factors in the transgenic brains. If the hypothesis that NAIP delayed cell death following TBI is valid, than as the cortical cells begin to die in greater numbers in the transgenic brain, growth factors would be withdrawn causing caspase-3 activation in the subcortical white matter. At this point, oligodendrocyte apoptosis in the transgenic brains might be further delayed compared to wildtype through the inhibition of caspase-3 activity by NAIP. Elucidation of the time course of neuronal and oligodendrocyte cell death in the NAIP transgenic brains will aid in determining the precise role of NAIP overexpression on caspase-3 activity and apoptosis in the subcortical white matter following TBI. However, the data presented in this study demonstrated for the first time that an overexpression of NAIP enhanced both cortical and subcortical white matter cell survival, thereby extending the therapeutic window following TBI.

4.5 Inflammation in C57/Bl6 CMV NAIP Transgenic Brains Following TBI

As inflammation during the acute period following TBI is known to be an important mediator of tissue damage, the inflammation in the transgenic cerebral cortex was measured to ensure that a similar response occurred in both CMV *NAIP* and wildtype brains post TBI. The generation of transgenic animals had been shown to occasionally cause phenotypically visible insertional mutations (5-15% of transgenic lines) which might deleteriously affect biological systems (72). To guarantee that the CMV *NAIP* transgenic mice did not express a defect in the inflammation response to TBI, immunofluorescent techniques were used to measure microglial activation and levels of TNF-α in the cerebral cortex at 24 hours following TBI. Similar levels of activated

microglia and TNF-α were present in wildtype and transgenic cerebral cortex at 24 hours after TBI indicating that insertion of *NAIP* did not alter the inflammation response in the transgenic animals. The data also showed that differences in the inflammation response between CMV *NAIP* and wildtype brains did not play a role in the reduced apoptosis observed in the transgenic cerebral cortex and provided further evidence that it was the role of NAIP in inhibiting apoptosis that promoted cell survival following TBI in the transgenic brain.

4.6 Neurological Outcome in Wildtype and CMV NAIP Transgenic C57/Bl6 Mice Following TBI

The ability of NAIP overexpression to improve cognitive outcome following TBI was investigated. Both clinical cases and animal models of TBI had been associated with deficits in cognitive (spatial memory and learning) and neuromotor function (60, 112, 140, 166). The deficits were thought to result from the apoptotic cell death that occurred within the sensory / motor cerebral cortex and hippocampus following TBI (140). In animal models of CNS trauma, deficits in cognitive and neuromotor function had been assessed with specific neurological scores. These scores had also been used to determine the ability of therapeutics to promote neurological recovery following TBI (140, 153, 160). The effect of overexpression of the endogenous antiapoptotic protein BCL-2 on neuromotor function following TBI had been investigated with a four point neurological score (140). Using this score Ragupathi et. al. (1998) demonstrated that, compared to wildtype, an overexpression of BCL-2 could attenuate cortical cell death but had no effect on neuromotor outcome following TBI (140). These results indicated that although an overexpression of BCL-2 was able to enhance cell survival, it was not able to preserve cell function following TBI. One possible explanation for the discrepancy is

that by inhibiting one step in the apoptotic pathway, cells were held in a state of 'suspended animation' between survival and death where normal function was not possible (140). A beneficial effect of BCL-2, or any antiapoptotic protein, on spatial learning and memory following TBI had not been reported. This was the first study to examine the effect of overexpression of NAIP on these cognitive factors post TBI using the Morris water maze neuroscore (16, 119). The Morris water maze is a well described neurological score that had been used with *in vivo* models of CNS trauma to detect deficits in spatial memory and learning which are associated with damage to the cerebral cortex and CA1 region of the hippocampus (16, 60, 118, 153). As NAIP overexpression had been shown to decrease cell death in the cortex and subcortical white matter following TBI, it was thought that the transgenic animals subjected to TBI would have improved cognitive function compared to wildtype litter mates. However, as the data indicated, due to the large standard deviations associated with the latency times within each experimental group conclusions about the effect of NAIP overexpression on spatial memory and learning could not be determined. It is possible that the Morris water maze might not have been the correct test to assess cognitive function in this study as this neurological score had been shown to be more sensitive to damage within the CA1 region of the hippocampus, an area where very minimal damage was detected in this model of TBI (118). The five point neurological score developed by Dunnett et. al. (1981) might be more useful than the Morris water maze in determining the effect of NAIP overexpression on neurological outcome following trauma (54). In comparison to the Morris water maze, the Dunnett score measures deficits in both motor and cognitive function and is highly sensitive to damage in the cortex and subcortical structures (44, 54). In future investigations, this score may prove beneficial in determining the role of NAIP overexpression on both motor and cognitive function following TBI.

4.7 Conclusion

This study was the first to provide evidence that NAIP promoted cell survival following TBI through the interaction of this protein with mediators of apoptosis. Previous studies had shown that NAIP was expressed in the brain and spinal cord and was deleted in the majority of type I SMA patients which suggested that this IAP was involved in promoting the survival of healthy CNS cells (147, 188). Additionally, NAIP had been shown to be an important mediator of cell protection in several *in vivo* models of CNS injury (73, 134, 187). However, prior to our study the role of NAIP in TBI, the most common form of pediatric CNS trauma, had not been investigated. As a member of the IAP family, NAIP had been shown to promote cell survival through the inhibition of apoptosis stimulated by a variety of agents including TNF-α (92). It had been demonstrated *in vitro* that this apoptosis inhibition occurred due to the ability of the BIR domains of NAIP to inhibit caspase-3 activity (92, J. Maier, personal communication). As previous studies had shown that the apoptotic cell death associated with TBI was primarily mediated through the TNF-α pathway and activation of caspase-3, it was hypothesized that an overexpression of NAIP would attenuate cell death and improve neurological outcome following TBI (38, 160, 190).

The data presented in this study suggested that, during the acute period post TBI, cortical neurons and subcortical white matter oligodendrocytes were selectively vulnerable to apoptotic cell death. Additionally, the occurrence of the apoptotic death correlated with increased levels of the proapoptotic cytokine TNF-α following TBI. This study was the first to show changing levels of endogenous Naip in the cerebral cortex during the acute period post TBI.

Transgenic animals that expressed human NAIP were used to investigate the role of this IAP on caspase-3 activity and neurological outcome following TBI. We were the first to demonstrate

that an overexpression of NAIP enhanced cell survival following head trauma. The indirect evidence that the cerebral cortex of NAIP transgenic animals contained significantly less caspase-3 activity following TBI compared to wildtype brains from the same time point was consistent with the theory that NAIP prevented apoptosis through the inhibition of caspase-3 activity. It is possible that an overexpression of NAIP might not perpetually halt caspase activity and cell death, but rather delay apoptosis thereby extending the therapeutic window in the brain following TBI. Comparison of the apoptosis time course in Naip1 deficient, NAIP transgenic, and wildtype animals would help to clarify the exact role of Naip and NAIP overexpression on apoptosis post TBI. It was postulated that due to the enhanced cell survival in the transgenic cerebral cortex, these animals would have improved neurological function compared to wildtype litter mates following TBI. Unfortunately, due to the large standard deviations in the Morris water maze data, the effect of NAIP overexpression on neurological outcome following TBI remains to be elucidated. Regardless, this study has identified NAIP as a new and exciting potential therapeutic target that could be utilized to attenuate the cell loss associated with TBI.

REFERENCES

1. Adams, J., and S. Cory. 1998. The Bcl-2 protein family: arbiters of cell survival. Science 281, 1322-1326.

2. Adams, G., D. Fuquay, B. Harley, T. Herr, K. Matthews, R. Mines, C. Lawrence, H. Weinblatt, and D. Young. 1999. The management of minor closed head injury in children. Pediatrics 104, 1407-1415.

3. Allen, J., S. Knoblach, and A. Faden. 1999. Combined mechanical trauma and metabolic impairment in vitro induces NMDA receptor-dependent neuronal cell death and caspase-3 dependent apoptosis. FASEB J. 13, 1875-1882.

4. Alnemri, E., D. Livingston, D. Nicholson, G. Salvesen, N. Thornberry, W. Wong, and J. Yuan. 1996. Human ICE/CED-3 protease nomenclature. Cell 87, 171.

5. Ambrosini, G., C. Adida, G. Sirugo, and D. Altieri. 1998. A novel antiapoptosis gene, *survivin*, expressed in cancer and lymphoma. Nat. Med. 3, 917-921.

6. Ashkenazi, A., and Dixit, V. 1998. Death receptors: signaling and modulation. Science 281, 1305-1308.

7. Banati, R., J. Gehrmann, P. Schubert, and G. Kreutzberg. 1993. Cytotoxicity of microglia. Glia 7, 7111-7118.

8. Barinaga, M. 1998. Is apoptosis key in Alzheimer's disease? Science 281, 1303-1304. Cotman, C., and J. Su. 1996. Mechanisms of neuronal death in Alzheimer's disease. Brain Pathol. 6, 493-506.

9. Barinaga, M. 1998. Stroke-damaged neurons may commit cellular suicide. Science 281, 1302-1303.

10. Barres, B., M. Jacobson, R. Schmid, M. Sender, and M. Raff. 1993. Does oligodendrocyte survival depend on axons? Current Biol. 3: 489-497.

11. Barres, B., and M. Raff. 1993. Proliferation of oligodendrocyte precursor cells depends on electrical activity in axons. Nature 361, 258-260.

12. Battaglia, G., A. Princivalle, F. Forti, C. Lizier, and M. Zeviani. 1997. Expression of the *SMN* gene, the spinal muscular atrophy determining gene, in the mammalian central nervous system. Hum. Mol. Gene. 6, 1961-1971.

13. Beg, A., and A. Baltimore. 1996. An essential role for NF-κB in preventing TNF-α induced cell death. Science 274, 781-784.

14. Berkenbosch, F., N. Robakus, and M. Blum. 1991. Interlukin-2 in central nervous system: role in the acute phase response and in brain development, brain repair, and the pathogenesis of Alzheimer's disease. In: R.C.A. Fredrichson, J.L. McGaugh, and D.L. Felton (Eds.) Peripheral Signaling of the Brain: Role in Neuronal Immune Interactions and learning Memory. Hogrefe and Huber, New York, N.Y. pp. 131-145.

15. Birnbaum, M., R. Clem, and L. Miller. 1994. An apoptosis inhibiting gene from a nuclear polyhedrosis virus encoding a polypeptide with Cys:His sequence motifs. J. Virol. 68, 2521-2528.

16. Block, F. 1999. Global ischemia and behavioral deficits. Prog. Neurobiol. 58, 279-295.

17. Boje, K., and P. Arora. 1992. Microglial-produced nitric oxide and reactive nitrogen oxides mediate neuronal cell death. Brain Res. 587, 250-256.

18. Boldin, M., E. Varfolomeev, Z. Pancer, I. Mett, , J. Carmonis, and D. Wallach. 1995. A novel protein that interacts with the death domain of Fas/APO1 contains a sequence motif related to the death domain. J. Biol. Chem. 270, 7795-7789.

19. Bratton, S., M. MacFarlane, K. Cain, and G. Cohen. 2000. Protein complexes activate distinct caspase cascades in death receptor and stress-induced apoptosis. Exp. Cell Res. 256, 27-33.

20. Brooke, M. 1985. A clinician's view of neuromuscular disorders. 2nd Ed., Williams and Wilkins, London, U.K. pp. 36-80.

21. Bruce, A., W. Boling, M. Kindy, J. Peschon, P. Kraemer, M. Carpenter, F. Holtsberg, and M.Mattson. 1996. Altered neuronal and microglial responses to excitotoxic and ischemic brain injury in mice lacking TNF receptors. Nat. Med. 2, 788-794.

22. Bruening, W., B. Giasson, W. Mushynski, and H. Durham. 1998. Activation of stress activated MAP protein kinases up regulates expression of transgenes driven by the cytomegalovirus immediate/early promoter. Nucleic Acids. Res. 26, 486-489.

23. Brzustowicz, L., T., Lehner, L. Castilla, G. Penchaszadeh, R. Daniels, K. Davies, , M. Leppert, F. Ziter, D. Wood, V. Dubowitz, K. Zerres, I. Hausmanowa-Petrusewicz, J. Ott, T. Munsat, and, T. Gilliam. 1990. Genetic mapping of chronic childhood-onset spinal muscular atrophy to chromosome 5q11.2-q13.3. Nature 344, 540-541.

24. Budihardjo, I., H. Oliver, M. Lutter, X. Lou, and X. Wang. 1999. Biochemical pathways of caspase activation during apoptosis. Ann. Rev. Cell Dev. Biol. 15, 269-290.

25. Bullock, R., R. Chesnut, G. Clifton, J. Ghajar, D. Marion, R. Narayan, D. Newell, L. Pitts, M. Rosner, and J. Wilberger. 1995. The Integration of Brain-Specific Treatments. In: Guidelines for the Management of Severe Head Injury. Brain Trauma Foundation, U.S.A. Chapter 3.

26. Bullock, M., B. Lyeth, and J. Muizelaar. 1999. Current status of neuroprotection trials for traumatic brain injury: lessons from animal models and clinical studies. Neurosurgery. 45, 207-217.

27. Burlet, P., A. Burglen, O. Clermont, S. Lefebvre, L. Viollet, A. Munnich, and J. Melki. 1996. Large-scale deletions of the 5q13 regions are specific to Werdnig-Hoffmann disease. J. Med. Genet. 33, 282-283.

28. Caggiano, A., and R. Kraig. 1996. Eicosanoids and nitric oxide influence induction of reactive gliosis from spreading depression in microglia but not astrocytes. J. Comp. Neurol. 369, 93-108.

29. Campagne, M., P. Lucassen, J. Vermeulen, and R. Balazs. 1995. NMDA and kainate induce interneucleosomal DNA cleavage associated with both apoptotic and necrotic cell death in the neonatal rat brain. Eur. J. Neurosci. 7, 1627-1640.

30. Canu, N., L. Dus, C. Barbato, M. Ciotti, C. Brancolini, A. Rinaldi, M. Novak, A. Cattaneo, A. Bradbury, and P. Calissano. 1998. Tau cleavage and dephosphorylation in cerebellar anule neurons undergoing apoptosis. J. Neurosci. 18, 7061-7074.

31. Carbonell, W., and M. Grady. 1999. Evidence disputing the importance of excitotoxicity in hippocampal neuron death after experimental traumatic brain injury. Ann. N. Y. Acad. Sci. 890, 287-298.

32. Chan, F., M. Lenardo. 2000. A crucial role for p80 TNF-R2 in amplifying p60 TNF-R1 apoptosis signals in T lymphocytes. Eur. J. Immunol. 30, 652-660.

33. Chen, Q., S. Baird, M. Mahadevan, A. Besner-Johnston, R. Farahani, J. Xuan, X. Kang, C. Lefebvre, J. Ikeda, R. Korneluk, A. MacKenzie. 1998. Sequence of a 131-kb region of 5q13.1 containing the spinal muscular atrophy candidate genes SMN and NAIP. Genomics 48, 121-127.

34. Cheng, Y., M. Deshmukh, A. D'Costa, J. Demaro, J. Gidday, A. Shah, Y. Sun, M. Jacquin, E. Johnson, and D. Holtzman. 1998. Caspase inhibitor affords neuroprotection with delayed administration in a rat model of neonatal hypoxic-ischemic brain injury. J. Clin. Invest. 101, 1992-1999.

35. Chinnaiyan, A., K. O'Rourke, M. Tewari, and V. Dixit. 1995. FADD, a novel death domain-containing protein, interacts with the death domain of Fas and initiates apoptosis. Cell 81, 505-512.

36. Chopp, M., Y. Li, N. Jiang, R. Zhang, and J. Prostak. 1996. Antibodies against adhesion molecules reduce apoptosis after transient middle cerebral artery occlusion in rat brain. J. Cereb. Blood Flow Metab. 16, 578-584.

37. Clark, R, J. Chen, S. Watkins, P. Kochanek, R. Stetler, J. Loeffert, and S. Graham. 1997. Apoptosis suppressor gene *bcl-2*expression after traumatic brain injury in rats. J. Neurosci. 17, 9172-9191.

38. Conti, A., R. Raghupathi, J. Trojanowski, and T. McIntosh. 1998. Experimental brain injury induces regionally distinct apoptosis during the acute and delayed post-traumatic period. J. Neurosci.18, 5663-5672.

39. Cotman, C., and J. Cu. 1996. Mechanisms of neuronal death in Alzheimer's disease. Brain. Pathol. 6, 493-506.

40. Crawford, T., and C. Pardo. 1996. The neurobiology of childhood spinal muscular atrophy. Neurobiol.Dis. 6, 397-408.

41. Crook, N., R. Clem, and L. Miller. 1993. An apoptosis inhibiting baculovirus gene with a zinc finger-like motif. J. Virol. 67, 2168-2174.

42. Crowe, M., J. Bresnahan, S. Shuman, J. Masters, and M. Beattie. 1997. Apoptosis and delayed degeneration after spinal cord injury in rats and monkeys. Nat. Med.3, 73-76.

43. Curfs, J., C. Hermsen, P. Kremsner, S. Neifer, J. Meuwissen, N. Van Rooyen, and W. Eling. 1993. Tumor necrosis factor-alpha and macrophages in Plasmodium berghei-induced cerebral malaria. Parasitology 107, 125-34.

44. Deckel, A., T. Moran, J. Coyle, P. Sanberg, and R. Robinson. 1986. Anatomical predictors of behavioral recovery following fetal striatal transplants. Behav. Res. 365, 249-258.

45. Deveraux, Q., E. Leo, H. Stennicke, K. Welsh, G. Salvesen, and J. Reed. 1999. Cleavage of human inhibitor of apoptosis protein XIAP results in fragments with distinct specificities for caspases. EMBO J. 18, 5242-5251.

46. Deveraux, Q., and J. Reed. 1999. IAP family proteins - suppressors of apoptosis. Genes Dev. 12, 239-252.

47. Deveraux, Q., N. Roy, H. Stennicke, T. Van Arsdale, Q. Zhou, M. Srinivasula, E. Alnemri, G. Salvesen, and J. Reed. 1998. IAPs block apoptotic events induced by caspase-8 and cytochrome c by direct inhibition of distinct caspases. EMBO J. 17, 2215-2223.

48. Deveraux, Q., R. Takahashi, G. Salvesen, and J. Reed. 1997. X lined IAP is a direct inhibitor of cell death proteases. Nature 388, 300-304.

49. Didenko, V., and P. Hornsby. 1996. Presence of double-strand breaks with single-base 3' overhangs in cells undergoing apoptosis but not necrosis. J. Cell Biol. 135, 1369-1376.

50. Diez, E., Z. Yaraghi, A. MacKenzie, and P. Gros. 2000. The neuronal apoptosis inhibitory protein (Naip) is expressed in macrophages and is modulated after phagocytosis and during intracellular infection with *Legionella pneumophila*. J. Immunol 164, 1470-1477.

51. Dubowitz, V. 1995. Muscle Disorders in Childhood, 2nd ed. Saunders, London, U.K. pp. 45-61.

52. Duckett, C., V. Nava, R. Gedrich, R. Clem, J. Van Dongen, M. Gilfillan, H. Shields, J. Hardwick, and C. Thompson. 1996. A conserved family of cellular genes related to the baculovirus iap gene and encoding apoptosis inhibitors. EMBO J. 15, 2685-2689.

53. Duncan, C., and L. Ment. 1990. Central nervous System: Head Injury. In: R.W. Reinhardt, M. Steube, and J Casey (Eds.) Pediatric Trauma. Mosby Year Book, St. Louis, MO. pp. 222-234.

54. Dunnett, S., W. Low, and S. Iverson. 1981. Learning impairments following selective kianic acid induced lesions within the neostriatum of rats. Behav. Brain Res. 2, 189-209.

55. Fadeel, B., B. Zhivotovsky, and S. Orrenius. 1999. All along the watchtower: on the regulation of apoptosis regulators. FASEB J. 13, 1647-1657.

56. Fan, L., P. Young, F. Barone, G. Feuerstein, D. Smith, T. McIntosh. 1996. Experimental brain injury induces differential expression of tumor necrosis factor-alpha mRNA in the CNS. Brain Res. Mol. Brain Res. 36, 287-291.

57. Fidzianska, A., H. Goebel, and I. Warlo. 1990. Acute infantile spinal muscular atrophy. Muscle apoptosis as a proposed pathogenetic mechanism. Brain 113, 433- 445.

58. Fidzianska, A., and I. Hausmanowa-Petrusewicz. 1984. Morphology of the lower motor neuron and muscle. In: I. Gamstroo and H. Sarnat (Eds.) Progressive Spinal Muscular Atrophies. Raven Press, New York, N.Y. pp. 55-89.

59. Flaris, N., T. Densmore, M. Molleston, and W. Hickey. 1993. Characterization of microglia and macrophages in the central nervous system of rats: definition of the differential expression of molecules using standard and novel monoclonal antibodies in normal CNS and in four models of parenchymal reaction. Glia. 7, 34-40.

60. Fox, G., L. Fan, R. Levasseur, and A. Faden. 1998. Sustained sensory/motor and cognitive deficits with neuronal apoptosis following controlled cortical impact brain injury in the mouse. J. Neurotrauma 15, 599-613.

61. Gao, L., and Y. Abu Kwaik. 1999. Activation of caspase 3 during Legionella pneumophila- induced apoptosis. Infect. Immun. 67, 4886-4894.

62. Gervais, F., N. Thornberry, S. Ruffolo, D. Nicholson, and S. Roy. 1998. Caspases

cleave focal adhesion kinase during apoptosis to generate a FRNK-like polypeptide. J. Biol. Chem. 273, 17102-17108.

63. Hall, E. 1985. Beneficial effects of acute intravenous ibuprofen on neurologic recovery of head-injured mice: comparison of cyclooxygenase inhibition with inhibition of thromboxane A2 synthetase or 5-lipoxygenase. Cent. Nerv. Syst. Trauma 2, 75-83.

64. Hauser, H., M. Bardroff, G. Pyrowolakis, and S. Jentsch. 1998. A giant ubiquitin-conjugating enzyme related to IAP apoptosis inhibitors. J. Cell Biol. 141, 1415-1422.

65. Hausmanowa-Petrusewicz, I., A. Fidzianska, I. Niebroj-Dobosz, and M. Strugalska. 1980. Is Kugelberg-Welander spinal muscular atrophy a fetal defect? Muscle Nerve 3, 389-402.

66. Haviv, R., and R. Stein. 1999. Nerve growth factor inhibits apoptosis induced by tumor necrosis factor in PC12 cells. J. Neurosci. Res. 55, 269-277.

67. Hengartner, M. 1997. Genetic control of programmed cell death and aging in the nematode *Caenorhabditis elegans*. Exp. Gerontol. 32, 63-74.

68. Hengartner, M., R. Ellis, and H. Horvitz. 1992. *Caenorhabditis elegans* gene *ced-9* protects cells from programmed cell death. Nature 356, 494-499.

69. Hengartner, M., and H. Horvitz. 1994. *C. elegans* cell survival gene *ced-9* encodes a functional homolog of the mammalian proto-oncogene bcl-2. Cell 76, 665-676.

70. Hickey, W., and H. Kimura. 1988. Perivascular microglial cells of the CNS are bone marrow-derived and present antigen in vivo. Science 239, 290-292.

71. Hisahara, S., S. Shoji, H. Okano, and M. Miura. 1997. ICE/CED-3 family executes oligodendrocyte apoptosis by tumor necrosis factor. J. Neurochem. 69, 10-20.

72. Hogan, B., R. Beddington, F. Costantini, and E. Lacy. 1994. Manipulating the mouse enbryo: Production of transgenic mice. In: Manipulating the Mouse Embryo. Cold Spring Harbor Laboratory Press USA pp. 217-251.

73. Holcik, M., C. Thompson, Z. Yaraghi, C. Lefebvre, A. MacKenzie, and R. Korneluk. 2000. The hippocampal neurons of neuronal apoptosis inhibitory protein 1 (NAIP1)-deleted mice display increased vulnerability to kainic acid-induced injury. Proc. Natl. Acad. Sci. U. S. A. 97, 2286-2290.

74. Holmin, S., and T. Mathiesen. 1999. Long-term intracerebral inflammatory response after experimental focal brain injury in rat. Neuroreport. 10, 1889-1891.

75. Hsieh-Li, H., J. Chang, Y. Jong, M. Wu, N. Wang, C. Tsai, and H. Li. 2000. A mouse model for spinal muscular atrophy. Nat. Genet. 24, 66-70.

76. Hsu, H., J. Xiong, and D. Goeddel. 1995. The TNF receptor 1-associated protein TRADD signals cell death and NF-kappaB activation. Cell 81, 495-504.

77. Huang, S., J. Scharf, J. Growney, M. Endrizzi, and W. Dietrich. 1999. The mouse Naip gene cluster on Chromosome 13 encodes several distinct functional transcripts. Mamm. Genome 10, 1032-1035.

78. Jaenisch, R. 1988. Transgenic animals. Science 240, 1468-1474.

79. Janicke, R., M. Spengart, M. Wati, and A. Porter. 1998. Caspase-3 is required for DNA fragmentation and morphological changes associated with apoptosis. J. Biol. Chem. 273, 9357-9360.

80. Jennett, B., G. Teasdale, J. Fry, R. Braakman, J. Minderhoud, J. Heiden, and T. Kurze. 1980. Treatment for severe head injury. J. Neurol. Neurosurg Psychiatry 43, 289-295.

81. Johnson, D. 1988. Head Injury. In: M.R. Eichelberger, and G. L. Pratsch (Eds.) Pediatric Trauma Care. Aspen Publishers, Inc., Rockville, MD. pp. 87-99.

82. Johnson, J. 1990. Comparative Development of Somatic Sensory Cortex, Rodents. In: E.G. Jones, and A. Peters (Eds.) Cerebral Cortex: Comparative Structure and Evolution of Cerebral Cortex. Plenum Press, New York, NY, pp. 385-398.

83. Johnson, D., and S. Krishnamurthy. 1998. Severe pediatric head injury: myth, magic and actual fact. Pediatr. Neurosurg. 28, 167-172.

84. Katayama, Y., T. Maeda, M. Koshinaga, T. Kawamata, and T. Tsubokawa. 1995. Role of excitatory amino acid-mediated ionic fluxes in traumatic brain injury. Brain Pathol. 5, 427-435.

85. Kermer, P., N. Klocker, and M. Bahr. 1999. Neuronal death after brain injury. Models, mechanisms, and therapeutic strategies in vivo. Cell Tissue Res. 298, 383-395.

86. Kerr, J., A. Wyllie, and A. Currie. 1972. Apoptosis: a basic biological phenomenon with wide-ranging implications in tissue kinetics. Br. J. Cancer. 26, 239-257.

87. Knoblach, S., L. Fan, and A. Faden. 1999. Related Early neuronal expression of tumor necrosis factor-alpha after experimental brain injury contributes to neurological impairment. J. Neuroimmunol. 95, 115-125.

88. Koshinaga, M., Y. Katayama, M. Fukushima, H. Oshima, T. Suma, and T. Takahata. 2000. Rapid and widespread microglial activation induced by traumatic brain injury in rat brain slices. J. Neurotrauma 17, 185-192.

89. Kothakota, S., T. Azuma, C. Reinhard, A. Klippel, J. Tang, K. Chu, T. McGarry, M.

Kirschner, K. Koths, D. Kwiatkowski, and L. Williams. 1997. Caspase-3-generated fragment of gelsolin: effector of morphological change in apoptosis. Science 278, 294-298.

90. Krajewski, S., J. Mai, M. Krajewska, M. Sikorska, M. Mossakowski, and J. Reed. 1995. Upregulation of bax protein levels in neurons following cerebral ischemia. J. Neurosci. 15, 6364-6376.

91. La Bella, V., C. Cisterni, D. Salaun, and B. Pettmann. 1998. Survival motor neuron (SMN) in rat is expressed as different molecular forms and is developmentally regulated. Eur. J. Neurosci. 10, 2913-2923.

92. LaCasse, E., S. Baird, R. Korneluk, and, A. Mackenzie. 1999. The inhibitors of apoptosis (IAPs) and their emerging role in cancer. Oncogene 18, 3247-3259.

93. LaHaye, P., G. Gade, and, D. Becker. 1991. Injury to the Cranium. In: K.L. Mattox, E.E. Moore, and D.V. Feliciano (Eds.) Trauma. Appleton and Lange, San Mateo, CA. pp. 237-251.

94. LeBrun, D., R. Warnke, and M. Cleary. 1993. Expression of bcl-2 in fetal tissues suggests a role in morphogenesis. Am. J. Pathol. 142, 743-753.

95. Lefebvre, S., L. Burglen, S. Reboullet, O. Clermont, P. Burlet, L. Viollet, B. Benichou, C. Cruard, P. Millasseau, M. Zeviani, D. Le Paslier, J. Weissenbach, A. Munnich, and J. Melki. 1995. Identification and characterization of a spinal muscular atrophy-determining gene. Cell 80, 155-165.

96. Lefebvre, S., P. Burlet, Q. Liu, S. Bertrandy, O. Clermont, A. Munnich, G. Dreyfuss, and J. Melki. 1997. Correlation between severity and SMN protein level in spinal muscular atrophy. Nat. Gen. 16, 265-269.

97. Li, F., G. Ambrosini, E. Chu, J. Plescia, S. Tognin, P. Marchisio, and D. Altieri. 1998 Control of apoptosis and mitotic spindle checkpoint by survivin. Nature 396, 580-584.

98. Li, G., G. Brodin, M. Farooque, K. Funa, A. Holtz, W. Wang, and Y. Olsson. 1996. Apoptosis and expression of BCL-2 after compression trauma to the rat spinal cord. J. neuropathol. 55, 280-289.

99. Li, X., and Z. Darzynkiewicz. 2000. Cleavage of Poly(ADP-ribose) polymerase measured in situ in individual cells: relationship to DNA fragmentation and cell cycle position during apoptosis. Exp. Cell Res. 255, 125-132.

100. Li, J., J. Kim, P. Liston, M. Li, T. Miyazaki, A. MacKenzie, R. Korneluk, and B. Tsang. 1998. Expression of inhibitor of apoptosis proteins (IAPs) in rat granulosa cells during ovarian follicular development and atresia. Endocrin. 139, 1321-1328.

101. Li, P., D. Nijhawan, I. Budihardjo, S. Srinivasula, M. Ahmad, E. Alnemri, and X. Wang. 1997. Cytochrome c and dATP-dependent formation of Apaf-1/caspase-9 complex initiates an apoptotic protease cascade. Cell 91, 479-489.

102. Li, H., H. Zhu, C. Xu, and J. Yuan. 1998. Cleavage of BID by caspase 8 mediates the mitochondrial damage in the Fas pathway of apoptosis. Cell 94, 491-501.

103. Liston, P., N. Roy, K. Tamai, C. Lefebvre, S. Baird, G. Cherton-Horvat, R. Farahani, M. McLean, J. Ikeda, A. MacKenzie, and R. Korneluk. 1996. Suppression of apoptosis in mammalian cells by NAIP and a related family of IAP genes. Nature 379, 349-353.

104. Liu, Q., U. Fischer, F. Wang, and G. Dreyfuss. 1997. The spinal muscular atrophy disease gene product, SMN, and its associated protein SIP1 are in a complex with spliceosomal snRNP proteins. Cell 90, 1013-1021.

105. Liu, X., C. Kim, J. Yang, R. Jemmerson, and X. Wang. 1996. Induction of apoptotic program in cell-free extracts: requirement for dATP and cytochrome c. Cell 86, 147-157.

106. Luo, X., I. Budihardjo, H. Zou, C. Slaughter, X. Wang. 1998. Bid, a Bcl2 interacting protein, mediates cytochrome c release from mitochondria in response to activation of cell surface death receptors. Cell 94, 481-90.

107. Lundar, T., and K. Nestvold. 1985. Pediatric head injuries caused by traffic accidents. A prospective study with 5-year follow-up. Child's Nerv. Syst.1, 24-28.

108. MacManus, J., A. Buchan, I. Hill, I. Rasquinha, and E. Preston. 1993. Global ischemia can cause DNA fragmentation indicative of apoptosis in rat brain. Neurosci. Lett. 164, 89-92.

109. Marks, N., and M. Berg. 1999. Recent advances on neuronal caspases in development and neurodegeneration. Neurochem. Int. 35, 195-220.

110. Mattson, M., B Cheng, SA Baldwin, VL Smith-Swintosky, J Keller, JW Geddes, SW Scheff, and S Christakos. 1995. Brain injury and tumor necrosis factors induce calbindin D-28k in astrocytes: evidence for a cytoprotective response. J. Neurosci. Res. 42, 357-370.

111. McIntosh, T., A. Rink, K. Fung, J. Trojanowski, V. Lee, and E. Neugebauer. 1995. Evidence of apoptotic cell death after experimental brain injury in the rat. Am. J. Pathol. 147, 1575-1583.

112. McIntosh, T., R. Vink, L. Noble, I. Yamakami, S. Fernyak, H. Soares, and A. Faden. 1989. Traumatic brain injury in the rat: characterization of a lateral fluid-percussion model. Neurosci. 28, 233-244.

113. Meda, L., M. Cassatella, G. Szendrei, L. Otvos Jr, P. Baron, M. Villalba, D. Ferrari, and

F. Rossi. 1995. Activation of microglial cells by beta-amyloid protein and interferon-gamma. Nature 374, 647-650.

114. Melki, J., P. Sheth, S. Abdelhak, P. Burlet, M. Bachelot, M. Lathrop, J. Frezel, and A. Munnich. 1990. Mapping of acute (type 1) spinal muscular atrophy to chromosome 5q 12-q14. The French Spinal Muscular Atrophy Investigators. Lancet 333, 271-273.

115. Menon, D. 1999. Cerebral protection in severe brain injury: physiological determinants of outcome and their optimization. Br. Med. Bull. 55, 226-258.

116. Mogi, M., M. Harada, P. Riederer, H. Narabayashi, K. Fujita, and T. Nagatsu. 1994. Tumor necrosis factor-alpha (TNF-alpha) increases both in the brain and in the cerebrospinal fluid from parkinsonian patients. Neurosci. Lett. 165, 208-210.

117. Monney, L., R. Olivier, I. Otter, B. Jansen, G. Poirier, and C. Borner. 1998. Role of an acidic compartment in tumor-necrosis-factor-alpha-induced production of ceramide, activation of caspase-3 and apoptosis. Eur. J. Biochem. 251, 295-303.

118. Montkowski, A., M. Poettig, A. Mederer, and F. Holsboer. 1997. Behavioral performance in three substrains of mouse strain 129. Brain Res. 762, 12-18.

119. Morris, R. 1982. Development of a water maze procedure for studying spatial learning in the rat. J. Neurosci. Methods 22, 47-60.

120. Morrison, K. 1996. Advances in SMA research: review of gene deletions. Neuromusc. Disord. 6397- 6408.

121. Munch, E., P. Horn, L. Schurer, A. Piepgras, T. Paul, and P. Schmiedek. 2000. Management of severe head injury by decompressive craniectomy. Neurosurg. 47, 315-323.

122. Murayama, S., T. Bouldin, and K. Suzuki. 1991. Immunocytochemical and ultrastructural studies of Werdnig-Hoffmann disease. Acta Neuropathol. 81, 408-417.

123. Muzio, M., R. Stockwell, G. Salvesen, and V. Dixit. 1998. An induced proximity model for caspase-8 activation. J. Biol. Chem. 273, 2926-2930.

124. Nagata S. 1997. Apoptosis by death factor. Cell 88, 355-365.

125. Newcomb, J., X. Zhao, B. Pike, and R. Hayes. 1999. Temporal profile of apoptotic-like changes in neurons and astrocytes following controlled cortical impact injury in the rat. Exp. Neurol. 158, 76-88.

126. Nicholson, D., and N. Thornberry. 1997. Caspases: Killer Proteases. TIBS 22, 303-306.

127. Nicotera, P., M. Leist, B. Single, and C. Volbracht. 1999. Execution of apoptosis:

converging or diverging pathways? Biol. Chem. 380, 1035-1040.

128. Oliver, F., G. de la Rubia, V. Rolli, M. Ruiz-Ruiz, G. de Murcia, and J. Murcia. 1998. Importance of poly (ADP-ribose) polymerase and its cleavage in apoptosis. Lesson from an uncleavable mutant. J. Biol. Chem. 273, 33533-33539.

129. Oppenheim, R. 1991. Cell death during development of the nervous system. Annu. Rev. Neurosci. 14, 453-501.

130. Pan, G., K. O'Rourke, and V. Dixit. 1998. Caspase-9, BCL-XL, and Apaf-1 form a ternary complex. J. Biol Chem. 273, 5841-5845.

131. Park, J., and D. Hockenbery. 1996. BCL-2, a novel regulator of apoptosis. J. Cell. Biochem. 60, 12-17.

132. Pellizzoni, L., N. Kataoka, B. Charroux, and G. Dreyfuss. 1998. A novel function for SMN, tthe spinal muscular atrophy disease gene product, in pre-mRNA splicing. Cell 95, 615- 624.

133. Peress, N., A. Stermann, R. Miller, C. Kaplan, and B. Little. 1986. "Chromalytic" neurons in lateral geniculate body in Werdnig-Hoffmann disease. Clin Neuropathol. 5, 69-72.

134. Perrelet, D., A. Ferri, A. MacKenzie, G. Smith, R. Korneluk, P. Liston, Y. Sagot, J. Terrado, D. Monnier, and A. Kato. 2000. IAP family proteins delay motor neuron cell death *in vivo*. Eur. J. Neurosci. 12, 2059-2067.

135. Perry, V., and S. Gordon. 1988. Macrophages and microglia in the nervous system. Trends Neurosci. 11, 273-277.

136. Pike, B., X. Zhao, J. Newcomb, C. Glenn, D. Anderson, R. Hayes. 2000. Stretch injury causes calpain and caspase-3 activation and necrotic and apoptotic cell death in septo-hippocanpal cell cultures. J. Neurotrauma 17, 283-298.

137. Pohl, D., P. Bittigau, M. Ishimaru, D. Stadthaus, C. Hubner, J. Olney, L. Turski, and I. Ikonomidou. 1999. N-Methyl-D-aspartate antagonists and apoptotic cell death triggered by head trauma in developing rat brain. Proc. Natl. Acad. Sci. U. S. A. 96, 2508-2513.

138. Raff, M. 1998. Cell suicide for beginners. Nature 12, 119-122.

139. Raghavendra, R., V. Rao, A. Dogan, K. Bowen, and R. Dempsey. 2000. Traumatic brain injury leads to increased expression of peripheral-type benzodiazepine receptors, neuronal death, and activation of astrocytes and microglia in rat thalamus. Exp Neurol. 161, 102-114.

140. Raghupathi, R., S. Fernandez, H. Murai, S. Trusko, R. Scott, W. Nishioka, and T. McIntosh. 1998. BCL-2 overexpression attenuates cortical cell loss after traumatic brain injury in transgenic mice. J. Cereb. Blood Flow Metab.18, 1259-1269.

141. Raine, C. 1995. Multiple sclerosis: TNF revisited, with promise. Nat Med. 1, 211-214.

142. Rodrigues, N., N. Owen, K. Talbot, S. Pate, F. Muntoni, J. Ignatius, V. Dubowitz, and K. Davies. 1996. Gene deletions in spinal muscular atrophy. J. Med. Gen. 33, 93-96.

143. Ross, S., M. Halliday, G. Campbell, D. Byrnes, and B. Rowlands. 1994. The presence of tumour necrosis factor in CSF and plasma after severe head injury. Br. J. Neurosurg. 8, 419-425.

144. Rothe, M., M. Pan, W. Henzel, T. Ayres, and D. Goeddel. 1995. The TNFR2-TRAF signaling complex contains two novel proteins related to baculoviral inhibitor of apoptosis proteins. Cell 83, 1243-1252.

145. Rothe, M., S. Wong, W. Henzel, and D. Goeddel. 1994. A novel family of putative signal transducers associated with the cytoplasmic domain of the 75 kDa tumor necrosis factor receptor. Cell 78, 681-692.

146. Roy, N., Q. Deveraux, R. Takahashi, G. Salvesen, and J. Reed. 1997. The c-IAP-1 and c-IAP-2 proteins are direct inhibitors of specific caspases. EMBO J. 16, 6914-6925.

147. Roy, N., M. Mahadevan, M. McLean, G. Shutler, Z. Yaraghi, R. Farahani, S. Baird, A. Besner-Johnson, C. Lefebvre, X. Kang, M. Salih, H. Aubry, K. Tamai, P. Ioannou, T. Crawford, P. de Jong,, L. Surh, J. Ikeda, R. Korneluk, and A. Mackenzie. 1995. The gene for neuronal apoptosis inhibitory protein is partially deleted in individuals with spinal muscular atrophy. Cell 80, 167-178.

148. Sakahira, H., M. Enari, and S. Nagata. 1998. Cleavage of CAD inhibitor in CAD activation and DNA degradation during apoptosis. Nature 391, 96-99.

149. Sarnat, H. 1984. Commentary: Research strategies in spinal muscular atrophy. In: I. Gamstorp and H. B. Sarnat (Eds.) Progressive Spinal Muscular Atrophies. Raven Press, New York, N.Y. p233.

150. Scaffidi, C., S. Fulda, A. Srinivasan, C. Friesen, F. Li, K. Tomaselli, K. Debatin, P. Krammer, and M. Peter. 1998. Two CD95 (APO-1/Fas) signaling pathways. EMBO J. 17, 1675-1687.

151. Scharf, J., D. Damron, A. Frisella, S. Bruno, A. Beggs, L. Kunkel, and W. Dietrich. 1996. The mouse region syntenic for human spinal muscular atrophy lies within the Lgn1 critical I interval and contains multiple copies of Naip exon 5. Genomics 38, 405-417.

152. Scharf, J., M. Endrizzi, A. Wetter, S. Huang, T. Thompson, K. Zerres, W. Dietrich, Wirth B, and L. Kunkel. 1998. Identification of a candidate modifying gene for spinal muscular atrophy by comparative genomics. Nat. Genet. 20, 83-86.

153. Scherbel, U., R. Raghupathi, M. Nakamura, K. Saatman, J. Trojanowski, E. Neugebauer, M. Marino, and T. McIntosh. 1999. Differential acute and chronic responses of tumor necrosis factor-deficient mice to experimental brain injury. Proc. Natl. Acad. Sci. U .S. A. 96, 8721-8726.

154. Schmeiser, K., E. Hammond, S. Roberts, and R. Grand. 1998. Specific cleavage of gamma catenin by caspases during apoptosis. FEBS Lett. 433, 51-57.

155. Schwartz, L., and B. Osborne. 1993. Programmed cell death, apoptosis and killer genes. Immunol. Today 14, 582-590.

156. Scott, N., A. Hale, M. Deakin, P. Hand, F. Adals, C. Hale, G. Williams, and J. Elder. 1998. A histopathological assessment of the response of rectal adenocarcinoma to combination chemo-radiotherapy: relationship to apoptotic activity, p53, and *bcl-2* expression. Eur. J. Surg. Oncol. 24, 169-173.

157. Sedgwick, J., A. Ford, E. Foulcher, and R. Airriess. 1998. Central nervous system microglial cell activation and proliferation follows direct interaction with tissue-infiltrating T cell blasts. J. Immunol. 160, 5320-5330.

158. Shah, G., S. Kaufmann, and G. Poirier. 1995. Detection of poly (ADP-ribose) polymerase and its apoptosis-specific fragment by a nonisotopic activity-western blot technique. Anal. Biochem. 232, 251-254.

159. Shohami, E., R. Bass, D. Wallach, A. Yamin, and R. Gallily. 1996. Inhibition of tumor necrosis factor alpha (TNFalpha) activity in rat brain is associated with cerebroprotection after closed head injury. J. Cereb. Blood Flow Metab.16, 378-384.

160. Shohami, E., R. Gallily, R. Mechoulam, R. Bass, and T. Ben-Hur. 1997. Cytokine production in the brain following closed head injury: dexanabinol (HU-211) is a novel TNF-alpha inhibitor and an effective neuroprotectant. J. Neuroimmunol. 72, 169-177.

161. Shohami, E., M. Novikov, R. Bass, A. Yamin, and R. Gallily. 1994. Closed head injury triggers early production of TNF alpha and IL-6 by brain tissue. J. Cereb. Blood Flow Metab. 14, 615-619.

162. Simons, M., S. Beinroth, M. Gleichmann, P. Liston, R. Korneluk, A. MacKenzie, M. Bahr, T. Klockgether, G. Robertson, M. Weller, and J. Schulz. 1999. Adenovirus-mediated gene transfer of inhibitors of apoptosis protein delays apoptosis in cerebellar granule neurons. J. Neurochem. 72, 292-301.

163. Sipe, K., D. Srisawasdi, R. Dantzer, K. Kelley, and J. Weyhenmeyer. 1996. An

endogenous 55 kDa TNF receptor mediates cell death in a neural cell line. Brain Res. Mol. Brain Res. 38, 222-232.

164. Skippen, P., M. Seear, K. Poskitt, J. Kestle, D. Cochrane, G. Annich, and J. Handel. 1997. Effect of hyperventilation on regional cerebral blood flow in head injured children. Crit. Care Med. 25, 1402-1409.

165. Slee, E., M. Harte, R. Kluck, B. Wolf, C. Casiano, D. Newmeyer, H. Wang, J. Reed, D. Nicholson, E. Alnemri, D. Green, and S. Martin. 1999. Ordering the cytochrome c-initiated caspase cascade: hierarchical activation of caspases-2, -3, -6, -7, -8, and -10 a caspase-9-dependent manner. J. Cell Biol. 144, 281-292.

166. Smith, D., H. Soares, J. Pierce, K. Pierce, K. Saatmann, D. Meaney, C. Dixon, and T. McIntosh. 1995. A model of parasagittal controlled cortical impact in the mouse: cognitive and histopathological effects. J. Neurotrauma 12, 169-178.

167. Soane, L., H. Rus, F. Niculescu, and M. Shin. 1999. Inhibition of oligodendrocyte apoptosis by sublytic C5b-9 is associated with enhanced synthesis of bcl-2 and mediated by inhibition of caspase-3 activation. J. Immunol 163, 6132-6138.

168. Soares, H., M. Thomas, K. Cloherty, and T. McIntosh. 1992. Development of prolonged local cerebral edema and regional cation changes following experimental brain injury in the rat. J. Neurochem. 58, 1845-1852.

169. Stahel, P., E. Shohami, F. Younis, K. Kariya, V. Otto, P. Lenzlinger, M. Grosjean, H. Eugster, O. Trentz, T. Kossmann, and M. Morganti-Kossmann. 2000. Experimental closed head injury: analysis of neurological outcome, blood-brain barrier dysfunction, intracranial neutrophil infiltration, and neuronal cell death in mice deficient in genes for pro-inflammatory cytokines. J. Cereb. Blood Flow Metab. 20, 369-380.

170. Stehlik, C., R. de Martin, I. Kumabashiri, J. Schmid, B. Binder, and J. Lipp. 1998. Nuclear factor (NF)-kappaB-regulated X-chromosome-linked iap gene expression protects endothelial cells from tumor necrosis factor alpha-induced apoptosis. J. Exp. Med.188, 211-216.

171. Styren, S., W. Civin, and J. Rogers. 1990. Molecular, cellular, and pathologic characterization of HLA-DR immunoreactivity in normal elderly and Alzheimer's disease brain. Exp. Neurol. 110, 93-104.

172. Takahashi, A., E. Alnemri, Y. Lazebnik, T. Fernandes-Alnemri, G. Litwack, R. Moir, R. Goldman, G. Poirier, S. Kaufmann, and W. Earnshaw. 1996. Cleavage of lamin A by Mch2 alpha but not CPP32: multiple interleukin 1 beta-converting enzyme-related proteases with distinct substrate recognition properties are active in apoptosis. Proc. Natl. Acad. Sci. U. S. A. 93, 8395-8400.

173. Takahashi, R., Q. Deveraux, I. Tamm, K. Welsh, N. Assa-Munt, G. Salvesen, and J.

Reed. 1998. A single BIR domain of XIAP is sufficient for inhibiting caspases. J. Biol. Chem. 273, 7787-7790.

174. Takahashi, A., P. Musy, L. Marins, G. Poirier, R. Moyer, and W. Earnshaw. 1996. CrmA/SPI-2 inhibition of an endogenous ICE related protease responsible for lamin A cleavage and apoptotic nuclear fragmentation. J. Biol. Chem. 271, 487-490.

175. Teasdale, G., and B. Jennett. 1974. Assessment of coma and impaired consciousness. A practical scale. Lancet 2, 81-84.

176. Tesco, G., T-W. Kim,, A. Diehlmann,, K. Beyreuther, and R. Tanzi. 1998. Abrogation of the presenilin 1 catenin interaction and preservation of the heterodimeric presenilin 1 complex following caspase activation. J .Biol. Chem. 273, 909-914.

177. Tewari, M., L. Quan, K. O'Rourke, S. Desnoyers, Z. Zeng, D. Beidler, G. Poirier, G. Salvesen, and V. Dixit. 1995. Yama/CPP32β, a mammalian homolog of CED-3, is a CrmA-inhibitable protease that cleaves the death substrate poly (ADP-ribose) polymerase. Cell 81, 801-809.

178. Thornberry, N., and Y. Lazebnik. 1998. Caspases: enemies within. Science 281, 1312-316.

179. Tizzano, E., C. Cabot, and M. Baiget. 1998. Cell-specific survival motor neuron gene expression during human development of the central nervous system: implications for the pathogenesis of spinal muscular atrophy. Am. J. Pathol. 153, 355-361.

180. Tracey K., and A. Cerami. 1993. Tumor necrosis factor: an updated review of its biology. Crit. Care Med. 21, S415-422.

181. Tussey, L., and, A. McMichael. 1995. General introduction to the MHC. In: G.E. Blair, C.R. Pringle, and D.J. Maudsley (Eds.) Modulation of the MHC antigen expression and disease. Cambridge University Press, Great Britain, pp. 1-18.

182. Vanhaesebroeck, B., J. Reed, D. De Valck, J. Grooten, T. Miyashita, S. Tanaka, R. Beyaert, F. Van Roy, and W. Fiers. 1993. Effect of *bcl-2* proto-oncogene expression on cellular sensitivity to tumor necrosis factor-mediated cytotoxicity. Oncogene 8,1075-1081.

183. Vartanian, T., Y. Li, M. Zhao, and K. Stefansson. 1995. Interferon-gamma-induced oligodendrocyte cell death: implications for the pathogenesis of multiple sclerosis. Mol. Med. 1, 732-743.

184. Wang, K., R. Posmantur, R. Nath, K. McGinnis, M. Whittan, R. Talanian, S. Glantz, and J. Morrow. 1998. Simultaneous degradation of alpha II and beta II spectrin by caspase-3 (CPP32) in apoptotic cells. J. Biol. Chem. 273, 490-497.

185. Weber, J., B. Rzigalinski, K. Willoughby, S. Moore, and E. Ellis. 1999. Alterations in calcium-mediated signal transduction after traumatic injury of cortical neurons. Cell Calcium 26, 289-299.

186. Woodroofe, M., A. Bellamy, M. Feldmann, A. Davison, and M. Cuzner. 1986. Immunocytochemical characterization of the immune reaction in the central nervous system in multiple sclerosis. Possible role for microglia in lesion growth. J. Neurol. Sci. 74, 135-152.

187. Xu, D., S. Crocker, J. Doucet, M. St-Jean, K. Tamai, A. Hakim, J. Ikeda, P. Liston C. Thompson, R. Korneluk, A. MacKenzie, and G. Robertson. 1997. Elevation of neuronal expression of NAIP reduces ischemic damage in the rat hippocampus. Nat. Med. 3, 997-1004.

188. Xu, D., R. Korneluk, K. Tamai, N. Wigle, A. Hakim, A. Mackenzie, and G. Robertson. 1997. Distribution of neuronal apoptosis inhibitory protein-like immunoreactivity in the rat central nervous system. J. Comp. Neurol. 382, 247-259.

189. Yachnis, A., M. Giovanini, T. Eskin, P. Reier, and D. Anderson. 1998. Developmental patterns of BCL-2 and BCL-X polypeptide expression in the human spinal cord. Exp. Neurol. 150, 82-97.

190. Yakovlev, A., S. Knoblach, L. Fan, G. Fox, R. Goodnight, and A. Faden. 1997. Activation of CPP32-like caspases contributes to neuronal apoptosis and neurological dysfunction after traumatic brain injury. J. Neurosci. 17, 7415-7424.

191. Yang, J., X. Liu, K. Bhalla, C. Kim, A. Ibrado, J. Cai, T. Peng, D. Jones, and X. Wang. 1997. Prevention of apoptosis by Bcl-2: release of cytochrome c from mitochondria blocked. Science 275, 1129-1132.

192. Yaraghi, Z., E. Diez, P. Gros, and A. MacKenzie. 1999. cDNA cloning and the 5'genomic organization of Naip2, a candidate gene for murine Legionella resistance. Mamm. Genome 10, 761-763.

193. Yaraghi, Z., R. Korneluk, and A. MacKenzie. 1998. Cloning and characterization of the multiple murine homologues of NAIP (neuronal apoptosis inhibitory protein). Genomics 51, 107-113.

194. Ye, P., A. D'Ercole. 1999. Insulin-like growth factor I protects oligodendrocytes from tumor necrosis factor-alpha induced injury. Endocrin. 140, 3063-3072.

195. Young, S. P. Liston, J. Xuan, C. McRoberts, C. Lefebvre, and R. Korneluk. 1999. Genomic organization of the physical map of the human inhibitors of apoptosis: HIAP1, HIAP2. Mamm. Gen. 10, 44-48.

196. Yuan, J., S. Shaham, S. Ledoux, H. Ellis, and H. Horvitz. 1993. The *C. elegans* cell

death gene *ced-3* encodes a protein similar to mammalian interleukin-1β-converting enzyme. Cell 75, 641-652.

197. Zou, A., W. Henzel, X. Liu, A. Lutschg, and X. Wang. 1997. Apaf-1, a human protein homologous to *C. elegans* CED-4, participates in cytochrome c dependent activation of caspase-3. Cell 90, 405-413.